2014: The Journal of Astronomical Data 20, 5.

Detectability of micro-variables in the ASAS database: the Scorpius – Centaurus Complex

M. David[1], H. Hensberge[2] and C. Nitschelm[3]

[1] Departement Wiskunde en Informatica, Universiteit Antwerpen, Middelheimlaan 1, B-2020 Antwerpen, Belgium
[2] Royal Observatory of Belgium, Ringlaan 3, B-1180 Brussels, Belgium
[3] Unidad de Astronomía, Facultad de Ciencias Básicas, Universidad de Antofagasta, Avenida Angamos 601, Antofagasta, Chile

Received October 31, 2013, accepted December 11, 2014

Abstract

We present a star-by-star discussion of the light variability of stars belonging to the Sco–Cen Complex, as detected in the ASAS–V database by David et al. (2013). Most of the variables (30) are young stars with irregular and/or cyclic patterns of variability, almost all with spectral types that indicate that they did not yet reach the zero-age main-sequence. The ZAMS starts at A3, F2 and F4 for the Upper-Scorpius, the Upper Centaurus-Lupus and the Lower Centaurus-Crux subgroups, respectively. A minority of stars (7), mainly of spectral type B or late-A, show strictly (multi-)periodic variability induced by rigid rotation of a spotted magnetic star, by slight deformation of the stellar shape in a binary, or by pulsation of stars situated in the instability domain of either SPB, δ Sct or γ Dor stars. For some stars comments on yet unpublished high-resolution spectra are included.

Keywords: Stars: variables: general – Techniques: photometric – open clusters and associations: individual: Sco–Cen Complex

1 Introduction

David et al. (2013) (henceforth referred to as paper I) have developed a method of analysis that allows to detect, in the All Sky Automated Survey ASAS–*V* data, variables of lower amplitude (0.02 mag peak-to-peak) than those commonly identified, see Table 2 in paper I. The technique is based on a consistency check between the results obtained in extraction apertures of different size for the quality–A measurements and eliminating quality–B, C and D data. This leaves on average 88% of the quality–A data (see Fig. 5 in paper I). David et al. (2013) applied this technique to a subset of the established members of the Scorpius–Centaurus Complex (de Zeeuw et al. 1999). Their tables 2 and 4 list 37 confirmed variables and 23 candidate variables, respectively. The stars cover the late–B to M3 spectral type range, the majority being pre–main sequence objects showing irregular or/and cyclic variability. Three stars (HD 146285 in Upper Scorpius, multi-periodic; HD 116794 in Lower Centaurus-Crux (LCC), irregular long-term variability; and HD 109022 in LCC, cyclic variability) were discussed in detail in paper I, as example cases.

The purpose of this paper is to present the discussion for the remaining 34 confirmed variables and comments on one of the other candidate variables. Unpublished high-resolution spectroscopy is discussed where applicable. In several cases, phase diagrams and power spectra illustrate the discussion. All necessary information is included to enable the reader to recover the data selection (Table 1) without need to repeat the iterative rejection procedure presented in paper I. Sect. 2 contains a short description of the general methodology, with the purpose to allow the reader to repeat our analysis exactly. Details of procedures specific for one or a few objects are mentioned in the subsections dedicated to that object.

Three sections group together the variable stars in Upper Scorpius, Upper Centaurus–Lupus and Lower Centaurus–Crux, respectively. B–type stars and early–A type stars are only found in Upper Scorpius, because in the other subgroups they are brighter than the saturation limit for the ASAS–V photometry. In each of these sections, subsections deal with different types of variability. Information on the stars and their light variability is given in each of these sections. In all tables and subsections stars are arranged in order of spectral type.

2 Methodology

Table 1 summarizes the selection criteria applied to all quality–A ASAS data sets of size $N > 75$. This lower limit to the size of the data sets is imposed in order to have a reasonable handle on the zero-point shifts between the data sets for each object. The photometric consistency criterion developed in paper I is as follows: for each ASAS data set a reference aperture is chosen (mostly #4, in two cases #2); an individual exposure in the data set is accepted if the magnitude obtained with each of the other apertures lies within a certain confidence region with respect to the magnitude obtained from the reference aperture. These confidence regions are obtained from a statistical analysis of all quality–A measurements in the data set. Columns 6-9 describe the confidence regions; they allow the reader to reproduce exactly our present selection from each data set, by the following rule: noting symbolically r for the reference aperture, $a_i \pm b_i$ for an entry of column d_{ri}, and m_i for the magnitude obtained with aperture i, an exposure is selected only if $a_i - b_i < (m_r - m_i)\mathrm{sgn}(r - i) < a_i + b_i$ simultaneously for all $i \neq r$.

We also list here the selected extraction aperture (corresponding to minimal scatter in the data, sometimes applied to a restricted time interval in case the object alternates 'quiet' periods with epochs in which the light variations are more pronounced), the relative magnitude shifts applied to the smaller data sets relative to the largest one for a specific object, the size of the quality–A data sets before and after the consistency check between apertures, and the time-interval covered by each data set (all quality–A data).

Searches for periodicity or cyclic behaviour are based on the periodogram analysis for unevenly spaced data (Scargle 1982); to ease the comparison between periodograms from data sets of different size N, we always plot a scaled periodogram value, notably $\left(\frac{4}{N}\right) P_X(f)$. Fits to periodic data were performed with a least-squares algorithm including sine/cosine terms in phase ϕ and, when required (see subsections for individual stars), in 2ϕ. No weights were used, since ASAS gives 'uncertainty' estimates applying to the whole frame rather than to individual objects. Extreme outliers to the fit (4.5 times the rms of the residuals) were omitted but, such outliers being rare, their elimination did not have a significant impact. Peak-to-peak amplitudes mentioned in the text for periodic variables or cycles refer to these fits.

In case of strictly periodic variability, an uncertainty on the period is estimated. For those objects for which both the HIPPARCOS data and the ASAS data independently define a phase diagram, the uncertainty is set dominantly by the allowable phase shift between both light curves. Indeed, the time elapsed between the midpoint of HIPPARCOS epochs, $t_{\rm hip}$ and the midpoint of ASAS epochs, $t_{\rm asas}$, is roughly 5 000 days, much larger than the time baseline for the HIPPARCOS data ($t_{\rm hip} \pm 500$ days) and for the ASAS data ($t_{\rm asas} \pm 1500$ days). In such case, the internal reshuffling in phase for data belonging to the same data set is small as compared to the shift of one data set relative to the other. The allowed phase shifts were estimated between ±0.08 (HD 145103) and ±0.2 in case of

Table 1: Selection of ASAS data used in this paper. Successive columns give the ASAS designation, the full data set identifier, the HJD-range, the number of quality–A measurements in the set, the range of allowed magnitude differences between the reference aperture and the other ones, the number of selected data, the aperture used in the photometric analysis, and (where applicable) the shift applied to the selected data.

ASAS	Data set	First, last HJD	n_A	d_{43}(mmag)	d_{42}(mmag)	d_{41}(mmag)	d_{40}(mmag)	n_{sel}	[ap]+shift
161625-2459.3	3;1;F1612-32_185	2040.74,5041.50	412	0.31±7.9	2.97±13.6	8.57±31.7	9.55±67.7	339	[4]
	1;1;F1600-40_146	1914.87,5024.56	247	3.52±7.6	6.17±17.4	6.46±33.8	-0.82±59.7	211	[4]+0.003
162005-2003.4	see bottom part of the table								
161828-2316.5	2;2;F1632-24_229	1932.86,5024.63	388	-0.22±7.6	-1.50±15.9	6.60±34.7	6.33±65.8	297	[4]
	1;1;F1600-24_228	2026.72,4258.61	111	3.89±10.1	4.96±19.0	6.65±39.7	6.88±57.3	87	[4]+0.010
164018-2353.7	2;1;F1632-24_229	1932.86,5024.63	402	2.86±9.5	7.07±17.1	15.21±38.8	14.25±48.0	294	[3]
161312-2229.1	1;2;F1600-24_228	1924.86,4985.66	361	4.66±7.7	6.39±16.8	10.48±38.9	8.66±50.0	311	[3]
	2;1;F1632-24_229	1932.86,5024.63	205	4.46±10.9	3.61±16.8	13.19±33.4	13.52±75.4	174	[3]
160713-2706.0	2;1;F1600-24_228	1924.86,4985.66	368	6.01±8.2	9.19±16.5	13.05±38.3	5.02±61.0	328	[3]
155321-1923.9	4;1;F1600-16_273	1931.86,4946.73	352	-7.27±9.1	-10.44±18.0	-7.72±43.0	-7.55±72.5	312	[4]
160118-2652.4	3;2;F1600-24_228	1924.86,4985.66	379	-11.84±18.3	-10.49±23.2	-6.82±36.2	-5.24±60.9	343	[3]
160244-3040.0	2;1;F1612-32_185	1919.87,5041.50	416	7.38±7.8	11.98±15.2	15.39±31.6	17.49±52.9	343	[4]
161023-2917.0	1;1;F1612-32_185	1919.87,5041.50	397	5.91±7.5	10.52±13.7	14.04±34.1	18.04±55.8	333	[2]
	3;2;F1632-24_229	3576.47,4948.74	80	-2.17±13.3	-8.59±24.5	-3.83±42.1	-1.00±77.3	73	[2]-0.010
	2;1;F1600-24_228	3397.87,4882.85	76	3.80±9.8	-3.40±19.6	5.03±38.8	10.84±72.5	71	[2]-0.005
145824-3721.7	1;1;F1440-40_144	1902.85,4615.78	307	3.89±7.9	8.63±18.0	9.38±37.9	8.11±64.7	236	[4]
	2;1;F1520-40_145	1914.85,4969.74	231	6.24±10.6	9.70±18.2	11.72±27.5	16.63±65.0	194	[4]
142958-5607.9	1;1;F1424-56_078	1907.86,4993.75	440	6.57±9.8	13.13±16.3	16.94±35.4	9.76±51.8	341	[3]
165445-3653.3	1;1;F1640-40_147	1931.86,5111.52	335	4.13±10.2	7.94±18.0	14.53±37.0	17.04±66.0	290	[2]
	3;1;F1648-32_186	1954.84,5056.70	219	7.04±11.6	11.72±17.6	19.04±39.3	19.14±67.3	196	[2]-0.035
144404-4059.4	2;3;F1440-40_144	1902.85,4994.68	441	6.45±7.6	11.42±12.8	15.36±34.5	17.62±50.1	386	[3]
135914-5152.6	4;2;F1415-48_109	1900.85,5037.55	278	-49.43±47.6	-14.10±20.3	-17.58±36.2	-12.89±79.7	256	[3]
	2;1;F1424-56_078	1903.85,3452.74	199	-52.31±69.0	-15.00±26.4	-16.47±39.7	-16.11±69.8	179	[3]-0.015
	1;2;F1336-56_077	1907.82,3433.81	176	-74.25±74.3	-12.89±22.7	-10.09±42.4	-4.52±66.2	164	[3]+0.003
154502-4050.5	3;1;F1600-40_146	1914.87,5024.56	408	9.46±10.7	15.54±17.9	20.03±33.5	24.12±67.4	355	[4]
153705-4009.4	2;3;F1520-40_145	1914.85,4969.74	540	5.94±9.4	8.92±21.1	11.04±39.6	14.15±56.3	367	[2]
	3;1;F1600-40_146	1918.87,5024.56	199	6.10±11.6	13.25±16.4	15.87±31.5	15.89±71.6	174	[2]-0.007
162752-3547.0	4;1;F1648-32_186	1926.88,5056.70	276	6.00±13.0	8.39±22.8	15.94±38.4	4.83±78.1	251	[3]
	3;1;F1612-32_185	1919.87,5051.50	258	0.54±10.1	7.56±17.8	3.88±38.6	4.94±58.0	226	[3]-0.010
	2;1;F1640-40_147	1931.86,3502.91	195	4.25±10.5	6.46±18.5	6.40±33.2	9.23±51.6	170	[3]+0.006
143010-4332.8	4;3;F1440-40_144	1902.85,4994.68	402	-2.32±9.7	-0.98±16.4	0.45±34.8	6.27±73.4	346	[4]
	1;1;F1415-48_109	1903.85,3393.85	184	-1.13±11.4	-7.89±15.7	-6.45±32.2	-7.97±79.7	168	[4]
160345-4355.8	3;1;F1600-40_146	1918.87,5024.56	242	13.43±8.9	16.58±15.9	15.89±36.7	16.52±71.6	225	[4]
	1;2;F1545-48_111	1920.87,3189.77	185	11.02±13.1	14.18±22.7	15.46±38.2	19.82±56.4	162	[4]-0.013
154945-3925.1	2;1;F1600-40_146	1914.87,5024.56	407	-6.31±17.8	-2.71±23.4	-0.57±36.5	11.35±69.3	364	[3]
150449-3949.4	2;1;F1520-40_145	1914.85,4969.74	436	-4.61±30.0	-6.42±43.0	-7.02±54.2	-7.63±72.3	400	[2]
113306-5419.5	2;1;F1200-56_075	1878.82,5057.48	520	9.90±10.6	18.04±20.5	26.09±31.7	26.49±63.9	447	[3]
	1;3;F1112-56_074	1885.76,5168.84	500	5.20±8.6	8.81±20.2	14.07±42.1	13.78±57.1	432	[3]
121212-5413.8	1;2;F1200-56_075	1878.82,5057.48	555	3.52±11.7	9.80±23.0	9.34±47.7	5.22±69.9	492	[3]
121451-5547.4	1;2;F1200-56_075	1878.82,5057.48	563	-12.55±19.9	-5.66±32.8	-11.80±56.1	-17.86±85.7	490	[4]
	2;2;F1248-56_076	2454.52,4938.83	120	-7.90±23.1	-5.39±53.2	-11.64±81.0	-18.85±96.8	112	[4]-0.005
130734-5254.3	1;2;F1248-56_076	1875.85,5023.60	434	8.56±10.0	12.98±19.2	17.43±35.0	18.83±58.7	417	[3]
	2;2;F1336-56_077	1900.82,5085.49	236	8.18±10.9	10.28±17.5	20.53±27.5	25.04±57.4	205	[3]-0.003
	4;1;F1330-48_108	1889.84,5031.62	182	6.50±11.2	8.19±18.4	12.73±33.0	17.17±63.3	164	[3]+0.004
	3;1;F1245-48_107	1878.84,4948.80	134	6.89±11.5	18.07±21.1	22.55±47.6	18.60±56.9	111	[3]-0.007
122455-5200.3	4;3;F1245-48_107	1878.84,5048.55	309	-5.71±17.6	-13.05±34.2	-17.64±41.5	-20.20±82.8	279	[3]
	2;2;F1248-56_076	1875.85,3452.68	246	-5.36±19.1	-12.25±40.6	-17.07±52.3	-18.43±67.8	214	[3]+0.006
	1;2;F1200-56_075	1884.83,3450.70	217	-5.84±15.7	-12.05±37.6	-16.93±53.7	-18.13±71.6	187	[3]+0.012
	3;2;F1200-48_106	1876.84,4700.47	131	-5.04±20.0	-11.30±37.8	-16.54±61.7	-19.49±76.7	126	[3]+0.008
132712-5938.2	4;1;F1336-56_077	1900.82,5085.49	386	22.46±11.7	37.01±19.2	51.00±32.5	55.16±69.1	346	[3]
	1;1;F1300-64_049	1886.83,3430.85	198	12.48±17.7	23.17±28.3	29.22±47.0	37.10±64.4	182	[3]-0.020
	2;1;F1400-64_050	1907.84,3430.84	133	19.31±22.7	30.80±32.9	42.23±51.3	53.68±75.0	129	[3]-0.020
121519-6325.5	1;1;F1200-64_048	1899.84,5048.52	510	16.00±10.2	28.20±17.5	40.34±39.9	52.59±48.8	439	[2]
122840-5527.3	2;2;F1248-56_076	1875.85,5023.60	542	7.92±9.1	9.97±16.1	13.04±33.1	16.95±65.3	460	[3]
	1;1;F1200-56_075	1884.83,4616.51	293	4.99±11.5	8.67±21.0	12.74±32.4	10.78±46.1	244?	[3]
120548-5100.2	2;1;F1200-48_106	1876.84,4884.72	438	13.50±10.9	21.77±17.9	26.53±39.0	29.52±61.6	396	[3]
134309-6907.7	1;2;F1320-72_028	1877.85,5087.48	504	4.98±12.2	5.81±24.9	10.46±45.6	11.21±56.5	439	[2]
	4;1;F1400-64_050	1954.79,5023.69	101	17.51±12.1	22.72±17.7	28.20±36.3	30.87±52.0	93	[2]-0.014
132435-5557.4	2;1;F1336-56_077	1900.82,5085.48	481	11.60±9.8	20.14±19.3	29.85±31.9	32.62±94.1	425	[3]
121628-5008.6	2;1;F1200-48_106	1876.84,4884.72	436	6.58±9.6	13.44±18.0	14.57±37.9	15.00±48.4	392	[4]
	3;1;F1245-48_107	2454.52,5048.55	176	6.20±12.9	13.99±22.4	16.15±35.2	15.11±70.4	158	[4]+0.006
130505-6413.9	2;2;F1300-64_049	1886.83,5041.52	524	10.46±12.6	18.95±17.5	30.95±35.5	34.64±44.9	466	[4]
133154-5113.5	2;1;F1330-48_108	1887.85,5089.48	569	11.01±12.2	18.54±20.9	19.33±42.7	21.42±67.4	497	[2]
124752-5126.6	3;1;F1245-48_107	1878.84,5048.55	514	6.21±9.4	10.53±17.0	11.90±36.9	15.69±69.6	434	[3]
	1;1;F1248-56_076	1913.84,3452.68	163	7.97±12.1	10.40±19.6	11.26±34.4	12.64±55.1	145	[3]+0.005
132548-4815.0	3;1;F1330-48_108	1887.85,5089.48	578	11.07±13.2	13.89±20.5	12.57±38.2	10.42±55.8	489	[4]
ASAS	Data set	First, last HJD	n_A	d_{24}(mmag)	d_{23}(mmag)	d_{21}(mmag)	d_{20}(mmag)	n_{sel}	[ap]+shift
162005-2003.4	4;1;F1632-16_274	1933.87,4951.76	210	185.80±77.0	63.70±68.0	-22.89±29.5	-13.41±84.5	193	[1]
	2;2;F1632-24_229	1932.86,3448.85	182	161.21±53.5	53.89±37.8	-29.24±37.5	-28.77±61.0	117	[1]+0.022

lower amplitudes, and in a single case ±0.3 (HD 141277), the latter including uncertainty due to multi-periodicity. With the different data sets defined by different symbols in the corresponding figures, the reader can easily evaluate the quoted uncertainties.

For those objects for which the uncertainty on the period was set by the ASAS data solely, uncertainties are consistent with the simplest procedure advocated by Schwarzenberg-Czerny (1991) to obtain an estimator taking into account the correlation of noise in observations (Sect. 6, (iii) of his paper). In practice, one finds the mean noise power level N^2 in the vicinity of the considered frequency, and uses the width of the power peak at f at a level N^2 below the top as uncertainty estimate.

In order to visualize long-term trends, and to remove such trends tentatively from the data with the purpose of looking for additional cyclic or periodic components, when appropriate, cubic splines were fit to the data over the whole time interval covered by the ASAS data. The algorithm implemented in the ESOMIDAS software is due to Dierckx (1982) and allows the user to control the smoothness of the spline (parameter s), returning for $s = 0$ the cubic spline passing through the data points, and for large s the least-squares cubic polynomial fit. s was adjusted to individual cases (see subsections for individual stars), and sometimes a range in smoothing values was explored (e.g. Sect. 4.2.2), iteratively improving the maximum power present in the residuals. Spline fits are generally not a good option in the case of variability patterns that change drastically over short parts of the time interval used in the fit.

Figure 1 gives basic information on the size of the HIPPARCOS data sets, and on the distribution of the estimated standard errors of the individual magnitudes. Data with quality flag values larger than 1 (see Perryman 1997, volume 3) are disregarded (except in one case, see Sect. 5.2.1). The shape of the histograms illustrates the fact that, for a specific object, there is often a large subset with uncertainty near the first mode value of the distribution, and a tail of less precise data. There is a tendency for the less precise data to fall in the later part of the mission.

For a significant part of the objects, the uncertainties on individual HIPPARCOS data are substantial when compared to the amplitudes of variability. Within each spin-period of the satellite (128 minutes) an object was observed twice, with an interval of about 20 minutes; in view of the relevant time-scales in our work, such data (if both available) may be averaged to obtain a better precision; they will be referred to as *paired observations*. In the study of long-term trends, averages over larger time intervals were considered, as mentioned in the specific subsections. In some cases, the analysis was repeated on a subset of data avoiding those with the largest uncertainties, especially when the ASAS data suggested a low amplitude. In other cases, substantial subsets obtained over a relatively short time interval (mostly of the order of days) were analysed separately to avoid impact of long-term trends in searches for short-time variability. This applied to cases where such combination of time scales was suggested by the ASAS data. When relevant, the applied selections are defined in the specific subsections.

Finally, when embedding the data discussed here in an ASAS set extending to more recent observations, which might become available in the future, the user is encouraged to apply to the extended set the iterative selection procedure explained in paper I.

3 Upper Scorpius

Table 2 lists the variable stars discussed in the following subsections or in paper I.

Table 2: Variable stars in Upper Scorpius. The columns show, successively, the ASAS designation, the HIPPARCOS– and HD numbers, the HIPPARCOS magnitude, the spectral type (taken from the Michigan Catalogue), our variability–type conclusion (see paper I), the period(s) or cycle-length(s), an estimate of the range (peak-to-valley) of brightness variation (in millimag, values for irregular or long-term variation are underlined) and a reference to the detailed discussion of the object. A (?) after a value signifies that the latter is an uncertain or somewhat subjective estimate; (a) after a period means that the true period could not be uniquely determined so that the quoted value may be an alias; (v) indicates a variable magnitude-range, the quoted value being the maximum range over the whole period of observations.

ASAS	HIP	HD	Hpmag	Sp.Type	V.C.	Period(s) (d)	ΔM	Ref.
161625-2459.3	79739	146285	7.984	B8V	**mP**	0.412077, 0.421591	17, 11	paper I
162005-2003.4	80024	147010	7.411	B9p(SiCrSr)	P	3.92076	58	3.1.1
161828-2316.5	79897	146706	7.559	B9V	P	0.422857	18	3.1.2
164018-2353.7	81624	150193	8.936	A2IVe	I		200(?)	3.2.1
161312-2229.1	79476	145718	8.932	A8III/IV	I		600(?)	3.2.2
160713-2706.0	78963	144499	8.620	A9V	**P**	0.157628	24	3.1.3
155321-1923.9	77813	142113	9.417	F8V	**mP**	2.95945(a), 1.45699(a)	21, 17	3.1.4
160118-2652.4	78483	143441	9.525	G0V	**I + qP**	1.1080(a), 8.299(a)	55, < 70(v), < 40(v)	3.3.1
160244-3040.0	78581	143637	9.199	G1V	I + **qP**	1.132–1.137	120, 30 (v)	3.3.2
161023-2917.0	79247	145103	8.028	M3III	**qP**	25.205	80	3.3.3

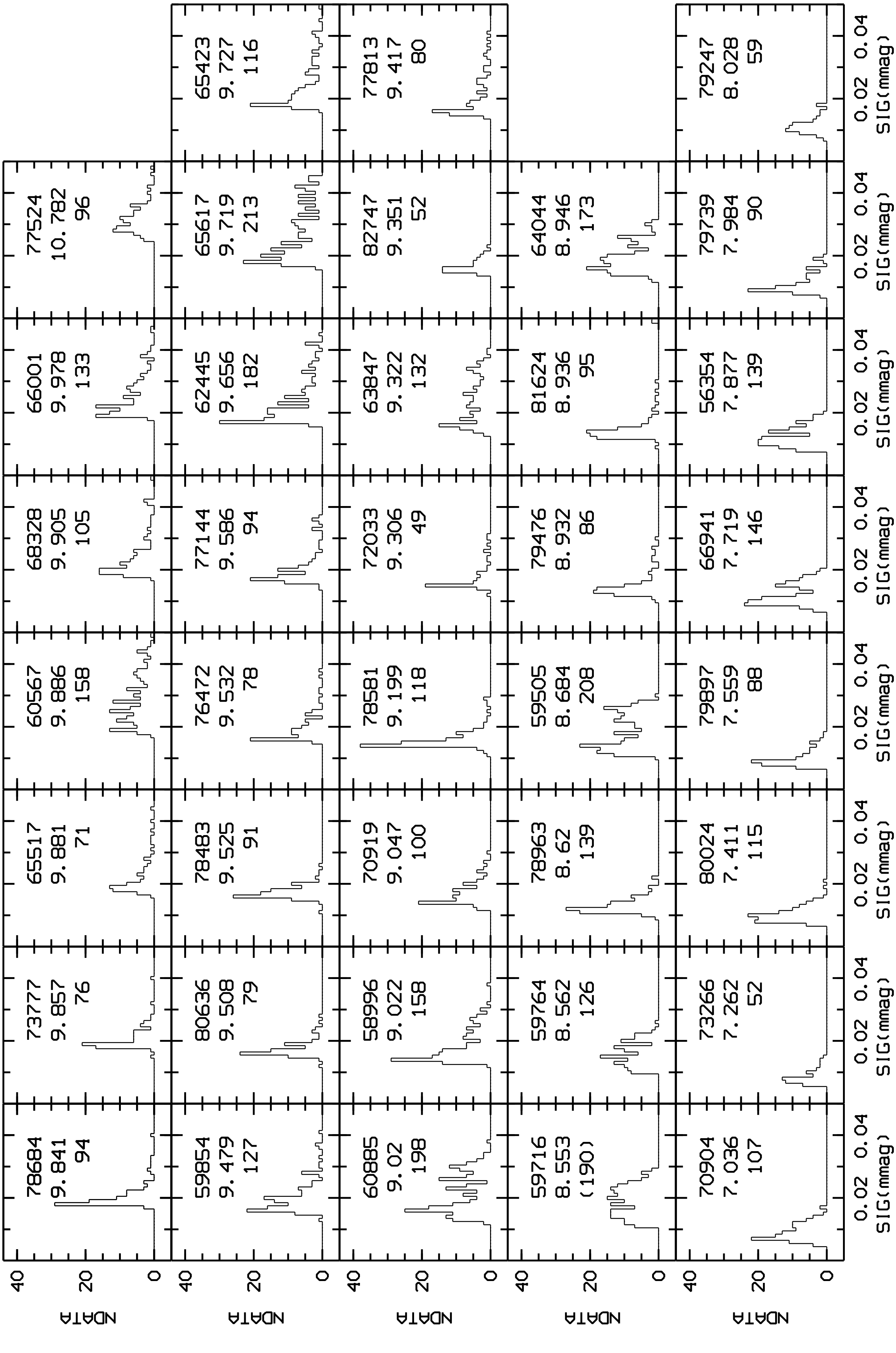

Figure 1: Distribution of standard errors in the HIPPARCOS data.

3.1 (Multi-)periodic variables

3.1.1 HD 147010 = HIP 80024

HD 147010 is a well-known, sharp-lined (21 km/s, Brown & Verschueren 1997) magnetic chemically peculiar B9p star of the type SiCrSr. Notice that the Michigan Spectral Survey classification B9 II-III (Houk & Smith-Moore 1988) is widespread in the literature without the remark about its peculiarity from the same catalogue, and therefore somewhat misleading. Various photometric studies (North 1984; Borra et al. 1985; Lanz & Mathys 1991; Adelman et al. 1992; Catalano & Leone 1993; Perryman 1997) and magnetic field studies (Thompson et al. 1987; Mathys 1991; Mathys & Lanz 1992; Mathys 1994) all agree on a period slightly shorter than 4 days and an amplitude that increases towards shorter wavelengths over the whole visible spectral range. The data span 16.3 years of photometry and 14.7 years in magnetic field data.

The ASAS photometry suffers from the adverse effect of the B-component of this wide visual binary, CCDM 116201-2003, at 47 arcsec. The larger apertures (commonly preferable) yield highly scattered data, but aperture–1 data confirm the known period (Fig. 2, bottom panel). This is the only case in our sample where the standard definition of the selection criteria was not efficient to remove outliers. In this case we used aperture 2 instead of aperture 4 as a reference for the magnitude differences between apertures (see also Table 1). In addition, the 33 data obtained in 2001 (all but one belonging to the smaller of both sets) were disregarded because of excessive scatter.

The uncertainty in the Lanz & Mathys (1991) period of 15×10^{-5} day results in an uncertainty of 0.05 P for the oldest literature data relative to the most recent ASAS data. Unfortunately, the enhanced scatter in the smaller aperture we are forced to use does not allow us to improve the

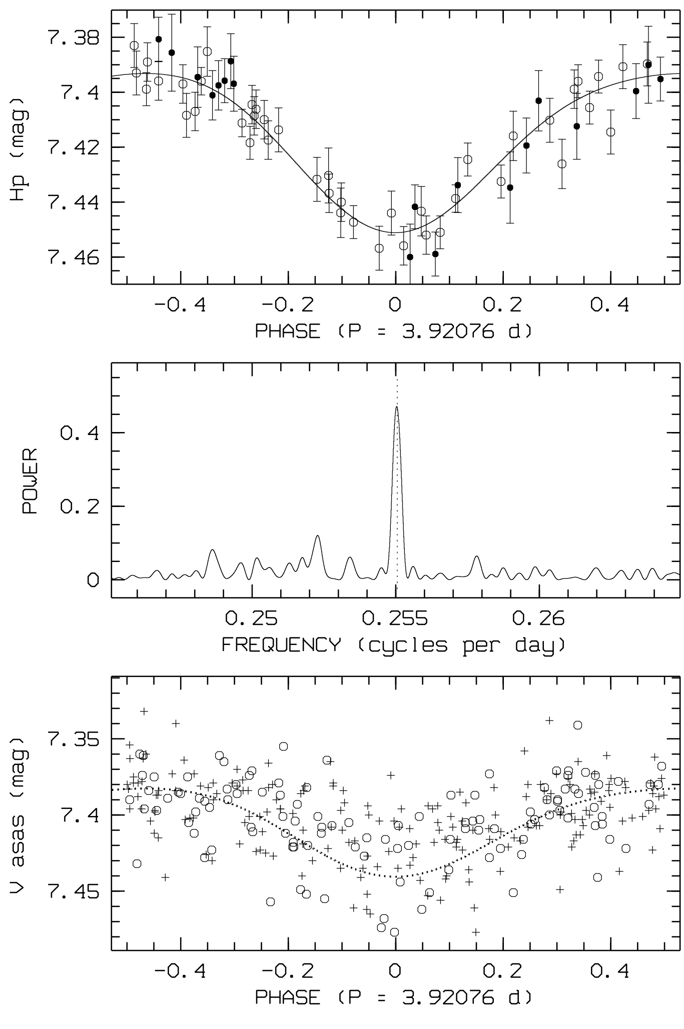

Figure 2: The HIPPARCOS data of HD 147010 (upper panel) and the aperture–1 ASAS V magnitudes (lower panel) phased in the rotation period of $P = 3^{\mathrm{d}}.92076$ (Lanz & Mathys 1991). In the upper panel, open circles represent paired observations and smaller closed symbols represent single observations. The middle panel shows the Scargle statistic for the ASAS data shown in the lower panel, with a vertical dashed line indicating the known rotation period of the star. In the lower panel, '+' symbols refer to aperture–1 data of the larger data set and 'o' to the smaller one, shifted by +0.022 mag (Table 1). One faint and two bright data of the 310 selected measurements fall outside the magnitude range shown in the lower panel, which is 1.8 times that of the upper panel. The fit curve in the upper panel corresponds to Eq. 1. In the lower panel, it is shifted appropriately in magnitude.

precision on the period. The new data merely confirm the known ephemeris. The HIPPARCOS data are well represented by a fit (upper panel in Fig. 2)

$$H_{\rm p} = 7.418 + 0.0288\cos(2\pi(\phi - 0.0071)) + 0.0044\cos(4\pi(\phi + 0.0132)) \qquad (1)$$

with the zero point of the phase at HJD 2 448 346.859 and period $P = 3^{\rm d}.92076$. The peak-to-peak amplitude of 0.058 mag is slightly larger than in Geneva V and smaller than in Geneva B (North 1984).

3.1.2 HD 146706 = HIP 79897

HD 146706 = HIP 79897 is a late–B type, fast rotating (≈230 km/s, Brown & Verschueren (1997)) known light variable. Koen & Eyer (2002) derived a $0^{\rm d}.422863$ period from the HIPPARCOS satellite data.

The much longer time baseline for the ASAS data allows us to refine the period of the light variations to $0^{\rm d}.422857 \pm 0^{\rm d}.000003$. The total range of variation, ≈18 millimag is slightly lower than indicated by the HIPPARCOS data (22 millimag), but whether this is due to the difference in passband or is a chance consequence of the coarser coverage of the light curve by HIPPARCOS remains unclear. Both HIPPARCOS and ASAS data show significant scatter, with rms comparable to the amplitude of the variations.

Two ASAS data sets are available (Table 1). The larger one (296 selected data) covers a 3000+ days time baseline and shows a formally significant trend towards more recent brighter values, with a mean gradient of 4.7 ± 1 millimag per 1 000 days. The smaller set (79 selected data) and the HIPPARCOS data are inconclusive in this respect, being compatible as well with this gradient as

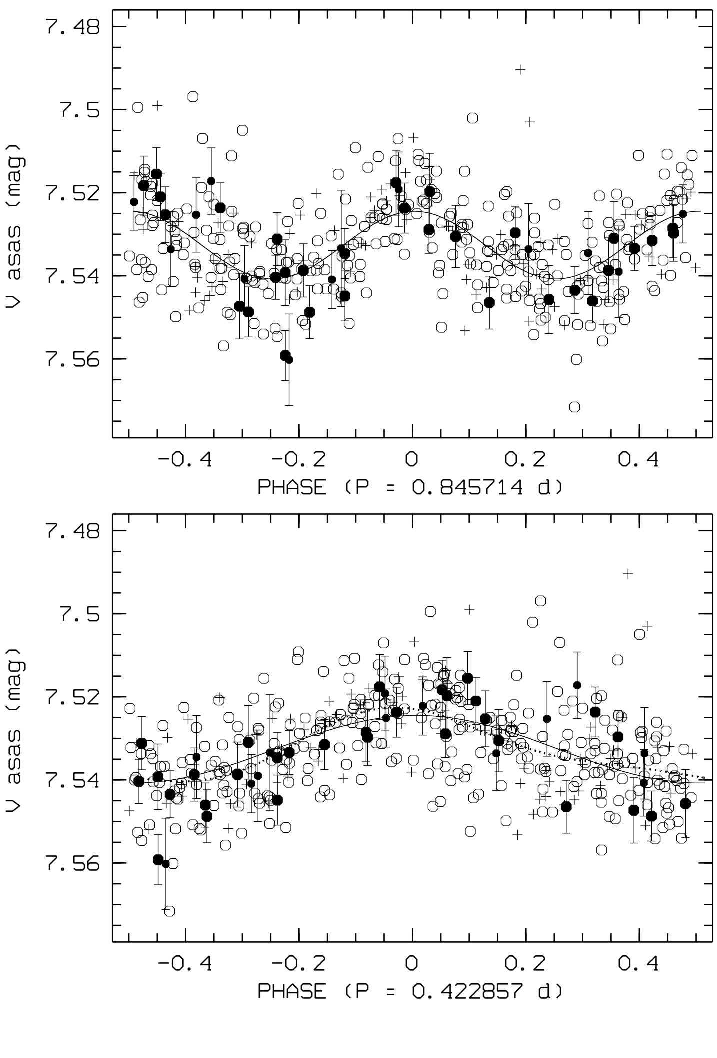

Figure 3: The light variations of HD 146706 folded on the derived light period and twice that period. Open circles: larger ASAS data set, plusses: smaller ASAS data set shifted in magnitude by +0.010 mag. Filled discs: HIPPARCOS data shifted by −0.025 mag (with error bars), larger symbols refer to paired observations. The fit curves shown are specified in the array of equations Eq. 2, with the dotted line representing the second equation. Four aperture–4 ASAS observations fainter than $V = 7.6$ are not visible in the figure.

with an absence of trend. It remains unclear to us whether this trend has an instrumental origin or represents a real brightening of the object. It was checked explicitly that a removal of the trend has no impact on the analysis, beyond slightly reducing the residuals in the phase-folded light curve. In Fig. 3 the trend was removed from all ASAS data, but not from the HIPPARCOS data, which refer to an earlier epoch. The curves in the figure correspond to three possible models which represent the data with similar success:

$$
\begin{aligned}
V_{\mathrm{ASAS}} &= 7.5326 - 0.0081\cos(2\pi(\phi - 0.0074)) \\
V_{\mathrm{ASAS}} &= 7.5327 - 0.0081\cos(2\pi(\phi - 0.0038)) - 0.0023\cos(4\pi(\phi + 0.0611)) \\
V_{\mathrm{ASAS}} &= 7.5326 - 0.0081\cos(4\pi(\phi_{\mathrm{d}} - 0.0027)) \qquad (2)
\end{aligned}
$$

The first two equations refer to the lower panel, the first and the third equation are shown in the figure with a full line, the second with a dotted line. Phases $\phi = 0$ (lower panel) and $\phi_{\mathrm{d}} = 0$ (upper panel) correspond to HJD 2 454 212.68.

With regard to the origin of the (quasi-)sinusoidal light variations, two hypotheses remain acceptable, given the spectral type of the star: either one sees a small ellipsoidality-effect in a close binary with an orbital period of twice the light period i.e. $0.^{\mathrm{d}}845714$ (see upper panel in Fig. 3), or the star is a slowly-pulsating B star (SPB). In the latter hypothesis, with its period very similar to the ones found in HD 146285, it would be the second late-B star in Upper Scorpius that is situated at the short-period edge of this class of stars. Its spectral type B9V, first established by Garrison (1967), raises the suspicion that this star may be out of the theoretical instability strip for SPB stars, but more precise fundamental stellar parameters should be derived before we can completely reject the SPB hypothesis. Spectroscopic observations will easily remove the SPB/ELL ambiguity, as the first moment of the spectral lines (relative to a fixed reference wavelength) should vary much less in the case of a slowly-pulsating star than in the case of Doppler shifts due to a binary with an orbital period shorter than one day.

3.1.3 HD 144499 = HIP 78963

This A9V star is a visual binary with separation of 9 arcsec. It is found to be a δ Scuti type variable with a total range of light variation of 24.2 ± 1.0 millimag in $0.^{\mathrm{d}}157628 \pm 0.000001$. The precision is obtained combining the ASAS data with the HIPPARCOS data. Maximum brightness occurs at HJD 2 452 755.9053. Fig. 4 shows the lightcurves.

In view of the amplitude, it might be expected that Koen & Eyer (2002) would have detected the variability in the HIPPARCOS data set. However, their procedure may have rejected it because, while the frequency corresponds to the highest peak in a power spectrum for the HIPPARCOS data, there is very strong aliasing due to the particular distribution of the data: 63 of the 110 observations are concentrated in $3.^{\mathrm{d}}66$ (and lead to a power spectrum with clear indication of the true period), 14 more are concentrated in two nearby epochs within less than 100 days of the former. Analysis with subgroups of the data (with and without the dense series of 63 observations) show excess power in a broad peak extending from $f \approx 4$ to $f \approx 7$ cycles per day masking the true frequency for the subset without the 63 observations.

A search for a second frequency was made with pre-whitened data. The 396 selected ASAS data suggest a 10.6 millimag peak-to-peak amplitude in $0.^{\mathrm{d}}1194296$, but neither the more precise old–catalogue[1] data (103 selected entries), nor the HIPPARCOS data confirm this. Thus, multi-periodicity is not well-established.

[1]At the time our investigation was begun, the ASAS data obtained before 2004 were still available in two versions. The old catalogue had a better precision for the early data, as shown in paper I, and might reveal lower–amplitude variability.

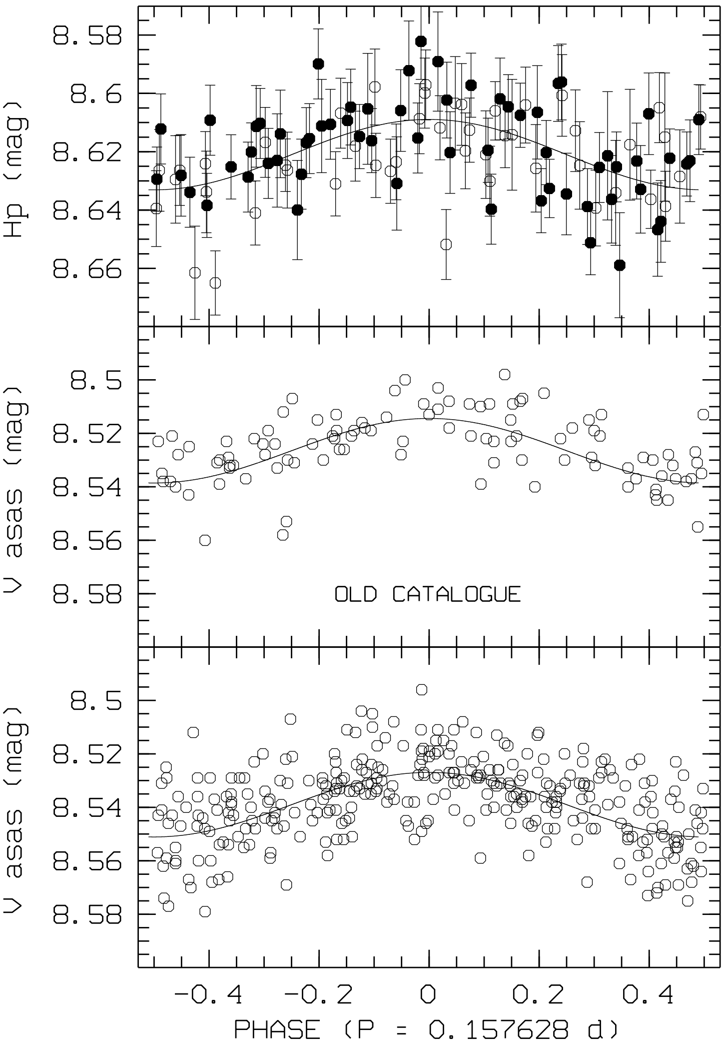

Figure 4: The light variations of HD 144499 folded on the $0^{\rm d}\!.157628$ period. From top to bottom, HIPPARCOS data, old–catalogue aperture–3 and standard aperture–4 ASAS data are shown, with a cosine model (peak-to-peak amplitude of 24 millimag and maximum light (phase 0.0) at HJD 2 452 755.905), as derived from the data in the lower panel. The same curve is overplotted in the mid- and upper panel with an offset of 0.0125 and 0.082 mag, respectively. Filled disks in the upper panel refer to the 63 observations obtained within $3^{\rm d}\!.66$, see Sect. 3.1.3, second paragraph. One anomalously faint data point falls outside the scale shown in the lower panel.

3.1.4 HD 142113 = HIP 77813

HD 142113 is clearly a short-periodic variable, but the distribution of the data does not permit to choose uniquely between aliased frequencies (Fig. 5). Both $f_1 = 0.337901 \pm 0.000024$ and $f_1' = 0.664817 \pm 0.000024$ represent the data well, with a total range of variation of 25 millimag and minimum light at HJD 2 453 501.497 or 2 453 501.838 respectively. After removal of either of these frequencies, the aliased peaks in the upper panel of Fig. 5 disappear. The power of the peak at $f_2 = 0.68649 \pm 0.00003$ remains almost intact, and the peak near $f_2 + 1$ strengthens, with somewhat weaker aliases near $1 - f_2$ and $f_2 + 2$. The lower panels of Fig. 5 show the phase diagrams for periods of $2^{\rm d}\!.95945$ and $1^{\rm d}\!.45699$ days after removal of the alternative frequency f_2 or f_1, respectively. Almost equally good are solutions with two periods near 3 days (f_1 and $1 - f_2$), or two periods near 1.5 days (f_1' and f_2). The HIPPARCOS data turn out to be too uncertain to allow any refinement or choice for the periodicities detected in the ASAS data set.

3.2 Early–type irregular variables

3.2.1 HD 150193 = HIP 81624

HD 150193 is a well-known Herbig star (V2307 Oph) with spectral type A2IVe (Mora et al. 2001). It is the brighter component of a visual binary detected by Zinnecker et al. (1990), with a F9Ve weak-lined T Tauri star (Carmona et al. 2007) of $V = 12.3$ mag at 1.16 arcsec as companion. The circumprimary disk was resolved by Fukagawa et al. (2003). Several sources mention light

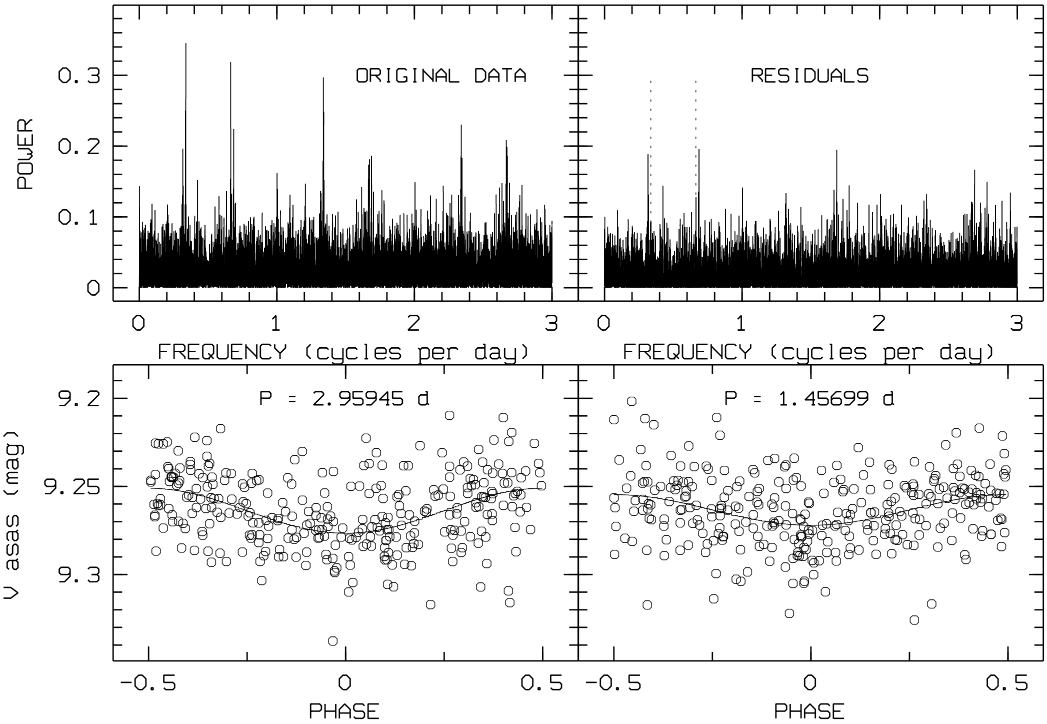

Figure 5: Scargle power for aperture–4 photometry of HD 142113 for the original data (upper left panel) and after prewhitening for $f_1 = 0.3379$ (upper right). In the latter panel, vertical dashed lines indicate f_1 and f_1' (see text). The lower panels show the phase diagrams for the two detected frequencies after removal of the sinusoidal fit to the other. Three anomalously faint data out of 312 fall outside the scale of the figure.

variability, with the largest series and highest amplitude ($8.56 < V < 8.78$) due to the extensive Maidanak Observatory series mentioned by Shevchenko et al. (1993) who find some evidence for a 0.04 mag cyclic component ($4^{\rm d}\!.92$).

While the HIPPARCOS data show no evidence of variability exceeding few hundredths of a magnitude, the ASAS data fully confirm the 0.2 mag peak-to-peak variability range claimed by Shevchenko et al. (1993), but just due to one obscuration event in 2009 (Fig. 6). Except for this short episode, the most obvious fadings, centered around HJD 2 452 650 and 2 454 150 and extending over almost one year, are restricted to ≈0.06 mag. We find no support for the cyclic $4^{\rm d}\!.92$ component mentioned by Shevchenko et al. (1993), even after removal of the data in the time intervals of the major fadings. However, this does not invalidate the result of Shevchenko et al. (1993), as the characteristics of the light curves in these young stars may change drastically with time due to the dynamical interaction of the star with the disk (Alencar et al. 2010).

3.2.2 HD 145718 = HIP 79476

HD 145718 is a known Herbig Ae star (V718 Sco) that was suggested to be an eclipsing binary with a period of the order of 2 days (Hoffmeister 1930), but this was never confirmed. Its spectral type is A8 III/IV. Guimarães et al. (2006) estimate $T_{\rm eff} = 7500$ K, $\log g = 3.4$ and $v \sin i = 115$ km/s and identify the presence of accreting hydrogen-rich material from high-resolution spectroscopy. They claim that the star presents a magnitude variation on the level of 1% in V, but this is based on only few single-epoch measurements from three sources given in their paper. In fact, both HIPPARCOS and ASAS show a complex variability pattern with a range of 0.1 up to 0.6 mag over any year or almost any 100–day interval (Fig. 7).

On the other hand, there is no periodicity and the early suggestion of a short-period eclipsing binary, can be firmly discarded.

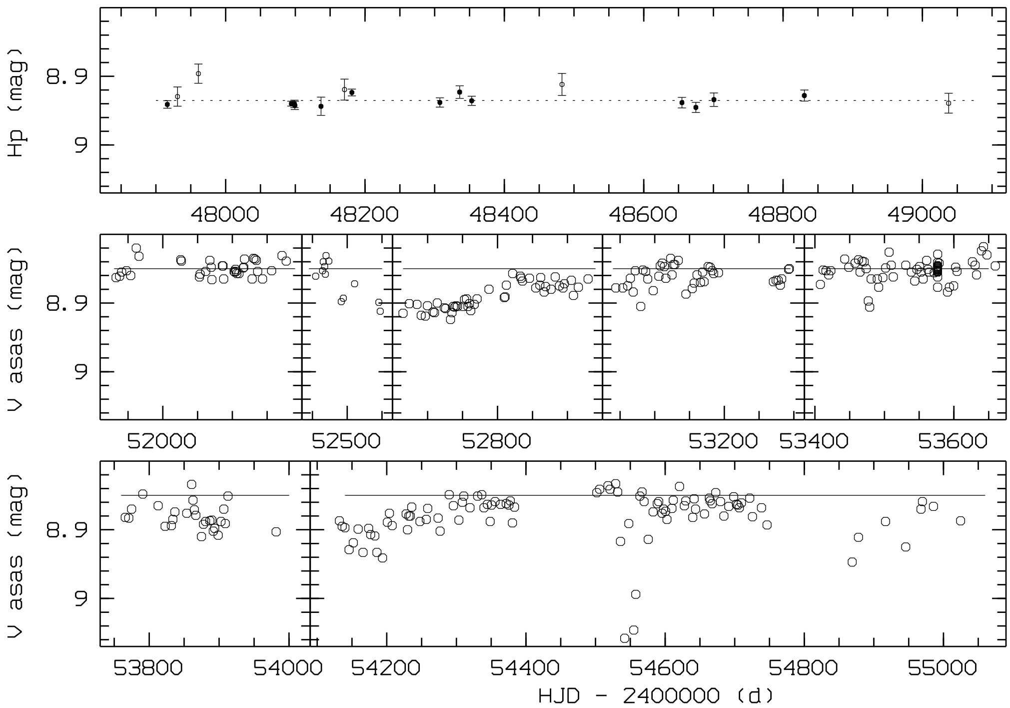

Figure 6: The light variations of HD 150193. Mid- and lower row panels show selected aperture–3 data of ASAS. HIPPARCOS data averaged within one day (filled discs indicating at least 4 contributing measurements) are given in the upper panel. Error bars are computed from the scatter in the hipparcos data contributing to each data point, rather than from the uncertainties on individual data points listed in the HIPPARCOS catalogue.

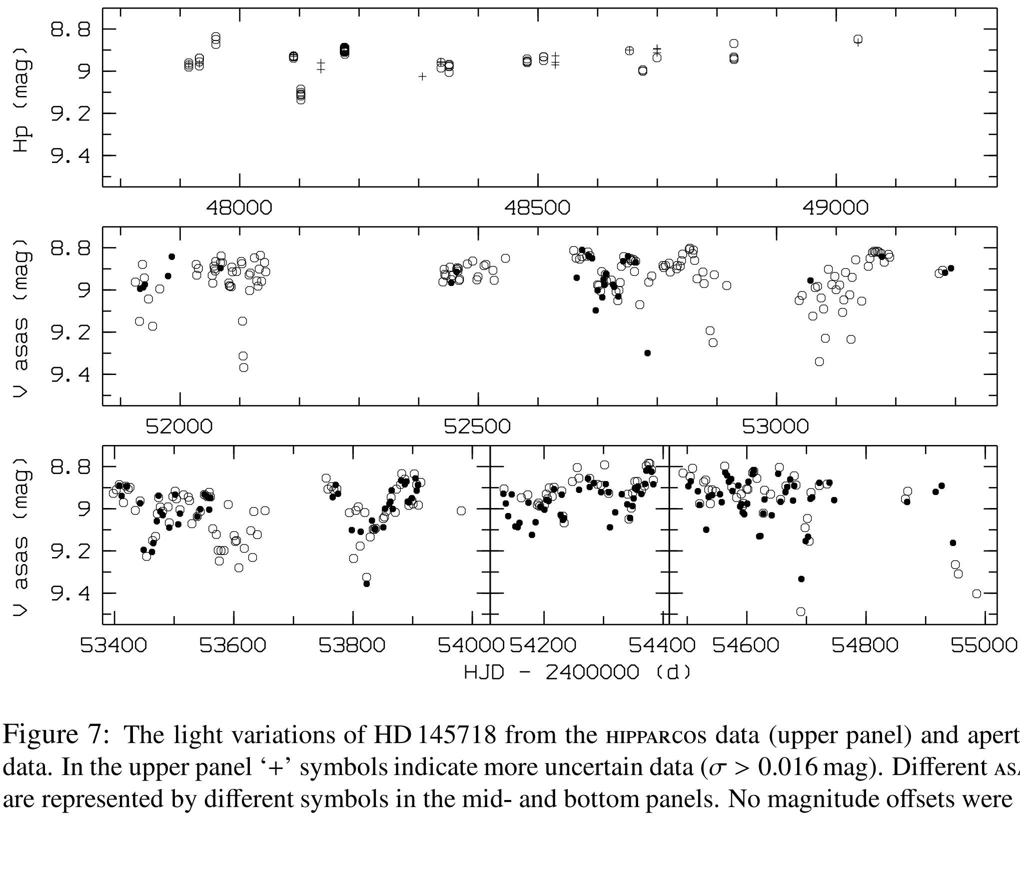

Figure 7: The light variations of HD 145718 from the HIPPARCOS data (upper panel) and aperture–3 ASAS data. In the upper panel '+' symbols indicate more uncertain data (σ > 0.016 mag). Different ASAS data sets are represented by different symbols in the mid- and bottom panels. No magnitude offsets were applied.

3.3 Late-type stars

3.3.1 HD 143441 = HIP 78483

HD 143441 is a wide T Tauri-type binary (Köhler et al. 2000; Kraus & Hillenbrand 2007) exhibiting long-term photometric variability below the 0.1 mag level over timescales of (tens of) years; Fig. 8 shows that the long-term trend is ill-defined over the HIPPARCOS mission and is not easily separable from the short-term variability. A slow brightening similar to the one observed in the early ASAS data should not be excluded.

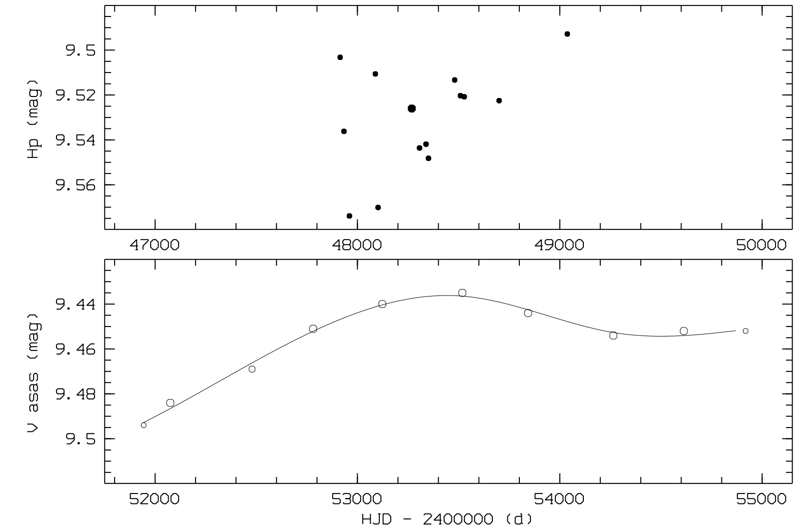

Figure 8: HD 143441: aperture–3 yearly averages of ASAS data (lower panel), and the applied detrending. The subsets cover resp. HJD 2 451 924–965 (9 data), HJD 2 452 026–130 (33 data), HJD 2 452 440–545 (20 data), HJD 2 452 659–916 (54 data), HJD 2 453 037–278 (38 data), HJD 2 453 397–652 (49 data), HJD 2 453 754–981 (35 data), HJD 2 454 128–383 (47 data), HJD 2 454 492–730 (49 data), HJD 2 454 865–985 (6 data). The curve is a smoothed (s = 0.005) spline fitting the yearly averages. The upper panel shows the 14 HIPPARCOS epochs, with the larger symbol indicating the dense set of observations during 2.3 days.

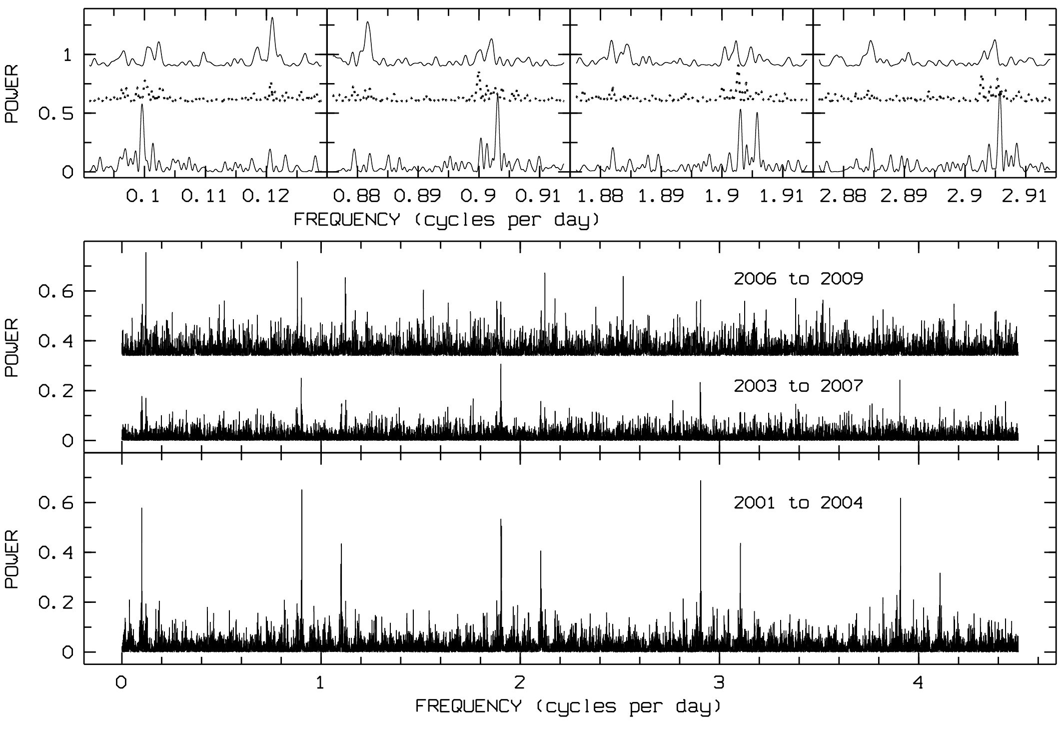

Figure 9: Scargle power for subsets of ASAS data for HD 143441, covering different time intervals as indicated in the panels. The upper panel zooms in on the stronger power peaks, with the 2001–2004 set (154 data points, HJD 2 451 924–3 278) at the bottom, the 2003–2007 set (223 data points, HJD 2 452 659–4 383) in the middle (dashed line) and the 2006–2009 set (138 data points, HJD 2 453 754–4 985) at the top.

The detrended ASAS data show power at higher frequencies. The Scargle power diagram (Fig. 9) suffers from strong aliases due to the ASAS observing cadence, and the HIPPARCOS data are not very helpful, because of the sparsity of epochs (14), the uneven distribution of the data (one epoch spreading over $2\overset{\mathrm{d}}{.}3$ contains 40% of all data) and the ill-defined long-term trend.

A closer look at the data excludes strictly periodic variability. Fig. 9 shows the situation for several subsets, with details around the most prominent power peaks displayed in the upper panel. The relative importance of the peaks varies from one set to the next, and the nominally strongest peak shifts from ≈2.9 cycles per day (early set) to ≈1.9 cycles per day (mid-time set) and ≈0.12 cycles per day (late set). The highest peaks in the early set are mostly due to the 2001–2002 data, and in the most recent set to the 2008 data. Observations with a cadence higher than the ASAS observations are needed to solve ambiguity due to aliased frequencies. At present we can only state that the data from the HIPPARCOS epoch around HJD 2 448 268.5, which covers $2\overset{\mathrm{d}}{.}3$, leave little support for high frequencies and indicate that, at least during that epoch, one of the true frequencies was near 0.9 cycles per day (Fig. 10, top panel).

Therefore our best guess is that there are two cycles with $f_1 \approx 0.9025$ and $f_2 \approx 0.1205$ cycles per day (Fig. 10). Their combined peak-to-peak variation varies from 0.07 in 2001 to 0.04 mag 2008, dominated by f_1 and f_2 respectively; it is lower in intermediate years, falling below the detection level in 2005. A search for additional frequencies was inconclusive, because of the many options generated by aliases and, more importantly, because of a lack of strict periodicity (phase shifts between data of different years; yearly subsets suggest changes of up to 0.0015 cycles per day between them). Whether both f_1 and f_2 are related to only one of the components of the binary is another open question.

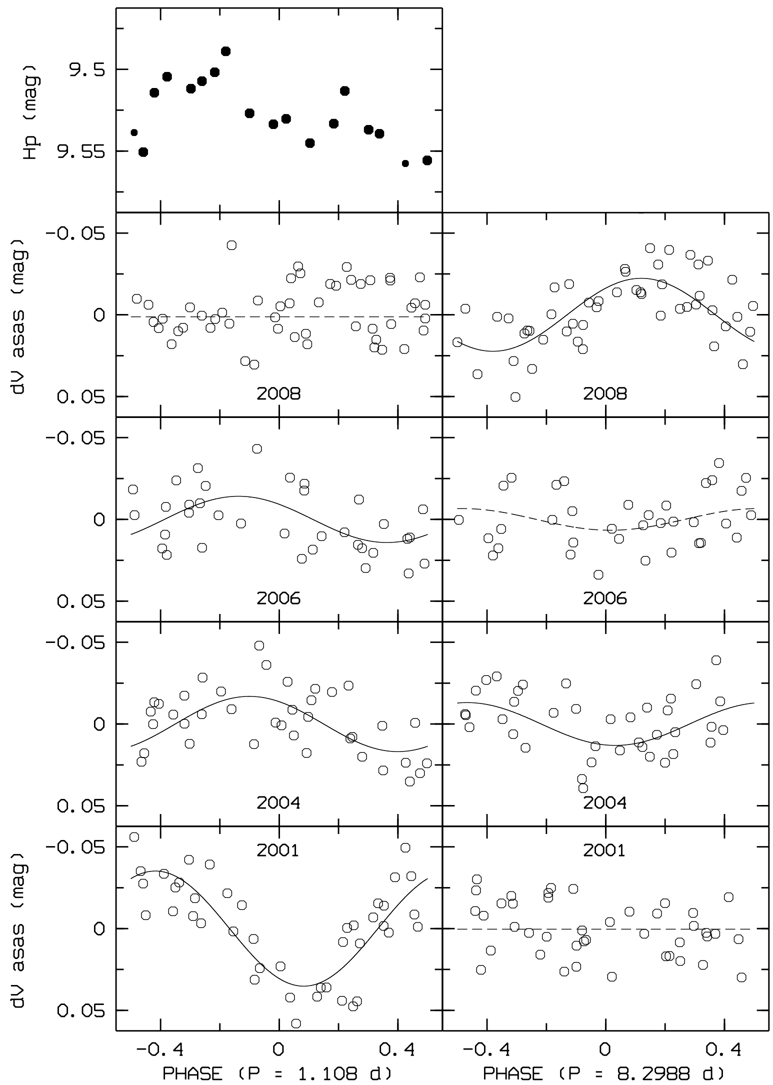

Figure 10: ASAS aperture–3 photometry of HD 143441 for selected, representative years, plotted in phase diagrams for the two suggested cycles. The long-term trend was removed, and also the variation in the alternative cycle, as determined by a sinusoidal fit simultaneously to the two frequencies. These sine fits are overplotted with full line, or with a dashed line in the case of low significance for either of the sine fits. A horizontal dashed line identicates non-detection of the second frequency. Phase zero is at HJD 2 453 436.85. Peak-to-peak amplitudes and phase of maximum light are, in the left-hand side panels: (0.0704, −0.417) for 2001, (0.0338, −0.100) for 2004, (0.0283, −0.137) for 2006; in the right-hand side panels: (0.0262, −0.467) for 2004, (0.0132, −0.484) for 2006, (0.0446, 0.120) for 2008. The upper panel shows the HIPPARCOS photometry during the 2.3 days around HJD 2 448 268.5, without any correction for long-term trends or for the eight-day cycle.

3.3.2 HD 143637 = HIP 78581

HD 143637 is suspected to be a long-period astrometric binary (Makarov & Kaplan 2005). There is no evidence of infrared excess at 24 or 70 μm (Chen et al. 2011). This star was classified recently as a variable star by Shaya & Olling (2011) but no details were given. In our study we find that it exhibits irregular brightness variations over years, with yearly averages varying over 0.1 mag (Fig. 11). Occasionally changes of 0.05 mag over time intervals as short as 100 days appear (JD 2 452 430– 2 452 550 in 2002; JD 2 453 760– 2 453 910 in 2006), interrupted by much longer time intervals wherein no light changes exceeding a few hundredths of a magnitude were observed (JD 2 452 650 to 2 453 500, and JD 2 454 350 to 2 455 050). Also at the HIPPARCOS epoch the star appears to have been relatively quiet, although it was probably somewhat fainter in the first year it was observed.

In addition, a cycle with frequency $f \approx 0.88$ cycles per day is detected in the 'quiet' time intervals covered by the HIPPARCOS data and by the ASAS data from JD 2 452 650 to 2 453 500, the latter extending from 2003 to early–2005 (Fig. 12). But the cycle was not detected in the second 'quiet' ASAS time interval JD 2 454 350 to 2 455 050 starting late–2007.

The HIPPARCOS set has some subsets with many observations over a few days, permitting to discern the frequency f_{ASAS} from aliases, but the frequent time gaps larger than one month hamper a unique separation of the cyclic variations from the slower variability. The upper panel of Fig. 12 shows the data obtained in January 1991 within three days as filled symbols. Obviously, they define a much neater pattern than obtainable from HIPPARCOS data scattered over larger time intervals. The early HIPPARCOS data (HJD < 2 448 135) are represented by '+' symbols in Fig. 12, and the remaining data out of the above mentioned three-day interval as 'o'. The early data were shifted by 0.02 mag upwards.

Since the detected frequency in the HIPPARCOS and the ASAS data is slightly (3.5%) different, $f_{\mathrm{hip}} = 0.8796$ cycles per day and $f_{\mathrm{ASAS}} = 0.88327$ cycles per day, respectively, we checked in some detail different ASAS subsets.

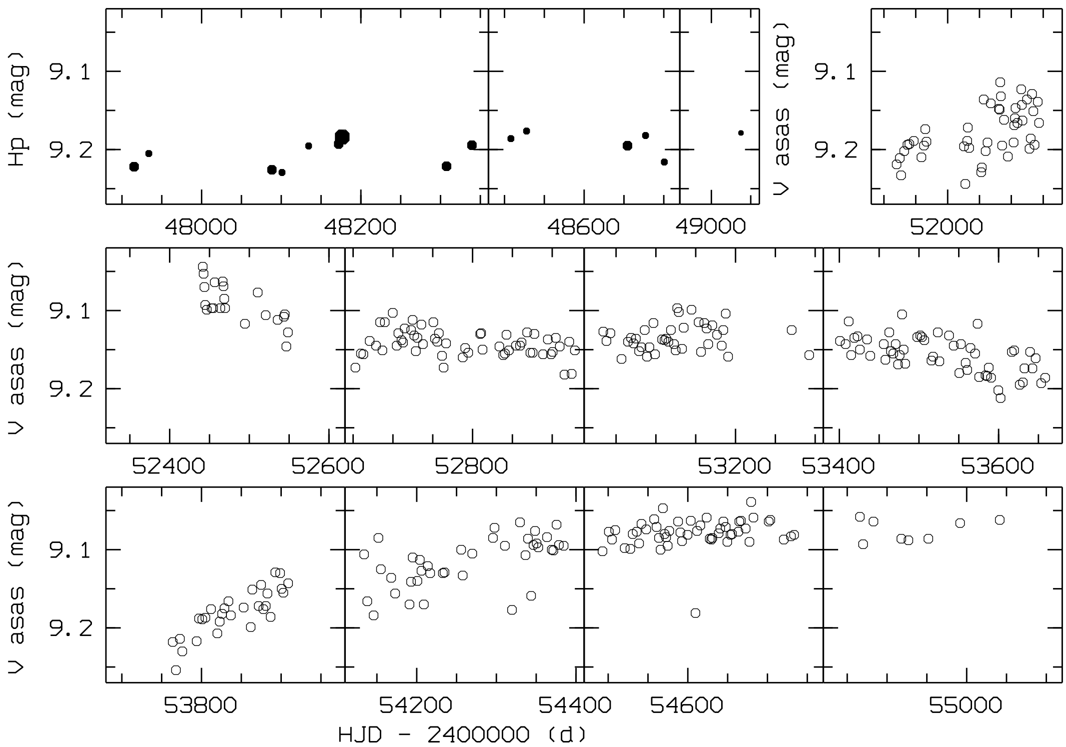

Figure 11: Long-term variability of HD 143637. HIPPARCOS magnitudes are averages over data obtained within few days, with the size of the symbols indicating the number of contributing observations (1–3, 4–10, 16 and 44, respectively).

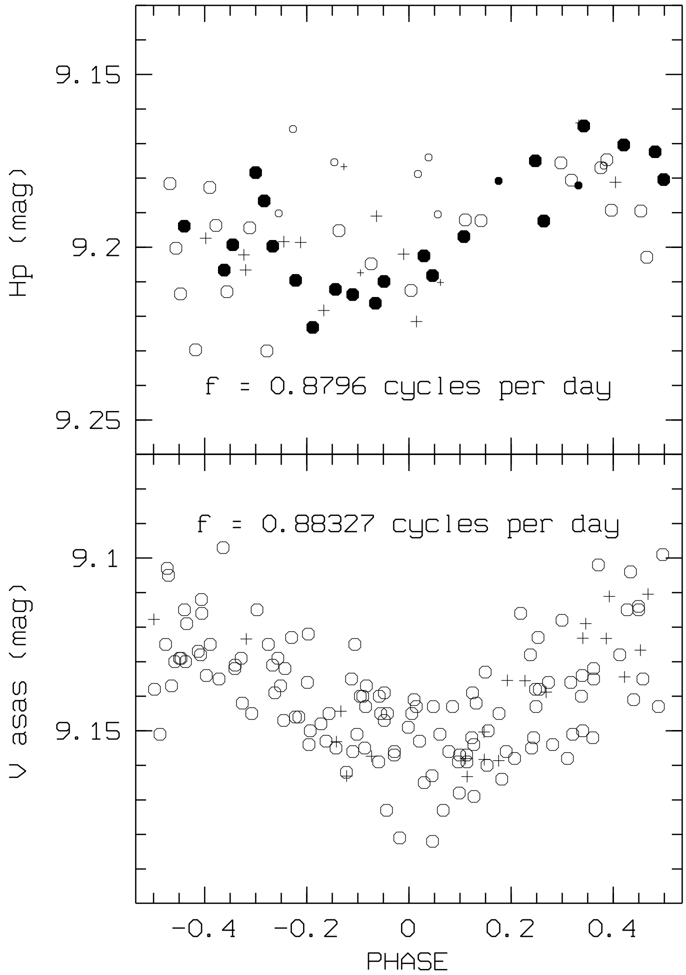

Figure 12: Evidence of cycles superposed on the long-term variability of HD 143637. Larger symbols in the upper panel refer to paired HIPPARCOS observations. See the detailed comments on this star in the text for the meaning of the symbols and the data selection.

Applying the best-fit sine model obtained from the 'quiet' 2003–early-2005 time interval to ASAS yearly subsets reduces the scatter in all those before 2008. This suggests that the cycle might be present over a much longer time baseline, albeit hidden by more prominent long-term trends. Hence, we investigated whether removing linear long-term trends in yearly subsets outside of the 'quiet' time intervals mentioned above would produce data showing a clear signature of the short cycle. The answer is positive for data observed before 2003, but negative for data observed after early–2005. It appears that the cycle weakened and then disappeared after 2005. In the lower panel of Fig. 12 the data obtained in the 'quiet 2003–early-2005 time interval are shown as open circles in the phase diagram. The long-term corrected data from 2002 (leftmost mid-row panel of Fig. 11) are shown in the phase diagram as '+' symbols.

The nature of the variations suggests that HD 143637 might be a BY Draconis type variable. In particular, the change in the cycle-length we observed from the HIPPARCOS to the ASAS epoch, is similar to the one found by Harmon et al. (2011) for LO Peg (HIP 106231) and ascribed tentatively to the migration of starspots over the surface, in combination with differential rotation. Using $v \sin i$ = 27 km/s (Chen et al. 2011) leads to $R \sin i$ = 0.6, suggesting that i is relatively small.

3.3.3 HD 145103 = HIP 79247

HD 145103 is a M-type giant and known HIPPARCOS variable, V1049 Sco, classified as a slow irregular variable of late spectral type (Kazarovets et al. 1999). The ASAS data reveal a cyclic character with a cycle length of $25\overset{\mathrm{d}}{.}19 \pm 0\overset{\mathrm{d}}{.}04$ and a peak-to-peak range of 0.08 mag (Fig. 13). The observing cadence of ASAS produces strong aliases near one day, but such solutions can be discarded based on the HIPPARCOS data. The bulk of the HIPPARCOS data also follow this cyclic character, although the data obtained at four epochs in the last year of the satellite (HJD 2 448 654–2 449 037) deviate

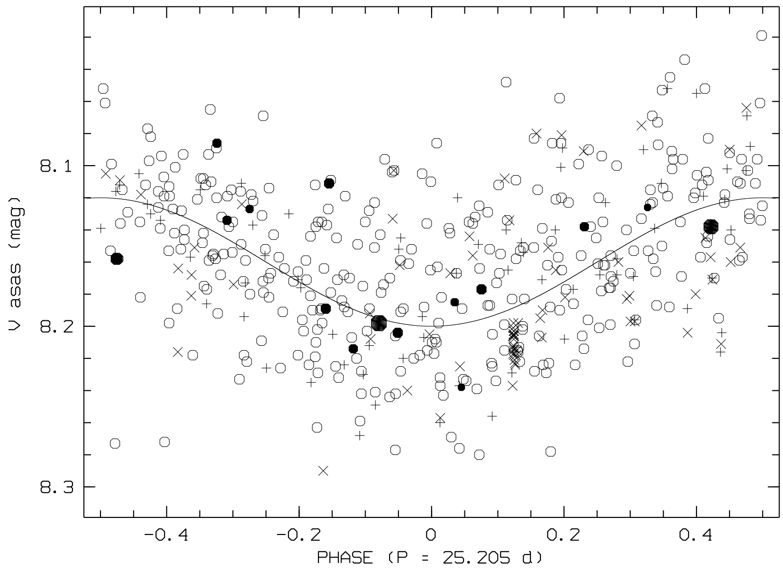

Figure 13: Phase diagram for HD 145103 using $P = 25^{\rm d}\!.205$. Symbols (o,+, x) correspond to aperture–2 data in three ASAS data sets (Table 1); filled symbols represent HIPPARCOS magnitudes averaged over less than $0^{\rm d}\!.63$ with the size of the symbol indicating the number (1–10) of contributing measurements. ASAS data represented by '+' were shifted by −0.005 mag, those represented by 'x' by −0.010 mag. Six faint ASAS data out of a total of 471 fall outside the magnitude range shown in the figure. The curve is a sine fit with 0.08 mag peak-to-peak amplitude and minimum light at JD 2 453 497.75.

somewhat from the general trend. Considering the combination of the HIPPARCOS and the ASAS data, the ephemeris is

$$\mathrm{HJD(min.light)} = 2\,453\,497.75 + (25^{\rm d}\!.205 \pm 0^{\rm d}\!.01)E \qquad (3)$$

The scatter in the pre-whitened ASAS data is still 0.04 mag, and the scatter in the HIPPARCOS data obtained in short time intervals is about a factor 2 higher than the expected 0.01–0.013 mag at 4 of 11 epochs with three or more measurements. This suggests that there is low-level (irregular?) light variability on shorter time scales.

4 Upper Centaurus–Lupus

Table 3 lists the UCL objects discussed in the following subsections.

Table 3: Variable stars in Upper Centaurus–Lupus; see Table 2 for a detailed explanation of the notations.

ASAS	HIP	HD	Hpmag	Sp.Type	V.C.	Period(s) (d)	ΔM	Ref.
145824-3721.7	73266	132094	7.262	B9V	?			4.1.4
142958-5607.9	70904	126859	7.036	A6V	P	0.05285375	13	4.1.1
165445-3653.3	82747	152404	9.351	F5V	I		>1000(?)	4.3.1
144404-4059.4	72033	129490	9.306	F7IV/V	**I? + P**	4600(?), 0.50214	62, 25	4.1.2
135914-5152.6	68328		9.905	G0	**I**		160(?)	4.3.2
154502-4050.5	77144	140421	9.586	G0/2 V	**I + qP**	1.05106	68, 42	4.2.1
153705-4009.4	76472	138995	9.532	G5V	**I + qP**	0.864	150, 98 (v)	4.2.2
162752-3547.0	80636	148187	9.508	G6V	qP + **I**	1.265–1.282	< 64, 46(?)	4.2.3
143010-4332.8	70919	126996	9.047	G8III	**qP + I**	53.87	160 (v), 150	4.2.4
160345-4355.8	78684	143677	9.841	G8V	**qP**	1.25423(a)	29	4.2.5
154945-3925.1	77524	141277	10.782	K0 (V)	**P + I**	2.2341	49, 40	4.1.3
150449-3949.4	73777	133259	9.857	K(1)V + G	**I**		90	4.3.3

4.1 Variables including a periodic component

4.1.1 HD 126859 = HIP 70904

HD 126859 is a known low-amplitude δ Sct star. Vander Linden & Sterken (1986) derived the main frequency (f_1 = 18.92186 cycles per day or any of the closest four 0.5 cycles per year aliases at each side) and identified tentatively a second frequency f_2 = 16.7520 from Strömgren photometry obtained in 1982 and 1984. Royer et al. (2002) list $v \sin i$ = 162 ± 7 km/s.

The ASAS photometry confirms the main frequency as the closest lower-frequency alias of the choice made by Vander Linden & Sterken (1986) (Fig. 14). A sinusoidal variation with a peak-to-peak amplitude of 13 millimag, consistent with the 15 millimag found from the Strömgren photometry, and a frequency of f'_1 = 18.920165 ± 0.00004 cycles per day represents the ASAS data. Analysing the data prewhitened for f'_1 does not reveal the frequency f_2 suggested by Vander Linden & Sterken. This does not invalidate their claim, as their photometry has uncertainties of ≈4 millimag to be compared with ≈10 millimag for the ASAS set, and their estimate for the total range of variability associated with f_2 is 4 millimag.

Neither we nor Koen & Eyer (2002) found this variability independently in the HIPPARCOS data set. However, limiting the set to the more precise observations, one of several Scargle power peaks of similar height is situated at the main frequency (Fig. 14). Thus, while the HIPPARCOS data are too sparse/uncertain to detect f'_1 uniquely, they are not incompatible with f'_1.

We conclude that the main frequency is well-determined and present with a stable amplitude from 1982 to 2010. The uncertainty on f'_1 as derived from the ASAS data corresponds to phase shifts slightly above ±0.2 at the HIPPARCOS epoch and slightly above ±0.3 for the observations in 1982. Phasing together all the data strongly favours frequencies near the lower ASAS limit for f'_1. Our final estimate, used in the phase diagrams shown in Fig. 14, is f'_1 = 18.920135 ± 0.000015 cycles per day, or $P = 0^{\rm d}.05285375 \pm 0.00000008$.

Four high-resolution spectra taken in a time interval of twenty days (2 452 802.4257, 804.3657, 806.4482, 822.8999) do not show radial velocity variations exceeding ±1 km/s nor obvious line profile variations.

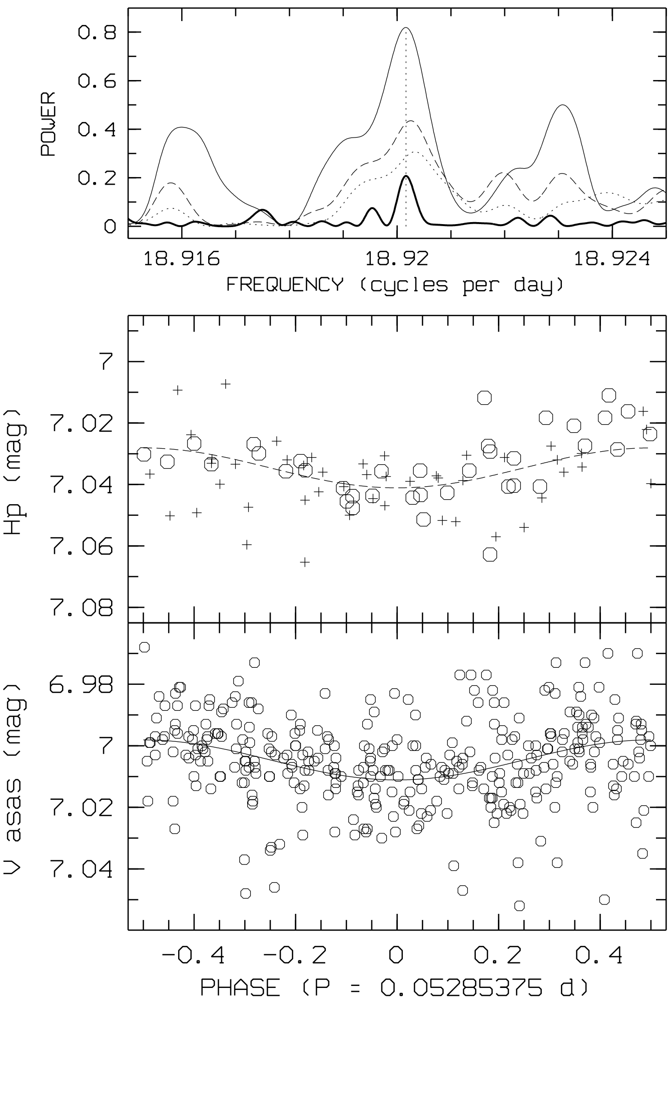

Figure 14: Light variability of HD 126859. The ASAS aperture–3 photometry is shown with a sine fit with peak-to-peak amplitude of 0.013 mag superposed (lower panel). Seven faint data points and one bright (out of a total of 341) fall outside the scale of the figure. The middle panel shows the HIPPARCOS data with different symbols for uncertainties of 5 to 7 millimag ('o') and 8 to 11 millimag ('+'). The dashed line is the ASAS sine fit shifted to 0.03 mag fainter magnitudes. Phases are computed for the period $0^{\rm d}.05285375$ and phase 0.0 (minimum brightness) at HJD 2 453 765.8044. The upper panel shows the Scargle power for the ASAS data (thick line), and three sets of HIPPARCOS data: all 107 data points (dotted line), the 84 with uncertainties of 0.011 mag and less (dashed line) and the 37 data points with uncertainties of 0.007 mag and less (thin line).

4.1.2 HD 129490 = HIP 72033

Christiansen et al. (2008) identified HD 129490 tentatively as an eclipsing binary of the W UMa type, with a period of $0\overset{d}{.}50383$ and an amplitude of 0.017 mag in the I filter based on a large number of observations obtained around April 2006 with a cadence of 15 images per hour. The ASAS photometry reveals that this star is in the first place a long-term variable, possibly with a period of 12.6 ± 0.7 year (bottom panels of Fig. 15), e.g.

$$V_{\rm ASAS} = 9.203 + 0.031 \sin(2\pi \frac{\rm HJD - 2454234}{4600}) \quad (4)$$

The time interval over which the ASAS project obtained data is about two thirds of the period, hence the periodicity is tentative. Interestingly, during the HIPPARCOS mission the star did not show a trend above the 0.01 mag level. Extrapolation of the ASAS ephemeris suggests that the star was at maximum brightness around HJD 2 448 484, i.e. near the middle of the satellite mission. This would be consistent with the absence of measurable long-term trends in these data. During the I photometry by Christiansen et al. (2008) around HJD 2 453 847, the star was becoming fainter at a rate of 1 millimag per 28 days, which went unnoticed over the relative short time interval of their observations.

A period search on the long-term detrended data reveals power at frequencies f = 1.99148 ± 0.00004 cycles per day (near the one detected by Christiansen et al., i.e. f_C = 1.9848 cycles per day), and f' = 0.98883 ± 0.00004 cycles per day. There is no power nearer to f_C, which could indicate that the frequency is slightly variable. The ASAS data set alone does not allow us to distinguish between f and f'. Unfortunately, at the time of writing we could not get access to the

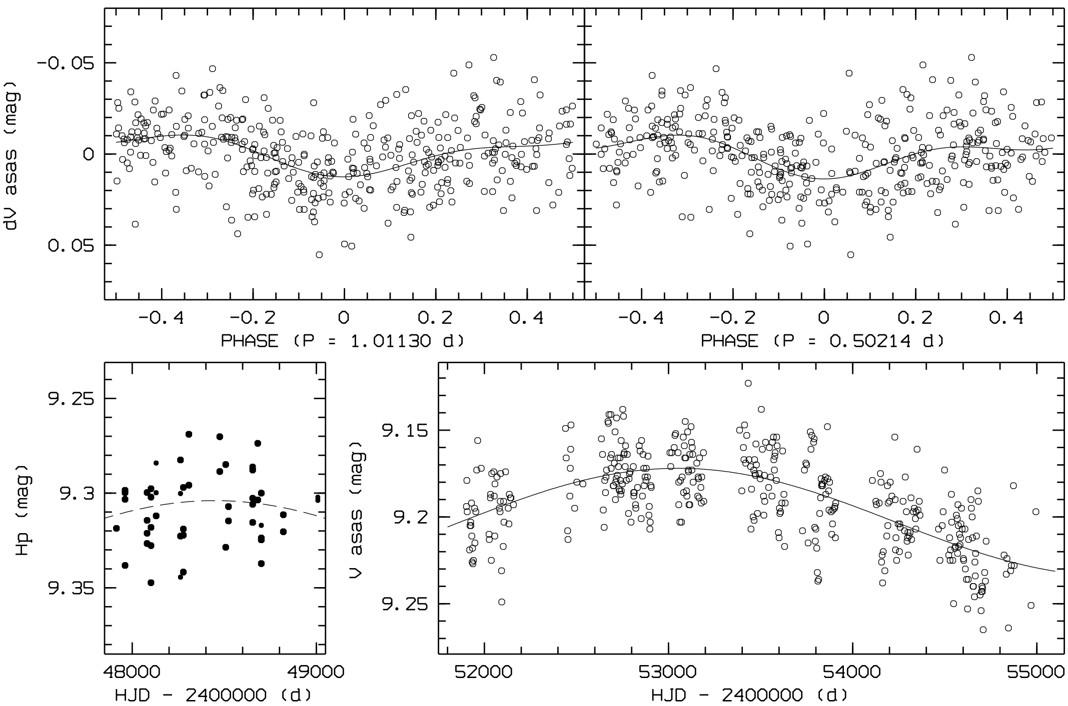

Figure 15: Long- and short-term variability of HD 129490. The lower panels show the HIPPARCOS measurements (smaller dots for data with uncertainties of 0.022 and higher) and the aperture–3 ASAS photometry in the left- and right-hand panels, respectively. A long-term sine fit to the ASAS data with a period of 12.6 year is shown as a full line, (Eq. 4) and its extrapolation to the HIPPARCOS epoch as a dashed line. The latter is shifted, arbitrarily, to 0.132 mag fainter magnitudes. Three anomalously faint observations in the set of 386 ASAS measurements fall out of the range of the figure. The upper panel shows the ASAS photometry, prewhitened for the long-term variation, and folded on the two candidate periods. The curves are fits with terms up to cos 2ϕ as specified in Eq. 5. Phase 0 is at HJD 2 453 456.806.

Christiansen data to clarify the issue. Observations at observatories at complementary latitudes during one night would offer the most efficient way to resolve the present indeterminacy. With $v \sin i = 193 \pm 13$ km/s (Chen et al. 2011), one finds $R \sin i = 1.9(3.9)$ solar radii assuming f (f'), respectively, which favours f if the star would be a spotted variable.

The peak-to-peak variation in this shorter period is 0.023–0.024 mag with the curves shown in Fig. 15 representing the functions

$$\begin{aligned} dV_{\rm ASAS} &= -0.0005 + 0.0097\cos(2\pi(\phi_1 - 0.0389)) + 0.0038\cos(4\pi(\phi_1 + 0.0299)) \\ dV_{\rm ASAS} &= -0.0001 + 0.0088\cos(2\pi(\phi_2 - 0.0456)) + 0.0055\cos(4\pi(\phi_2 + 0.0190)) \end{aligned} \quad (5)$$

where dV refers to the residuals of the ASAS magnitude with respect to the long-term trend and phase $\phi_1 = 0$ and $\phi_2 = 0$ corresponds to HJD 2 453 456.806. The first formula refers to the $1\overset{\rm d}{.}01130$ period and the second to the $0\overset{\rm d}{.}50214$ period. Minimum light occurs at phase −0.003 and −0.006, respectively. A Scargle power analysis does not detect microvariability in the HIPPARCOS data which, unfortunately, do not contain chains of measurements covering a significant part of a day. No firm conclusion can be formulated on whether the lack of detection is due to the level of the uncertainties in the HIPPARCOS photometry (both the random uncertainties and the hidden long-term trend) combined with their sampling in time, or due to absence (or weakness) of the short-term variability at the HIPPARCOS epoch. On the one hand, a sine-fit to the 42 HIPPARCOS data with rms uncertainties of 0.021 mag or less shows that they do not exclude microvariability with a frequency and range close to the estimates given above. On the other hand, the assumption of constant light leads to a reduced $\chi^2 = 1.44$, which is not sufficient to reject this assumption. Anyway, our findings indicate that this star might be a spotted variable rather than a W UMa type binary.

4.1.3 HD 141277 = HIP 77524

HD 141277 was identified as a weak-line T Tauri star by Krautter et al. (1997). Neuhäuser & Brandner (1998) estimate its mass and age at 1.5 solar masses and 5 Myr. The star shows some long-term trends below the 0.1 mag level (even below the 0.05 mag level over the whole ASAS period (see Fig. 16) but obviously also variations on shorter time scales. Both the ASAS and HIPPARCOS data indicate, independently, an almost identical frequency (0.44767 ± 0.00015 and 0.44735 ± 0.0003 cycles per day, respectively). Phasing the data together results in the ephemeris for maximum brightness

$$\text{HJD(max.light)} = 2\,453\,470.94 + (2\overset{\rm d}{.}2341 \pm 0\overset{\rm d}{.}0003)E \quad (6)$$

The ASAS data set shows relative strong aliases for $1 - f$ and $2 - f$, but the HIPPARCOS data support only $f \approx 0.4476$ cycles per day. A sine fit indicates a peak-to-peak variation of 0.049 mag. Removing the periodic component reduces the range of variability in the long-term trend (and the rms scatter around it), and removing the long-term trend indicated in Fig. 16 (a smoothed $s = 22.2$ cubic spline) reduces also the rms around the sine fit for the periodic component (Fig. 17). The fact that the rms scatter is more strongly reduced in the years where the scatter of the measurements around the yearly mean was higher ($\sigma > 0.04$) suggests a possible variation of the amplitude of the periodic component, but this cannot be firmly established.

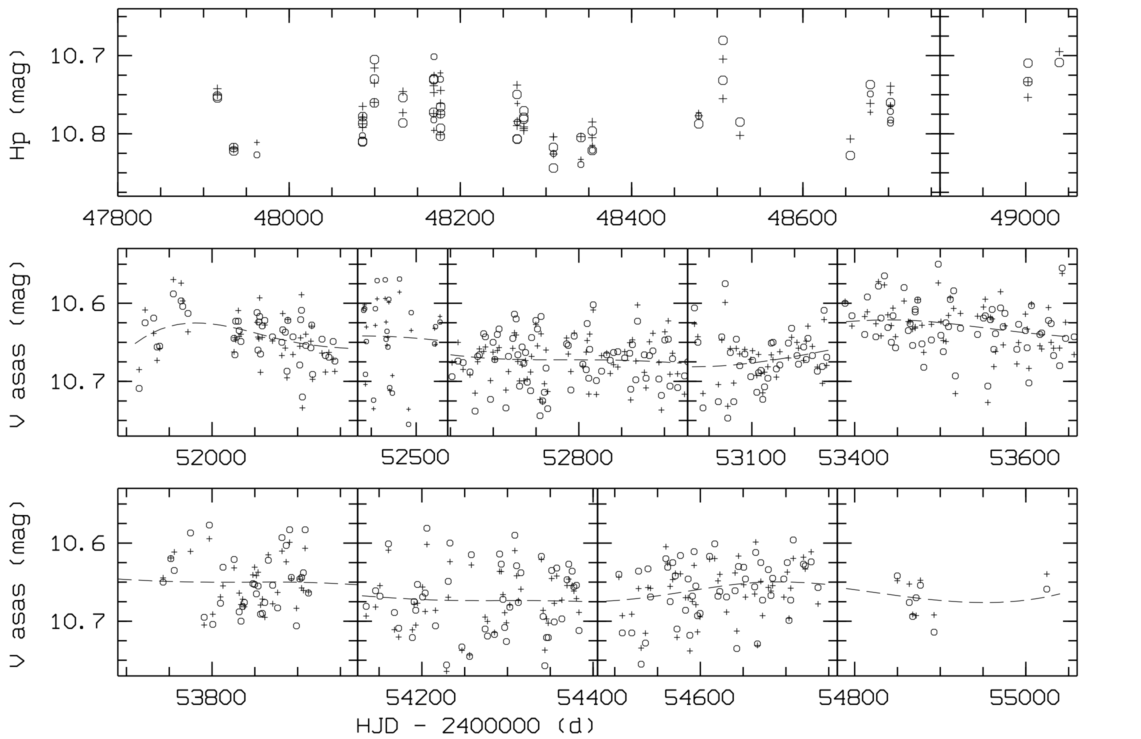

Figure 16: ASAS aperture–3 and HIPPARCOS photometry of HD 141277. Open circles represent the observed data, with larger symbols in the HIPPARCOS panel indicating paired observations. The '+' symbols are the same data corrected for the short-term periodic component shown in Fig. 17. The dashed line is a smoothed (s = 22.2) cubic spline fit to the long-term trend.

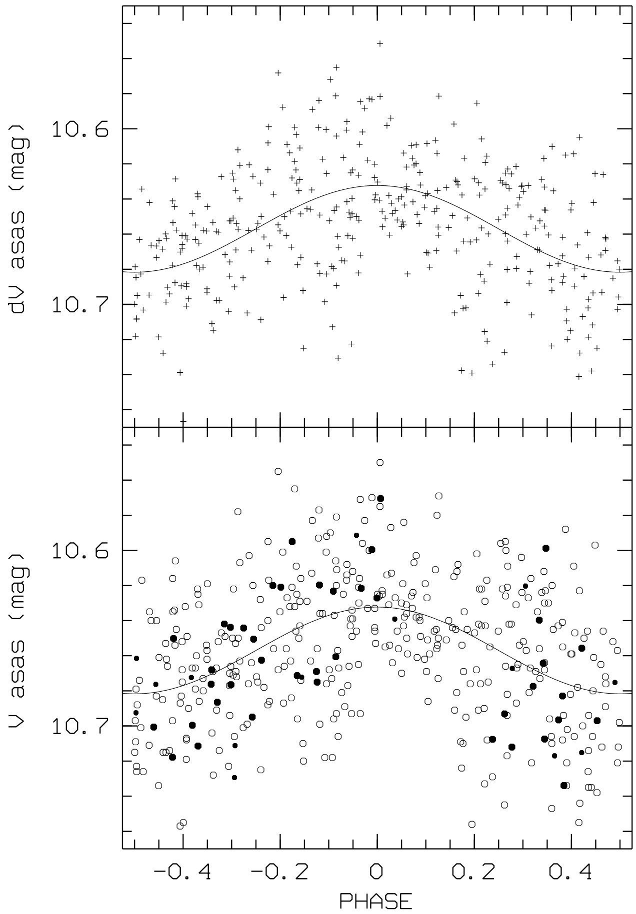

Figure 17: Phase diagram for HD 141277 using a period of $2\overset{d}{.}2341$. Filled symbols represent HIPPARCOS data shifted by −0.11 mag (larger symbols for the 21 paired observations with uncertainty on the average of 0.023 mag or less) and open circles represent the aperture–3 ASAS data (bottom panel). The upper panel shows the same ASAS data, but corrected for the long-term trend traced in Fig. 16.

4.1.4 Comment on the spectroscopic variable HD 132094 = HIP 73266

There is no convincing evidence for light variability in this late–B star up to the detection level of HIPPARCOS and ASAS photometry. However, high resolution spectra reveal that its spectrum is variable over time intervals as short as 0.1 days (Fig. 18). The variation in the shape of strong lines, e.g. Mg II λ4481, suggests line doubling reminiscent of a SB2, but the option that it is a slowly-pulsating B-star should not be excluded. More data are required to clarify the cause of the spectrum variability and its presumed periodicity. A preliminary analysis favours a number of candidate periods in the ranges $0^{\rm d}_{.}458 \pm 0^{\rm d}_{.}003$, $0^{\rm d}_{.}534 \pm 0^{\rm d}_{.}003$, $0^{\rm d}_{.}867 \pm 0^{\rm d}_{.}009$ and, with slightly less stringent criteria, $0^{\rm d}_{.}678 \pm 0^{\rm d}_{.}004$.

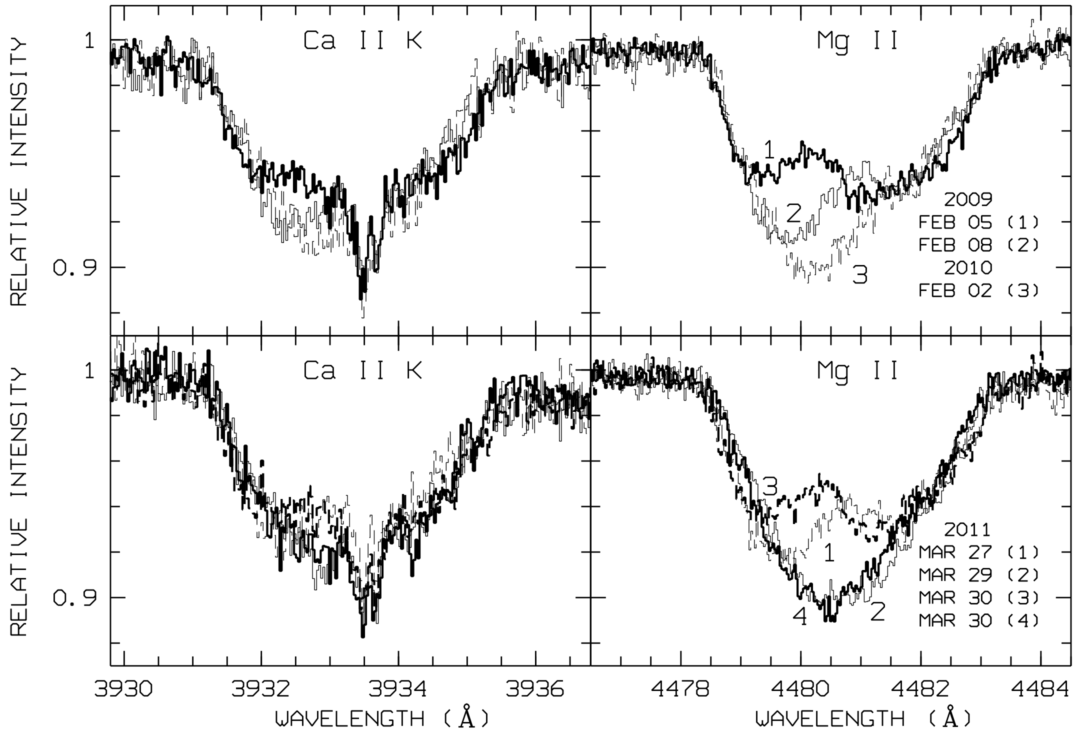

Figure 18: Variable line profiles of Ca IIK λ 3934 and Mg II λ 4481 in HD 132094. Spectra were taken with the FEROS echelle spectrograph at ESO in 2009–2010 (upper panels) and 2011 (lower panels). The spectra labeled 3 and 4 in the lower panel differ by ΔHJD = $0^{\rm d}_{.}116$.

4.2 Variables including a cyclic component

4.2.1 HD 140421 = HIP 77144

HD 140421 is a G0IV pre-main sequence star (Mamajek et al. 2002), fast rotating (65 km/s) and showing evidence of a magnetic field (Waite et al. 2011). It is an unsolved variable in the HIPPARCOS variable star catalogue. The ASAS data set shows low-level irregular variability and, even before any detrending, considerable power at the related frequencies $f \approx 0.951$, 0.051 and 1.051 cycles per day, with the first mentioned frequency corresponding to the highest power peak. This power peak is strengthened and the frequency slightly lowered to $f \approx 0.949$), by applying consecutively more detailed long-term detrending (Fig. 19, upper panel).

The HIPPARCOS data clearly reject the lower of the three frequencies, 0.051 cycles per day, as they indicate variability over fractions of a day; otherwise they are inconclusive with respect to periodicity. A denser subset of observations obtained at 5 epochs in the short time interval HJD 2 448 084–177 generates power at the frequencies near one cycle per day. But data taken over the whole HIPPARCOS time baseline do not confirm this, even if limited to the 76 data with uncertainties of 0.022 mag or less. The lower panel of Fig. 19 illustrates the situation. One might suspect that

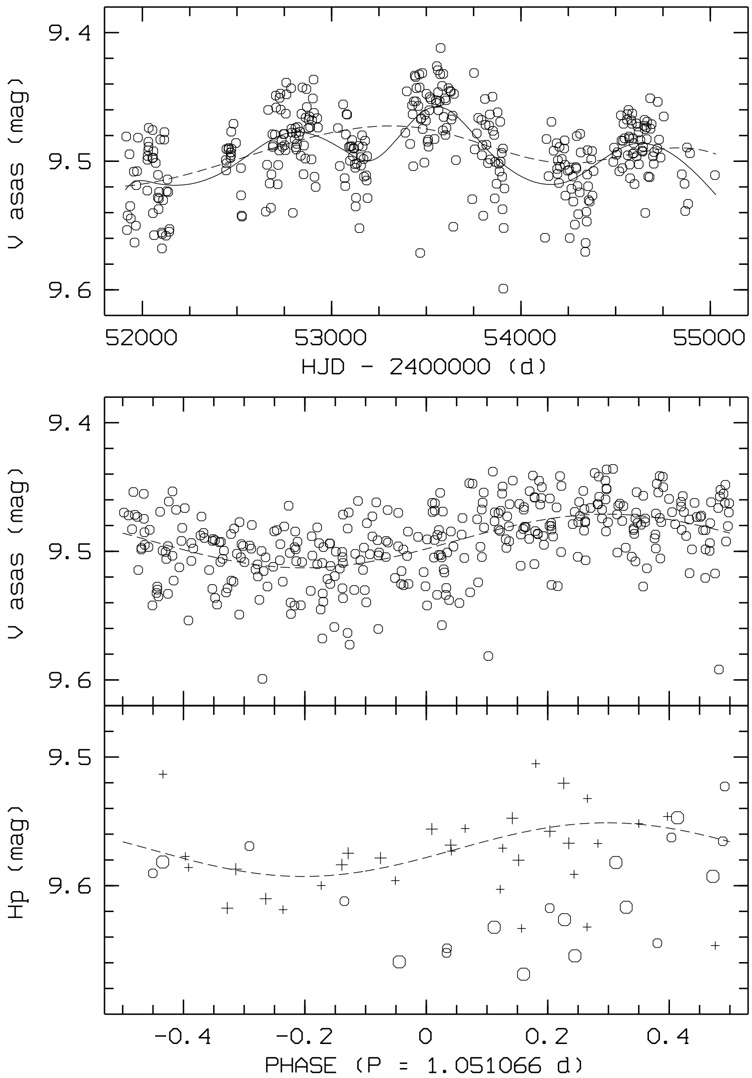

Figure 19: Irregular and cyclic variability of HD 140421. Upper panel: ASAS aperture–4 photometry prewhitened for the cyclic component with the sine curve with peak-to-peak amplitude of 0.042 mag shown in the mid-panel. The spline representations were computed in the ESO-MIDAS software with the smoothing parameter set to 0.19 and 0.12 for the dashed and full line, respectively. Mid panel: ASAS data prewhitened for the long-term drift (full line in upper panel; the much smoother dashed line was the initially assumed long-term drift) and folded on the detected cycle length. Phase 0.0 corresponds to HJD 2 453 446.247, maximum light is at phase 0.297. Lower panel: HIPPARCOS photometry folded on the ASAS cycle and phase 0.0 definition. The symbols '+' and 'o' correspond to the subsets obtained in and out of the time interval 2 448 084–177, respectively, as discussed in the text. Smaller symbols refer to single measurements, larger ones to paired observations. Only data with uncertainties of 0.022 mag and less were included. The dashed curve is the sine model for the ASAS cycle shifted to 0.08 mag fainter magnitudes.

irregular variations contribute to the non-detection, as the ASAS set shows that changes up to 0.07 mag may occur over time intervals of the order of one year.

In conclusion, a cycle length of $\approx 1^{\mathrm{d}}\!.051066$ is detected. When assigned to the rotation of stellar spots, the apparent rotational velocity measured by Waite et al. (2011) and Chen et al. (2011), 65 and 73 ± 5 km/s respectively, implies $R \sin i$ = 1.35–1.5 solar radii, in excellent agreement with the stellar radius estimated by Waite et al. (2011) and Mamajek et al. (2002).

4.2.2 HD 138995 = HIP 76472

HD 138995 was identified during the HIPPARCOS mission as a light variable. Mamajek et al. (2002) classify it as a G1V pre-main sequence star, while Torres et al. (2006) give G6Ve, closer to the classification in the Michigan Catalogue.

The ASAS photometry confirms the existence of long-term variability as seen in the HIPPARCOS photometry without exceeding the amplitude observed in the early satellite data. With indications of non-monotonic fluctuations within time intervals less than one year, detrending is not as unique as one would wish (Fig. 20). Locally, uncertainties of ±0.025 mag occur. At some epochs the trend is well-defined with relatively small scatter around it (e.g. HJD 2 452 700–900), leaving little room for shorter-term (quasi)-periodic trends. However, power appears at a number of frequencies (aliases of each other), independent of the details of the detrending (Fig. 21), prompting a finer

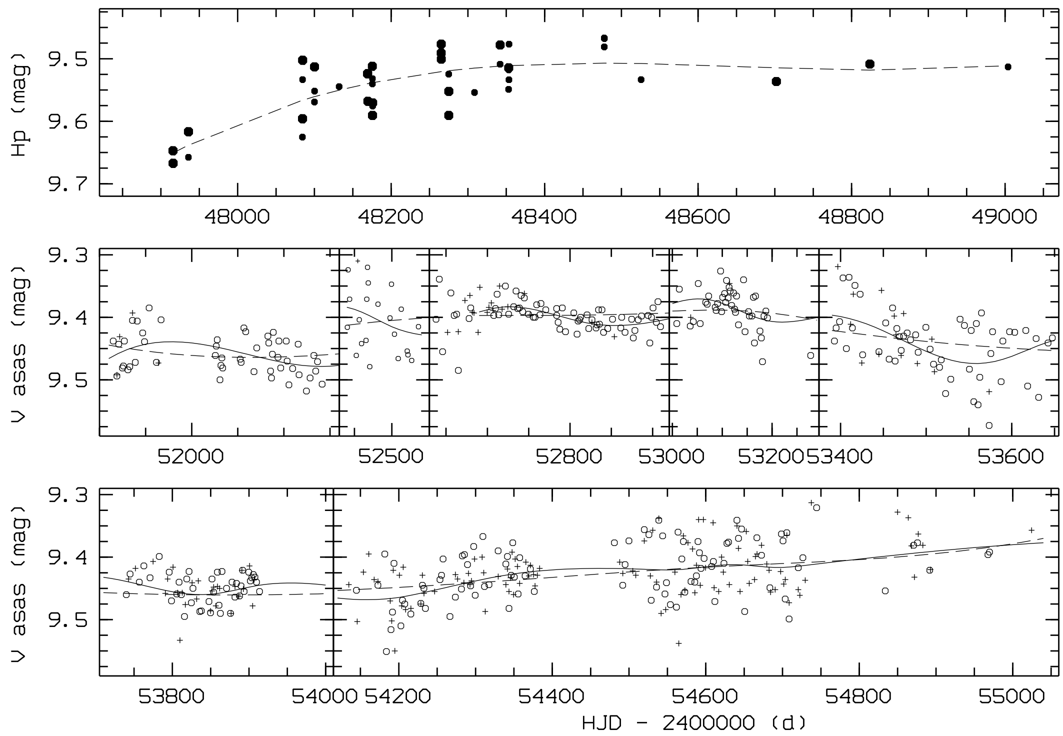

Figure 20: HIPPARCOS and ASAS aperture–2 photometry of HD 138995. Larger symbols in the HIPPARCOS panel represent paired observations. Only the 64 out of 78 data with uncertainty up to 0.022 mag were used. The long-term trend of the HIPPARCOS data is traced by a third degree polynomial. For the ASAS data, the long-term trend is tentatively represented by smoothed cubic splines with s = 25 (full line) and s = 29.5 (dashed line). The symbols in the ASAS panels refer to two data sets (Table 1), with the '+' symbols for the smaller set shifted to 0.007 mag brighter magnitudes.

analysis. Therefore, in this case, exceptionally, we tried to detrend also the HIPPARCOS data despite the involved uncertainties. The fact that the frequency of the highest power peak for the detrended HIPPARCOS data, $f_{\rm hip}$ = 1.1578 cycles per day differs by less than 0.1% from one of the stronger ASAS power peaks adds confidence to the reality of a short-term cycle.

Hence, the Scargle power analysis was applied to seasonal subsets of the ASAS data, in order to check whether a cycle around f = 1.157 cycles per day persists in all years. Seven subsets with 44–99 measurements were selected (2001, and 2003–2008, see the corresponding HJD intervals mentioned in the caption of Fig. 21). In 2005 and 2008, when the scatter in the data was obviously large (Fig. 20), the power is largest (Fig. 21). When the scatter was smallest (2003), the cycle might have been approximately 0.7% shorter, but differences are on the 0.1% level in other years, if real; this still holds if we include the much earlier HIPPARCOS data in the comparison. Assuming that the cycle is of rotational origin, using $v \sin i$ = 97 ± 7 km/s (Chen et al. 2011) implies $R \sin i$ = 1.7 solar radii.

Fig. 22 shows the data folded on the cycle length around $0\overset{\rm d}{.}864$. The amplitude differs significantly from year to year (a peak-to-peak amplitude of 0.1 down to 0.03 mag) and phase shifts seem to correlate with changes in amplitude. The figure suggests a semi-regular modulation in roughly three years. Except for 4 data points, the HIPPARCOS data were obtained in 1990–1991 and show a total range of variation of 0.067 mag (sinusoidal fit), which is in between the amplitudes seen in the ASAS data of 2008 and 2007 (or 2005 and 2004). This would fit in a modulation scheme of 2.9 years, but the gap between the two data sets is large and the HIPPARCOS data set is too short to deliver proof of the existence of such scheme over 20 years.

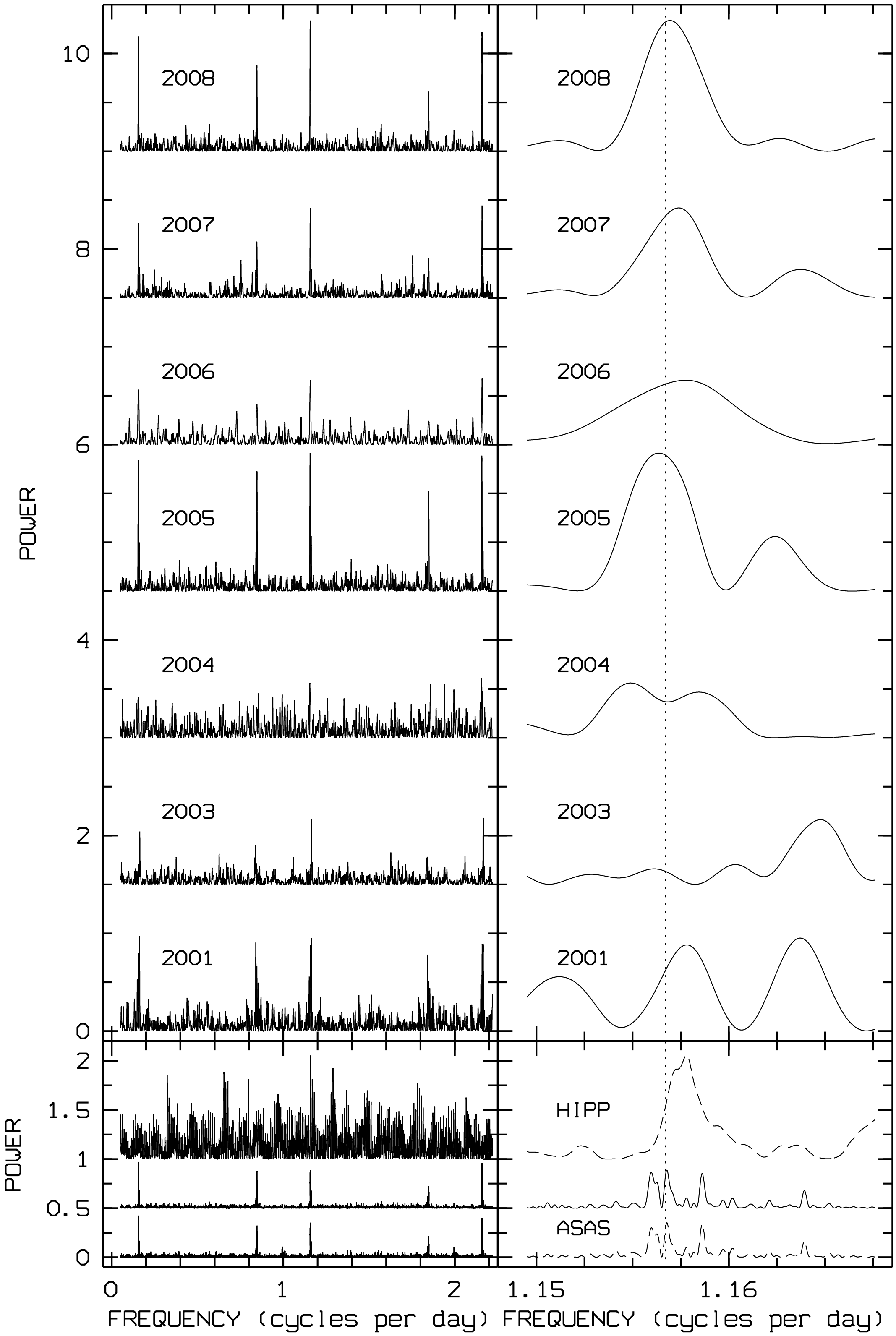

Figure 21: Scargle power diagrams for HD 138995, with in the right-hand side a zoom on the major peak. The bottom panels show the results for the detrended ASAS data (twice, the unshifted one is for the dashed-line detrending shown in Fig. 20) and for the detrended HIPPARCOS data. The panels refer to the 7 seasonal subsets with 54 (2001, JD 2 451 914–2 142), 85 (2003, JD 2 452 637–910), 33 (2004, JD 2 453 008–277), 66 (2005, JD 2 453 392–648), 69 (2006, JD 2 453 739–914), 88 (2007, JD 2 454 134–384), and 99 data points (2008, JD 2 454 480–745) respectively. The dashed vertical line in the right-hand panels indicates the frequency corresponding to the highest power peak in the whole, detrended, ASAS data set.

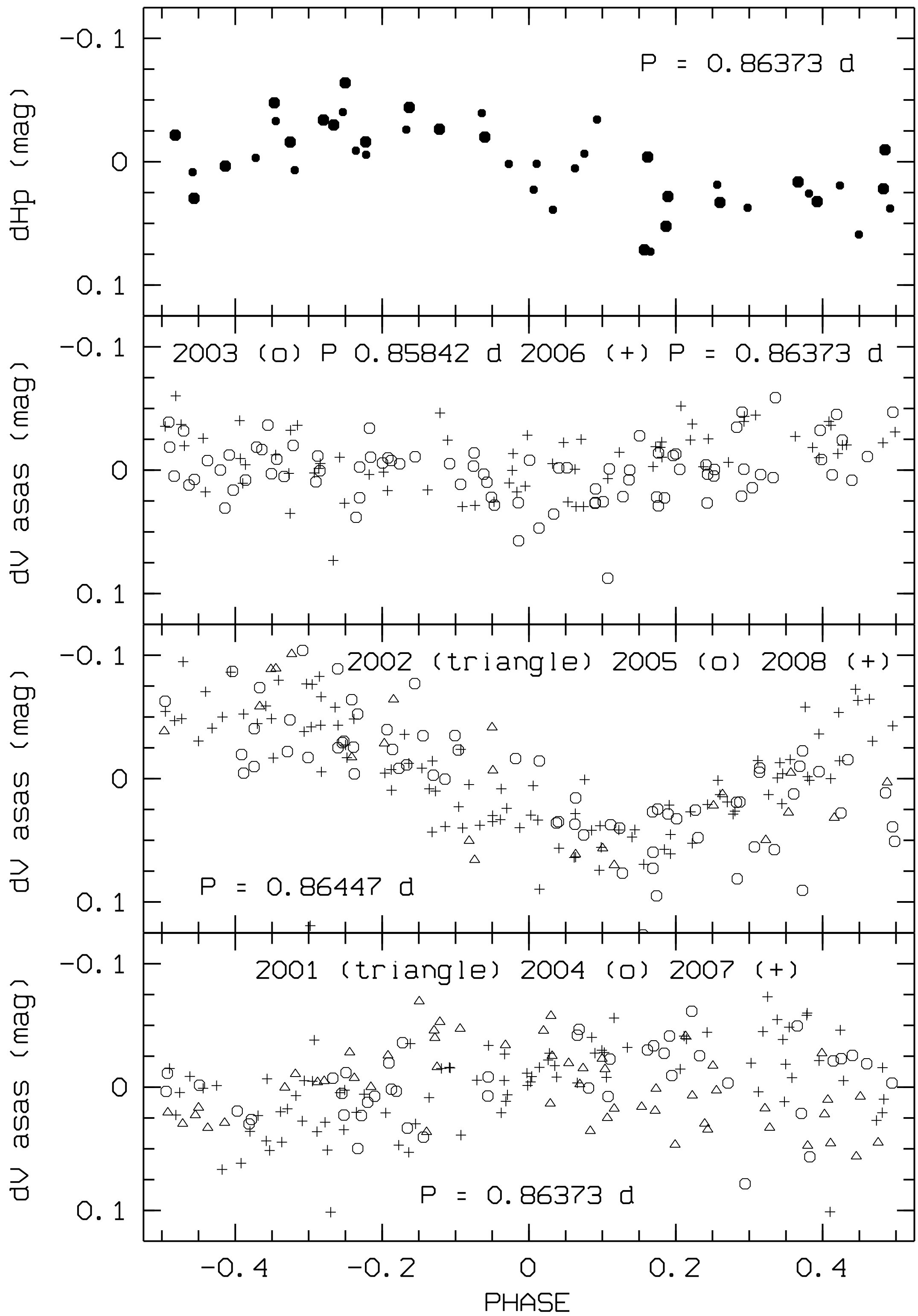

Figure 22: HIPPARCOS (upper panel) and ASAS aperture–2 detrended data for HD 138995, folded on the indicated cycle lengths. Different ASAS panels show the results for seasons differing by 3 years. Larger symbols in the HIPPARCOS panel refer to paired observations. The detrending indicated by a full-line in Fig. 20 was used. Zero phase was fixed arbitrarily at HJD 2 453 500.

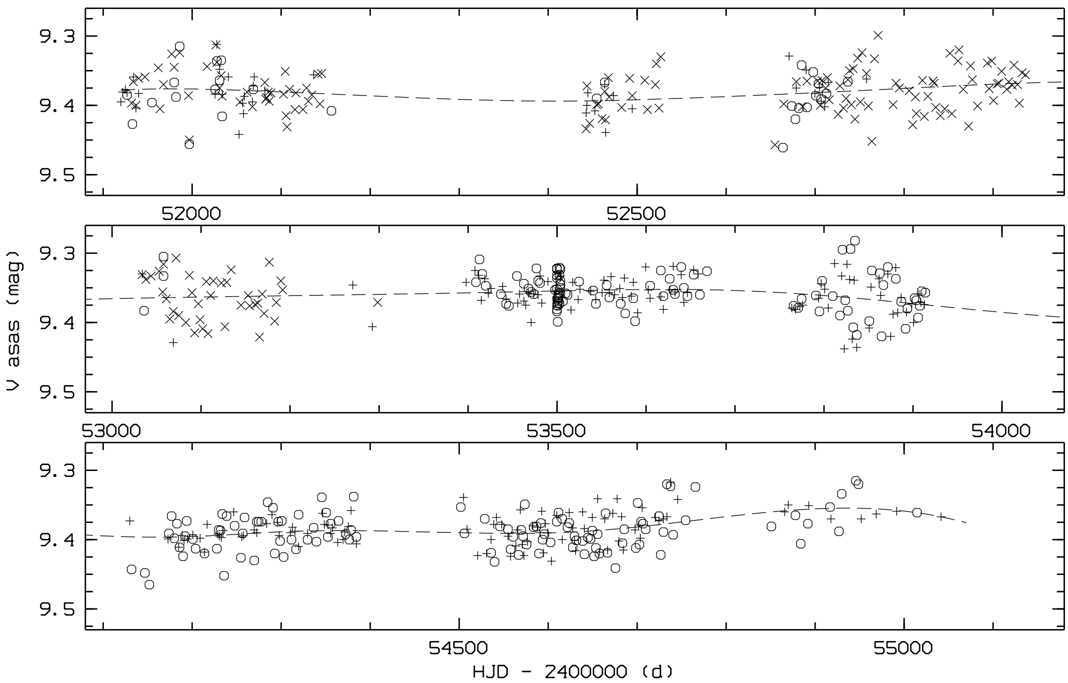

Figure 23: The aperture–3 ASAS data of HD 148187 with a tentative long-term trend traced by a smoothed (s = 26.1) cubic spline (dashed line). Four out of 647 measurements fainter than V = 9.48 fall outside the range shown in the figure. The data sets represented by 'x' and '+' were shifted to 0.006 mag fainter and 0.01 mag brighter magnitudes, respectively (see also Table 1).

4.2.3 HD 148187 = HIP 80636

HD 148187 is the variable V1056 Sco detected by HIPPARCOS with the variable star annex mentioning a period of $1^{\mathrm{d}}_{.}2819$. Kazarovets et al. (1999) suggest it is a BY Dra-type variable. The HIPPARCOS data consist of two subgroups: almost half of the observations is obtained in dense series at two epochs within 6 days. The remaining observations are shorter series with much larger time gaps in between.

This periodicity is not strictly confirmed by the ASAS data, although a nearby frequency is detected, f = 0.79017 cycles per day, or $P = 1^{\mathrm{d}}_{.}2656$. A slightly weaker peak at f' = 0.78203 is nearer to the dominant frequency detected by HIPPARCOS, but still significantly different. The ASAS data were tentatively corrected for a weak long-term trend as shown in Fig. 23. We notice that the HIPPARCOS data also show two comparable peaks at f_{hip} = 0.7800 (corresponding to the period mentioned in the HIPPARCOS catalogue) and f'_{hip} = 0.7675. While the ASAS data set shows also peaks at aliases of f and f', and at integer-number cycles per day related to the one-day sampling, the HIPPARCOS power diagrams clearly reject those.

Finally, a closer look at seasonal subsets in the ASAS data (Fig. 24) shows that only in 2001, 2004 and 2006 the variability range (54 millimag peak-to-peak) approaches the 64 millimag range seen in the HIPPARCOS set in July 1990 (HJD 2 448 091–097). During roughly half of the ASAS time interval, the cycle is not or barely detectable. A model including second order Fourier terms, with a period of $1^{\mathrm{d}}_{.}28216$ as derived from the time interval HJD 2 447 960–448 700, is shown in the HIPPARCOS panel of Fig. 24:

$$Hp = 9.5035 + 0.0315 \cos 2\pi(\phi + 0.3329) + 0.0066 \cos 4\pi(\phi - 0.1104) \qquad (7)$$

The highest–amplitude ASAS data suggest a somewhat different shape, with a broader minimum rather than a broader maximum:

$$V_{\mathrm{ASAS}} = 9.3746 + 0.0265 \cos 2\pi(\phi + 0.3252) + 0.0057 \cos 4\pi(\phi - 0.2084) \qquad (8)$$

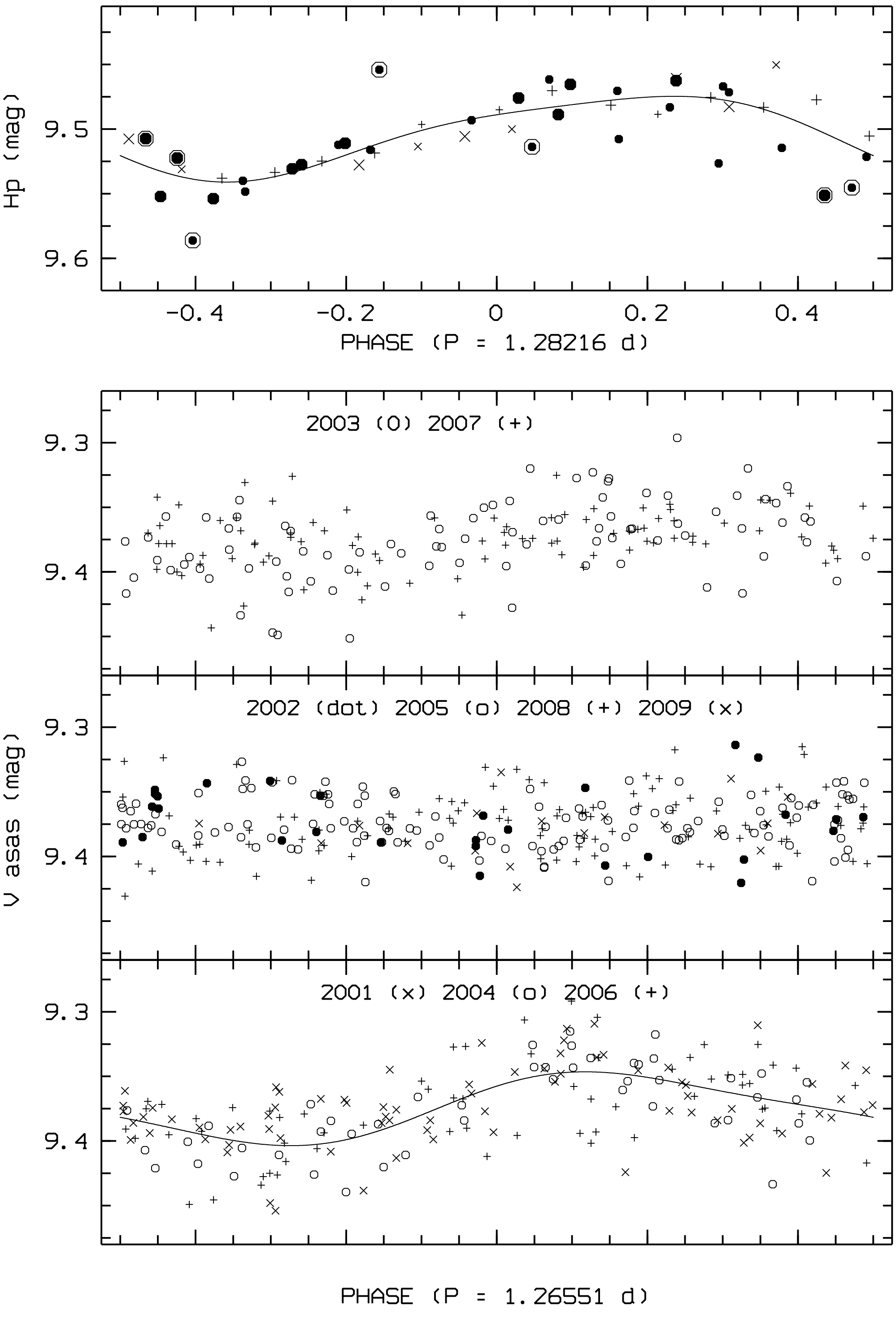

Figure 24: Phase diagrams for HD 148187. Upper panel: HIPPARCOS data. '+' data obtained at HJD 2 448 091.14–92.30; 'x' data obtained at HJD 2 448 096.04–97.01. Encircled data were obtained outside the interval HJD 2 447 960–448 700. Larger symbols indicate paired observations. Other panels: long-term detrended (see Fig. 23) aperture–3 ASAS data with symbols discerning seasonal subsets. The size of the subsets is 77 (2001; HJD 2 451 919–2 156), 29 (2002; HJD 2 452 442–526), 88 (2003; HJD 2 452 663–936), 47 (2004; HJD 2 453 033–298), 122 (2005; HJD 2 453 397–668), 63 (2006; HJD 2 453 763–913), 90 (2007; HJD 2 454 129–384), 112 (2008; HJD 2 454 501–765), and 19 (2009; HJD 2 454 850–5 041). Phase zero is arbitrarily set at HJD 2 448 093.7 for the HIPPARCOS data and HJD 2 453 512.0 for the ASAS data. The fits are described in Eq. 7 and Eq. 8.

Some of the earliest and latest HIPPARCOS data, outside the above mentioned time interval, show larger deviations. In conclusion, the BY Dra type variability classification is confirmed. Using $v \sin i = 76 \pm 6$ km/s (Chen et al. 2011) implies $R \sin i = 1.9$ solar radii.

4.2.4 HD 126996 = HIP 70919

HD 126996 is a late-G or K-type giant that shows variability on different time scales. The ASAS data reveal that the star became fainter during the interval HJD 2 452 025–3 141 (2003–2006) and started to brighten again from HJD 2 454 411 onwards (2008). Fig. 25 shows this long-term trend in the upper left panel.

In addition, cyclic variability with a period of $\approx 53\overset{\mathrm{d}}{.}87$ persists, but the amplitude of the variability varies. The upper right panel of Fig. 25 zooms in on the gradual reduction of the amplitude in the observing season 2005–2006, and Fig. 26 shows with open symbols that high amplitudes were reached in the 2002–2003 season (HJD 2 452 420–770) and from late–2005 on (after HJD 2 453 670).

This is the only object in our sample of candidate variables that is listed in the ASAS catalogue of new variables (Pojmański & Maciejewski 2004), as a periodic variable (with $P = 54\overset{\mathrm{d}}{.}4267$). It is also the highest–amplitude (quasi)-periodic variable in our sample. Koen & Eyer (2002) suggested a much higher frequency $f_{\mathrm{KE}} = 0.19627 \pm 0.0011$ cycles per day, from analysis of HIPPARCOS photometry. The lower panels of Fig. 25 show the Scargle power for the ASAS data (after removing the long-term trend) and the HIPPARCOS data set. At the time of the ASAS observations, there was no evidence for this higher frequency, although the observing schedule was well-suited to detect such periodicity.

We notice that it appears impossible to single out one frequency from the HIPPARCOS data. Actually, we found as much power at a frequency half as high, and even more power in these data for $f = 0.20146$ cycles per day. The exact power depends a bit on which data with high uncertainty estimate are rejected.

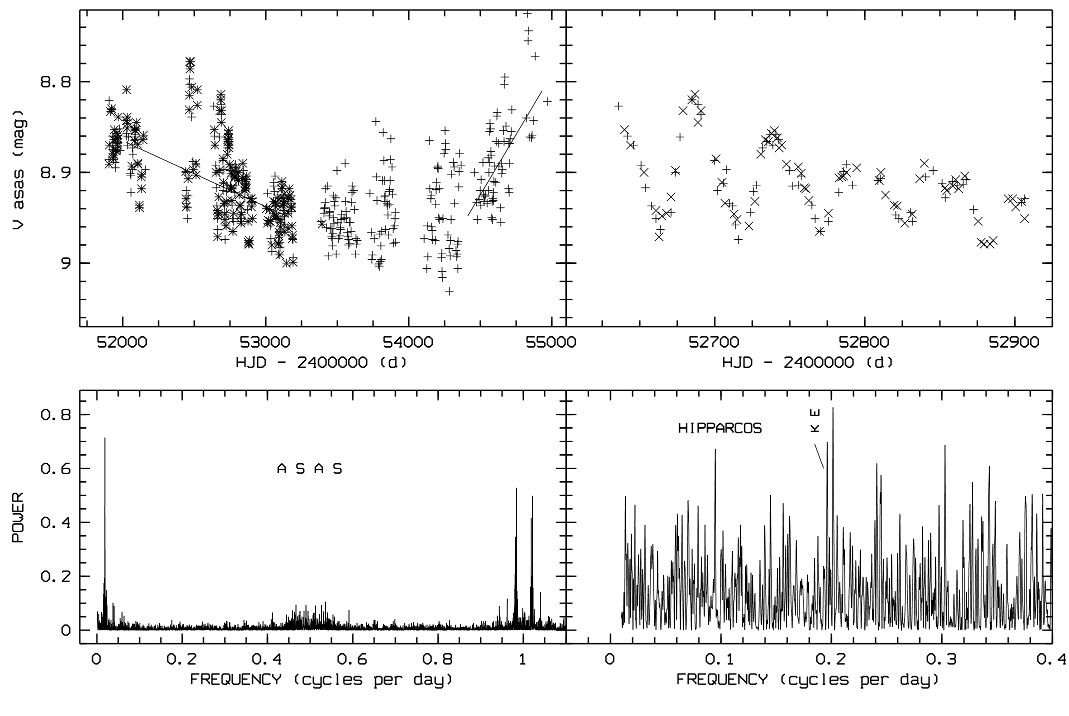

Figure 25: Upper left: V magnitudes of HD 126996 for two data sets of ASAS represented by '+' and 'x' (no shifts between the data sets). Three abnormally faint data points are not shown. Upper right: zoom on the data obtained during one observing season. Lower panels: Scargle power for the detrended ASAS data and the HIPPARCOS data. The frequency selected by Koen & Eyer (2002) is labeled 'KE'.

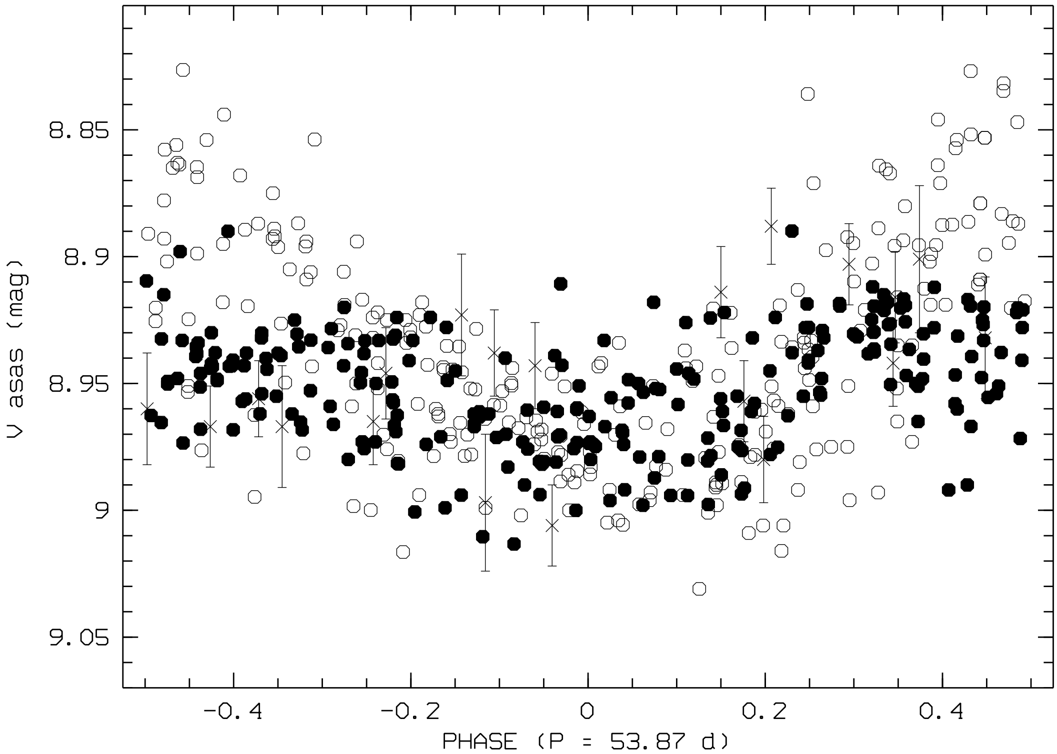

Figure 26: Phase diagram for HD 126966 corresponding to the ephemeris 2 453 522.62 + $53^{\rm d}.87$E for minimum light (phase 0). The HIPPARCOS data ('x' with vertical bars indicating the rms estimate for the original data around the plotted averages for each epoch) were shifted by −0.1 mag. Open symbols refer to data within the HJD-ranges 2 452 420–770 and 2 453 670–4 994; closed symbols represent data observed in a 300-day interval before HJD 2 452 420 and in the 900-day interval between the time intervals with high amplitudes. ASAS data were detrended roughly, using the linear gradients of +0.08 mag per 1 000 days before HJD 2 453 141 and −0.265 mag per 1 000 days after HJD 2 454 411, as shown in the upper left panel of Fig. 25.

With a varying amplitude and the fact that HIPPARCOS measured the star at only 20 different epochs (counting series of subsequent observations) with no more than 3 epochs within a same $53^{\rm d}.87$ cycle, it is not surprising that the cycle detected in the ASAS data remained undetected in the HIPPARCOS data. Fig. 26 shows that the hipparcos data are not incompatible with such a cycle which appears to have had low amplitude during the epoch the satellite was observing. Indeed, the ASAS cycle phases well with the HIPPARCOS data, such that the existence of this cycle over a longer time interval cannot be excluded.

If this would be a spotted variable, the apparent rotation velocity of 13 km/s (Chen et al. 2011) implies $R \sin i = 13.8$ solar radii. Based on the reddening and the weak lithium line, Chen et al. (2011) rejected this star as belonging to the Sco-Cen Complex. If this is an evolved giant star, the apparent rotation velocity might include a non-negligible contribution from macroturbulence, and the stellar radius might be smaller than suggested above.

4.2.5 HD 143677 = HIP 78684

HD 143677 is a late–G post–T Tauri star (G9.5 IV, Mamajek et al. 2002) and unresolved binary (separation 0.3 arcsec). It was identified as a young ROSAT star by Krautter et al. (1997). The ASAS and HIPPARCOS photometry reveal a quite different photometric variability pattern in the early 1990s and the first decade of the 21st century. The HIPPARCOS photometry shows a long-term trend, most clearly in the initial year of the satellite observations, while no significant long-term trends are visible over the much longer time interval covered by the ASAS project (Fig. 27). The star was also

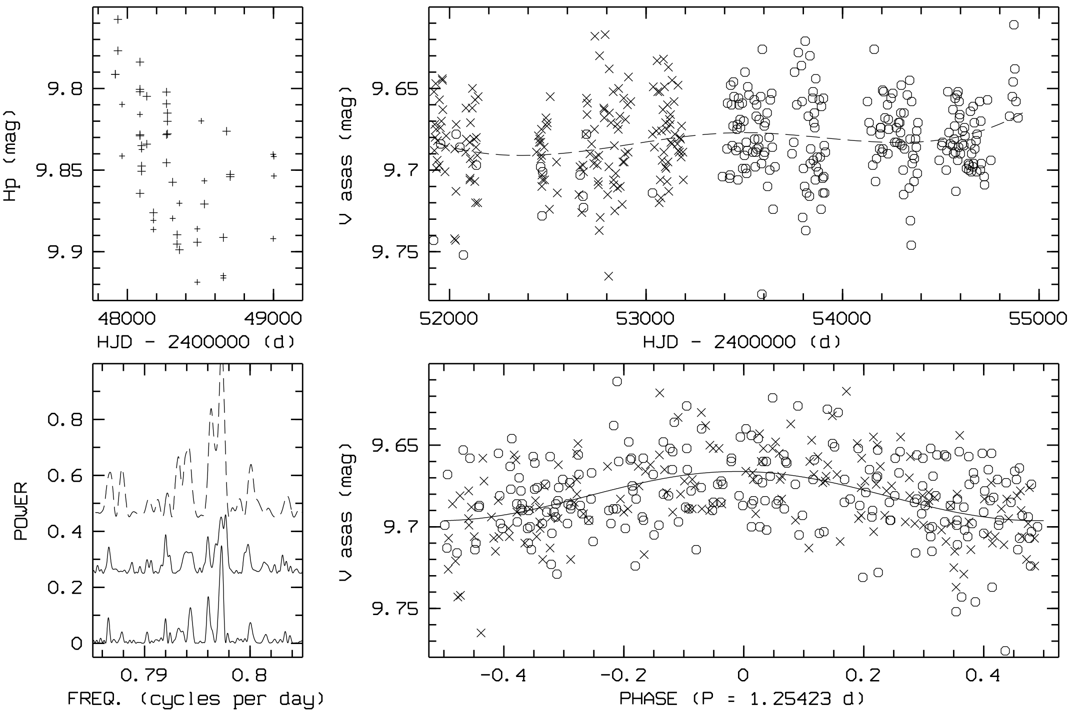

Figure 27: Photometry of HD 143677. The upper panels show the HIPPARCOS data (larger symbols representing paired observations) with uncertainties up to 0.025 mag on single measurements, and two sets of ASAS data (Table 1). A dashed line traces a tentative long-term trend with a smoothed (s=13.7) cubic spline. The smaller set ('x') was shifted to 0.013 mag brighter magnitudes. One out of 387 data points, near $V = 9.8$, falls out of the scale of the figure. The ASAS data are folded on the $1\overset{d}{.}25423$ period in the bottom right diagram, with maximum light (phase 0) at HJD 2 452 999.556. The bottom left diagram shows the Scargle power in the whole ASAS set (unshifted) and in the separate data sets (both shifted upwards along the power axis). Dashed and full line correspond to the 161 and 225 data shown by 'x' and 'o', respectively, in the right upper panel.

fainter over most of the HIPPARCOS epoch, as compared to the early 21st century.

In addition, the ASAS data show a periodic or possibly cyclic variability pattern ($P = 1\overset{d}{.}25423 \pm 0\overset{d}{.}00004$) with a peak-to-peak amplitude of 0.03 mag (right hand side bottom panel of Fig. 27). It is absent at the epoch of the HIPPARCOS observations, or at least hidden by larger long-term or irregular variations, and by the noise level in a much sparser data set.

In view of the possible temporary character of this cycle, the period search analysis was repeated separately for the two ASAS data sets which only have a small overlap in time. Fig. 27 shows that the periodicity is detected in both sets, so it persists over the whole ASAS time interval. Nevertheless, the amplitude of the variations might have been somewhat larger in the initial half of the 9-year time interval. Although less probable, the alias period near $P' = 0\overset{d}{.}83$ cannot be completely excluded. Using $v \sin i = 71 \pm 4$ km/s (Chen et al. 2011) and assuming that the short-period cycle is of rotational origin, leads to $R \sin i = 1.8$ solar radii.

4.3 Irregular variables

4.3.1 HD 152404 = HIP 82747

HD 152404 is the famous pre-main sequence irregular variable AK Sco consisting of two almost equal-mass mid-F stars in an eccentric ($e = 0.47$) orbit of $13\overset{d}{.}6$ days (Andersen et al. 1989; Alencar et al. 2003). Alencar et al. (2003) show that both components exhibit many of the same signs of accretion as typical classical T Tauri stars.

The ASAS data confirm the known irregular patterns on short and long time scales (Fig. 28),

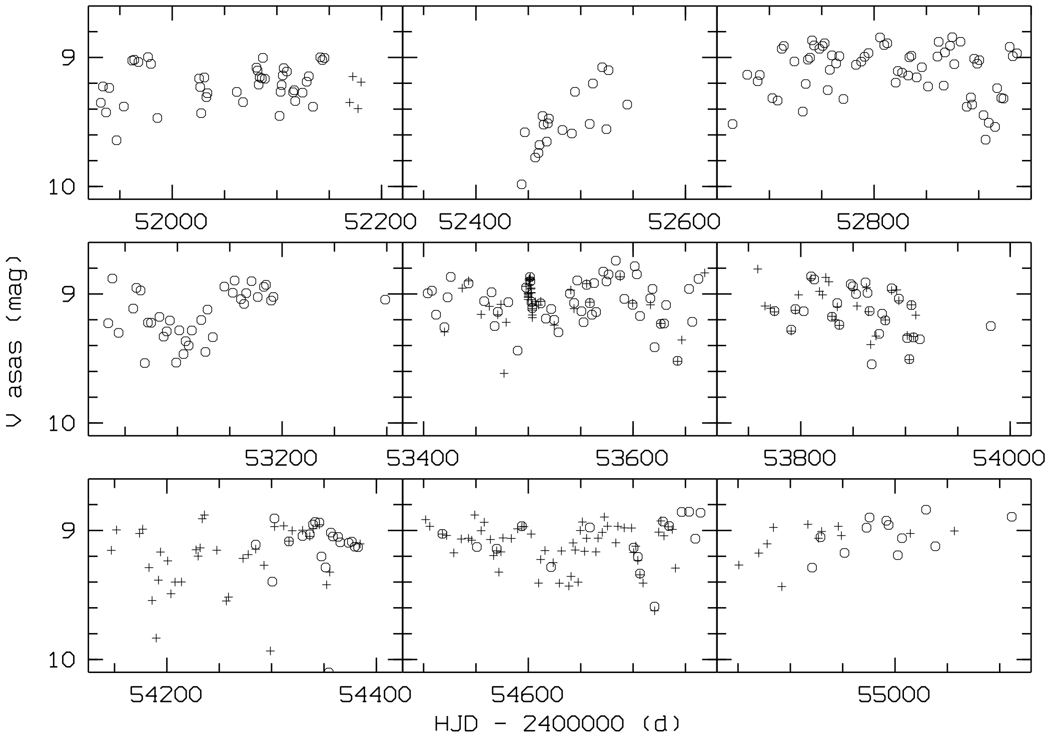

Figure 28: Light variability of AK Sco from ASAS aperture–4 photometry. The smaller subset represented by '+' symbols was shifted to 0.035 mag brighter magnitudes.

without any evidence of cyclic components, and the absence of eclipses. The data are distributed quite homogeneously over all orbital phases, with 44 to 58 data points in bins of one tenth of the orbital period. Folding the photometry in orbital phase gives essentially a scatter plot, although there might be a statistical variation in the sense that the fraction of data with aperture–4 V photometry brighter than $V = 9.25$ equals or exceeds 80% for bins centered on phases -0.1 to 0.2 (with periastron situated at phase 0.0), and falls below to 65–67% for bins centered on 0.3 and 0.4. The bins with an excess of bright magnitudes coincide with the larger absorption equivalent widths of H α in the sample of spectra presented by Alencar et al. (2003), see their Fig. 11.

4.3.2 HIP 68328

HIP 68328 was listed as a new suspected variable after the HIPPARCOS mission. The ASAS data confirm a long-term variability with a dominant smooth component (Fig. 29). Bright and faint states seem to be separated by more than one year. Variability on shorter time scales is probably irregular and of low amplitude; no cycles were found after removing tentatively the long-term trend. HIP 68328 is rotating relatively slowly in comparison to most F-type or G-type stars in the Sco-Cen Complex (10 km/s, Chen et al. 2011)

The star HD121835, $V = 8.44$, F5V, at 68″ strongly deteriorates the photometry in aperture 4. Aperture 3 is a bit better than aperture 2 considering the rms scatter, and was therefore used. The aperture–3 magnitudes are apparently offset by the bright star at the 0.01 mag level, but nevertheless useful for a variability study.

4.3.3 HD 133259 = HIP 73777

Houk (1982) classifies HD 133259 as K(1)V + G with the remark "overlapped, probably composite". In a study of X-ray active young stellar objects near the Lupus star forming region, Wichmann et al. (1997) classify it from higher resolution spectroscopy as a weak-lined T Tauri star of spectral type F8. Koen & Eyer (2002) suggest a period of $1^{\mathrm{d}}.85656$ and an amplitude of 0.0325 mag

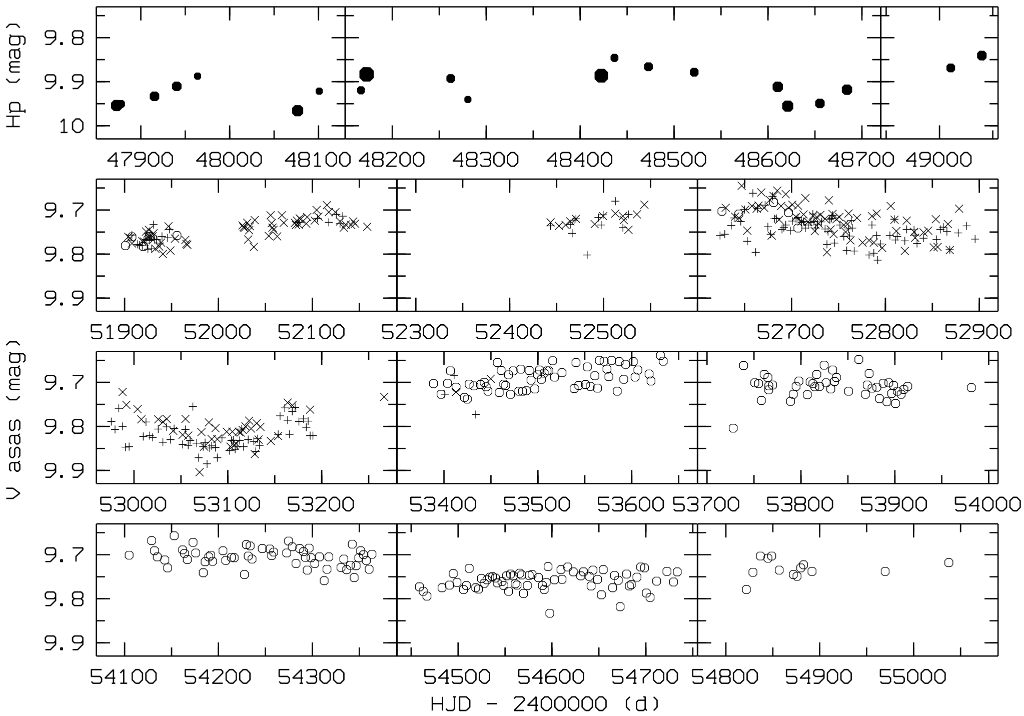

Figure 29: Long-term variability of HIP 68328. Upper panel: HIPPARCOS data averaged over sub-day fractions, with symbol size indicating the number (1–10) of contributing measurements. The aperture–3 data sets from ASAS are represented by 256 'o', 164 '+' (shifted by +0.003 mag) and 179 'x' (shifted by −0.015 mag); the shifts with respect to the larger data set are rather uncertain because of lack of overlap of the time series.

(= 0.065 peak-to-peak) from HIPPARCOS photometry. We find no confirmation of such a period (or cycle) over the much longer time baseline of the ASAS data.

A straightforward Scargle test on the ASAS data reveals some power at frequencies $f = 1.4355$ cycles per day, $f+1$, $f-1$ and $2-f$, but nothing with an amplitude comparable to the one mentioned by Koen & Eyer (2002). A closer look at the data shows that irregular variability may hide cyclic trends: at least between HJD 2 454 300–400, a gradual change of about 0.08 mag is apparent (Fig. 30). In an attempt to minimise the influence of superposed irregular variations, the subset observed in 2003 (second panel in the middle row of the figure) was analysed separately, as it is the largest of the yearly subsets and it shows the lowest rms scatter. In addition, the complete ASAS set was detrended using a smoothed ($s = 12.9$) cubic spline to describe slow variations. Both trials confirm the frequency f, but at $f' = 0.41056$ cycles per day the power grows to being dominant for the detrended set, slightly stronger than the one at f, while the other prominent peaks weaken. However, at any of these frequencies the peak-to-peak variation does not exceed 0.024 mag and irregular variability seems dominant at any time.

The HIPPARCOS data set consists of a dense subset obtained within 48 hours (37% of all observations, second panel in upper row of figure) embedded within a sparser set encompassing 900 days. Scargle power diagrams for these two sets separately show that the dense set is compatible with a broad range of frequencies around 0.5 cycles per day, but not with higher ones; while the subset covering the whole time domain outside of these 48 hours does not allow us to single out a unique period or cycle. This is presumably due to the superposition of large irregular light variations.

In conclusion, the light variation of HD 133259 is dominantly irregular over a range of roughly 0.1 mag and over relatively short time scales. With the typical integer-day spacing, the ASAS data are inadequate to confirm any underlying low-level cyclic component, in contrast to cases with slower irregular variability. Indications for a cyclic component depend on an uncertain detrending for irregular variability. Much denser sets of observations should be obtained to confirm or deny

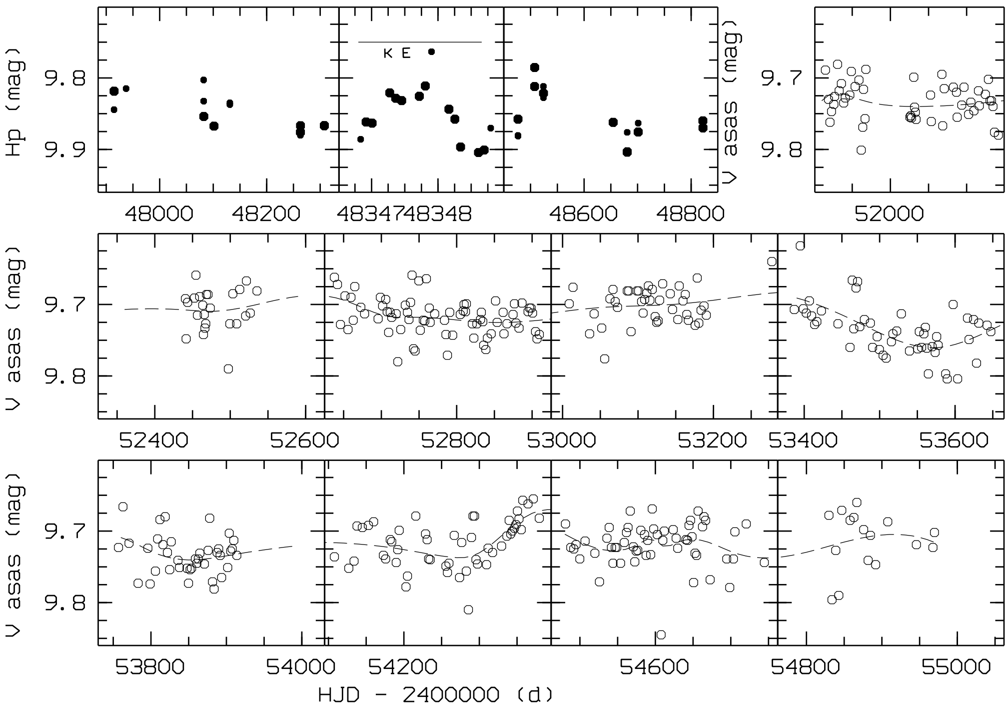

Figure 30: Light variability of HD 133259, from HIPPARCOS and ASAS aperture–2 photometry. The dashed line in the ASAS panels is the smoothed (s = 12.9) cubic spline used for the tentative long-term detrending discussed in the text. The horizontal line labeled 'KE' in the mid-HIPPARCOS panel shows the length of the period suggested by Koen & Eyer (2002). HIPPARCOS paired observations are shown as larger dots; two measurements with uncertainty larger than 0.028 mag, out of a total of 76, were not included.

whether the short-term variability seen in the HIPPARCOS data around HJD 2 448 348 is part of a cyclic or part of an irregular pattern. Anyway, the length of a possible cycle is much more uncertain than suggested by Koen & Eyer (2002).

5 Lower Centaurus–Crux

Table 4 lists the variable stars identfied in Lower Centaurus–Crux and discussed in the following subsections or in paper I.

Table 4: Variable stars in Lower Centaurus–Crux; see Table 2 for a detailed explanation of the notations.

ASAS	HIP	HD	Hpmag	Sp.Type	V.C.	Period(s) (d)	ΔM	Ref.
113306-5419.5	56354	100453	7.877	A9Ve	I		100(?)	5.3.1
121212-5413.8	59505	106048	8.684	A9V	**mP**	0.505382, 0.600128	23, 23	5.1.1
121451-5547.4	59716	106444	8.553	F5V	**I?**	2800(?)	70	5.3.2
130734-5254.3	64044	113901	8.946	F5V	**I**		90	5.3.3
122455-5200.3	60567	108016	9.886	F6/7V	**I**			5.3.4
132712-5938.2	65617	116794	9.719	F7/G0V	**I**		65	paper I
121519-6325.5	59764	106506	8.562	F8/G0(V)	**I + qP**	0.58373	70, 21	5.2.1
122840-5527.3	60885	108568	9.020	G0/2	**I + qP**	1.7698	63, 59	5.2.2
120548-5100.2	58996	105070	9.022	G1V	**I + qP**	2.5832, 2.6468, 2.6568, . . .	90, 41, 22, 20	5.2.3
134309-6907.7	66941	119022	7.719	G2IV/V	**qP + I**	0.7073(v)	95(v), 56	paper I
132435-5557.4	65423	116402	9.727	(G3w)F7	**I + qP**	1.85896(a),. . .	140, < 60 (v)	5.2.4
121628-5008.6	59854	106725	9.479	G3V	**I + qP**	2.3298(a)	40, 36	5.2.5
130505-6413.9	63847	113466	9.322	G5 (V)	**I + qP**	2.91593	50, 23	5.2.6
133154-5113.5	66001	117524	9.978	G5/6V	**I**		100(?)	5.3.5
124752-5126.6	62445	111170	9.656	G8/K0V	**I**		> 300(?)	5.3.6
132548-4815.0	65517	116650	9.881	K0/2(V)+(G)	I		130	5.3.7

5.1 Variable including a periodic component

5.1.1 HD 106048 = HIP 59505

This star of spectral type A9 V (Houk & Cowley 1975) has been found by Koen & Eyer (2002) as a periodic variable from HIPPARCOS photometry, with a frequency $f = 1.66659$ cycles per day and a peak-to-peak amplitude of 33.4 millimag. The ASAS photometry reveals two frequencies with very similar amplitude. The HIPPARCOS data set spans an unusually large range of uncertainties that, in a statistical sense, deteriorate from early to more recent observations. Nonetheless a re-analysis of the HIPPARCOS photometry considering all 208 data, as well as only the 99 data with uncertainties up to 0.017 mag, shows that both power peaks are present in both data sets. The broader HIPPARCOS Scargle power peaks and the narrower (longer time baseline) ASAS peak overlap completely. Hence, assuming strict periodicity over the combined time interval and phasing both data sets together, a unique, more precise value of the frequencies can be obtained:

$$f_1 = 1.66631 \pm 0.00002 \text{ cycles per day } (P_1 = 0\overset{d}{.}600128 \pm 0\overset{d}{.}000007)$$
$$f_2 = 1.97868 \pm 0.00002 \text{ cycles per day } (P_2 = 0\overset{d}{.}505382 \pm 0\overset{d}{.}000005)$$

Phase diagrams corresponding to P_1 and P_2, respectively, for data prewhitened for the variability in the alternate period, are shown in Fig. 31. From the ASAS data the peak-to-peak variation is 0.023 mag for both f_1 and f_2. The amplitude was apparently higher at the epoch of the HIPPARCOS observations. A formal solution to the higher quality data suggests 0.037 ± 0.007 mag for both frequencies. The ASAS data obtained in 2003 ('x' symbols, HJD 2 452 622–878) show a minor offset to fainter magnitudes, presumably an instrumental zero-point offset.

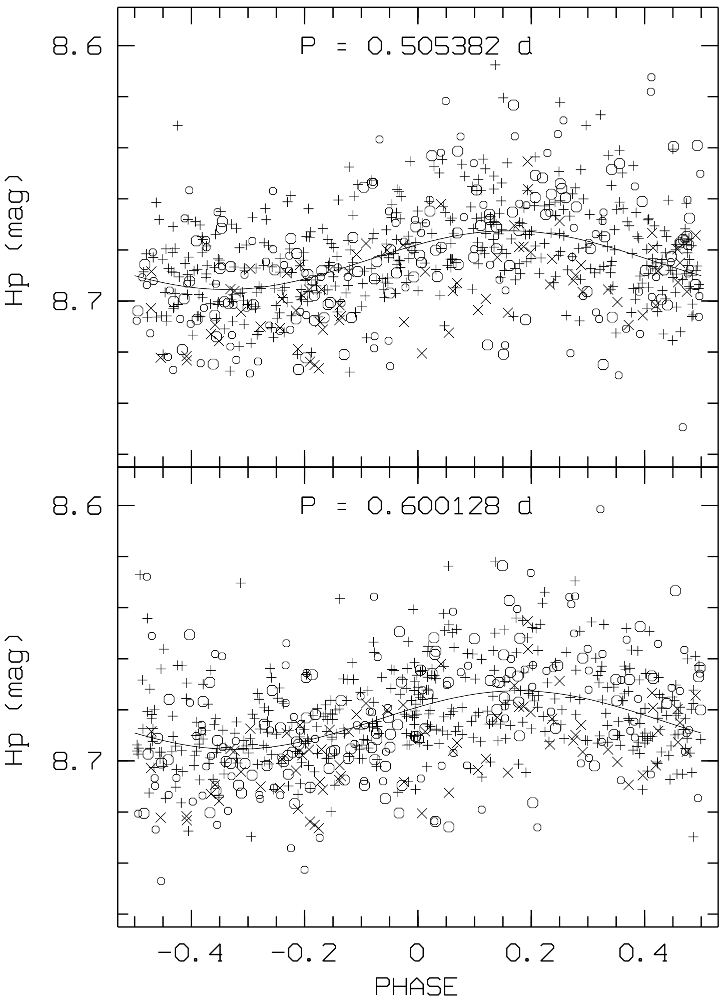

Figure 31: Light-curves of HD 106048. Phase 0.0 was taken arbitrarily at HJD 2 452 000.00. The ASAS aperture–3 magnitudes were shifted to HIPPARCOS magnitudes by adding 0.07 mag. Both panels show the data for one frequency (after removing the variation in the other frequency) and a sine fit to the ASAS data, with 0.023 mag peak-to-peak amplitude and maximum light at phase 0.177 and 0.161 for the shorter and the longer period, respectively. Symbols: 'o' HIPPARCOS data, smaller size corresponding to uncertainties larger than 0.017 mag; '+' ASAS except for data obtained in HJD 2 452 622–878 (Dec. 2002 – Aug. 2003); 'x' ASAS data obtained in HJD 2 452 622–878. Six faint and two bright data points in the set of 492 ASAS data fall out of the range of the figure.

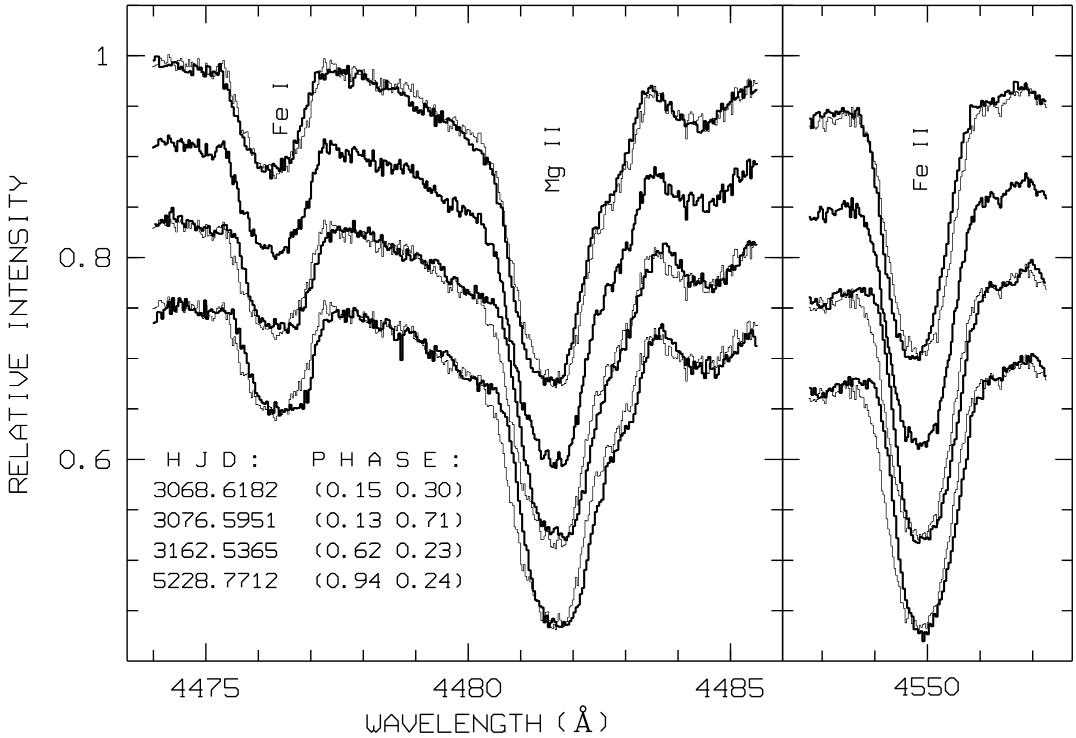

Figure 32: Positional and shape variability in selected line profiles of HD 106048. The curves are labeled with HJD – 2450000 and pulsational phase (ϕ_1 ϕ_2), with phase 0.0 as defined in the caption of Fig. 31. In order to facilitate the comparison, thin lines represent the spectrum at HJD 2 453 076.5951 shifted vertically to coincide with the other spectra.

The spectral type, the length of the periods, the modest changes in line shape and the radial velocity variations within a range of 13 km/s, as measured from four FEROS spectra (Fig. 32), are compatible with high-order, non-radial, g-mode pulsations as seen in γ Doradus type variable stars (Henry et al. 2007, 2011). The line widths indicate an apparent projected rotational velocity of 68 km/s. Analysis of the ASAS data set prewhitened for f_1 and f_2, which has a rms scatter of 16.6 millimag, hints at the presence of additional frequencies, but with a peak-to-peak variation below 0.013 mag. This requires independent confirmation. The most apparent ones are $f_3 \approx$ 1.81635 cycles per day and aliases $f_3 \pm 1$. Notice that f_3 is situated roughly mid-between f_1 and f_2.

5.2 Variables including a cyclic component

5.2.1 HD 106506 = HIP 59764

Waite et al. (2005) identify HD 106506 as a star with strong chromospheric activity and deformation of spectral lines indicating the presence of large starspots. They estimate $v \sin i$ = 80 km/s.

The ASAS photometry shows magnitudes weakening with increasing aperture, and the lowest rms is obtained for aperture 2, despite the star being slightly brighter than V = 8.5. Low-amplitude long-term variations over years are apparent (Fig. 33). In 2007, a faster brightening over 0.07 mag occurs between HJD 2 454 150–350. Another indication of a long-term trend is visible in the HIPPARCOS photometry, with magnitudes after HJD 2 448 500 being statistically brighter than before this date.

Detrending the ASAS data using the smooth (s = 12.6) cubic spline shown in Fig. 33 reveals a short cycle of $\approx 0\overset{d}{.}58373$ (Fig. 34), with a peak-to-peak variation of 0.021 mag. The cycle length is compatible with the rotational modulation of the light by starspots given the $v \sin i$ of Waite et al. and a radius of the order of the solar radius ($R \sin i$ = 0.92).

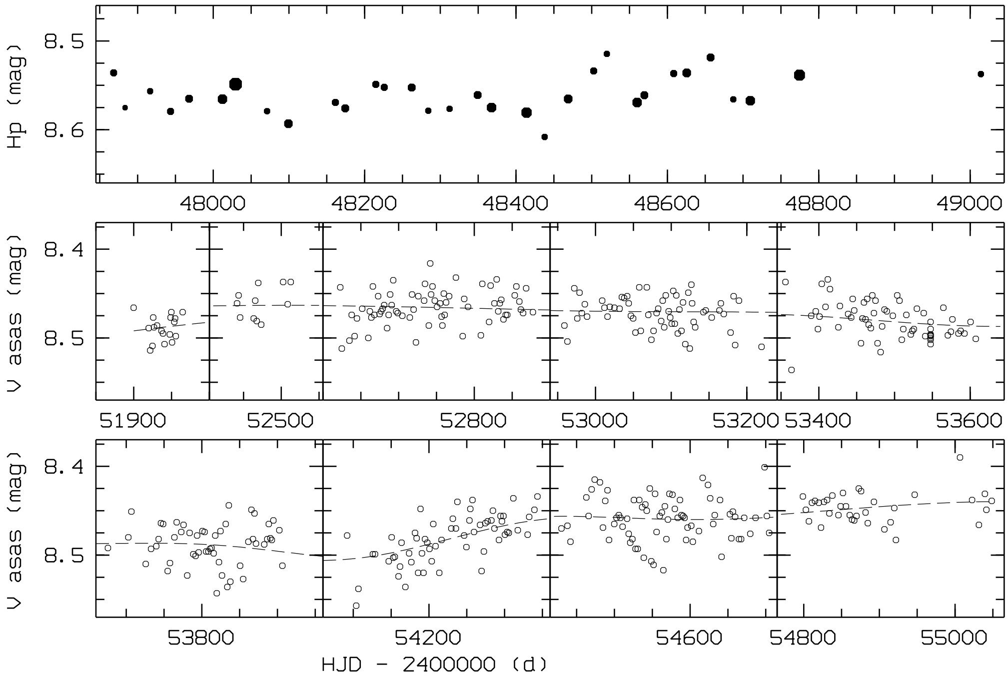

Figure 33: HIPPARCOS and ASAS aperture–2 photometry of HD 106506. The dashed line in the ASAS panels is a tentative smoothed (s = 12.6) cubic spline representation of long-term trends. Increasing size of the symbols in the panel with the HIPPARCOS data indicates averages over 1–10 measurements within a day.

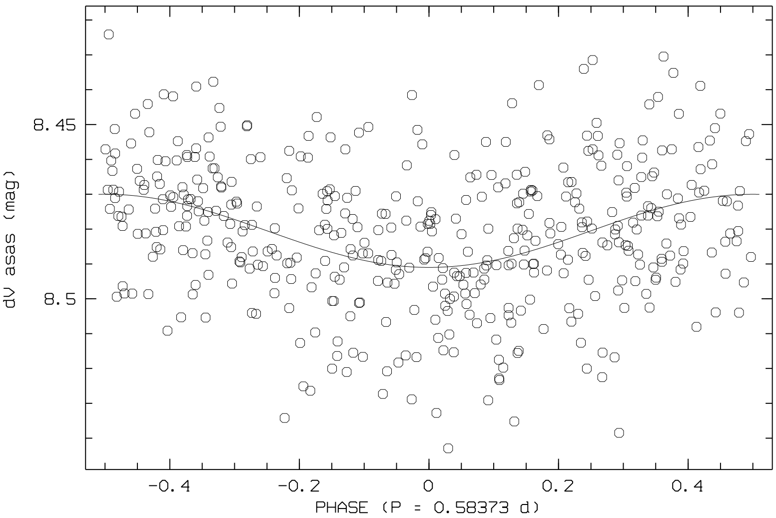

Figure 34: ASAS aperture–2 photometry of HD 106506 folded on a period of $0^{\rm d}.58373$, with phase 0 at HJD 2 453 653.317 (minimum light in a sine fit with peak-to-peak amplitude of 0.021 mag).

At some epochs, HIPPARCOS obtained several observations within a significant part of such cycle (in particular on HJD 2 448 029 and HJD 2 448 367), but the data do not support the findings from ASAS. Neither the total HIPPARCOS set, nor shorter subsets presumably less sensitive to long-term trends, support it, suggesting that the life time of the starspots is less than the time separation between the two data sets.

5.2.2 HD 108568 = HIP 60885

HD 108568 is a Li-rich G0 IV subgaint following Mamajek et al. (2002), who labelled it therefore as "PMS?". Chen et al. (2011) give $v \sin i$ = 56 ± 4 km/s. The ASAS photometry shows a long-term trend in the early observations (Fig. 35), as well as a fairly weak indication of a short-term periodicity when the whole sample is analysed. However, a closer look reveals that the power detected near f = 0.566 cycles per day is due to a subset of data (Fig. 36). The photometry

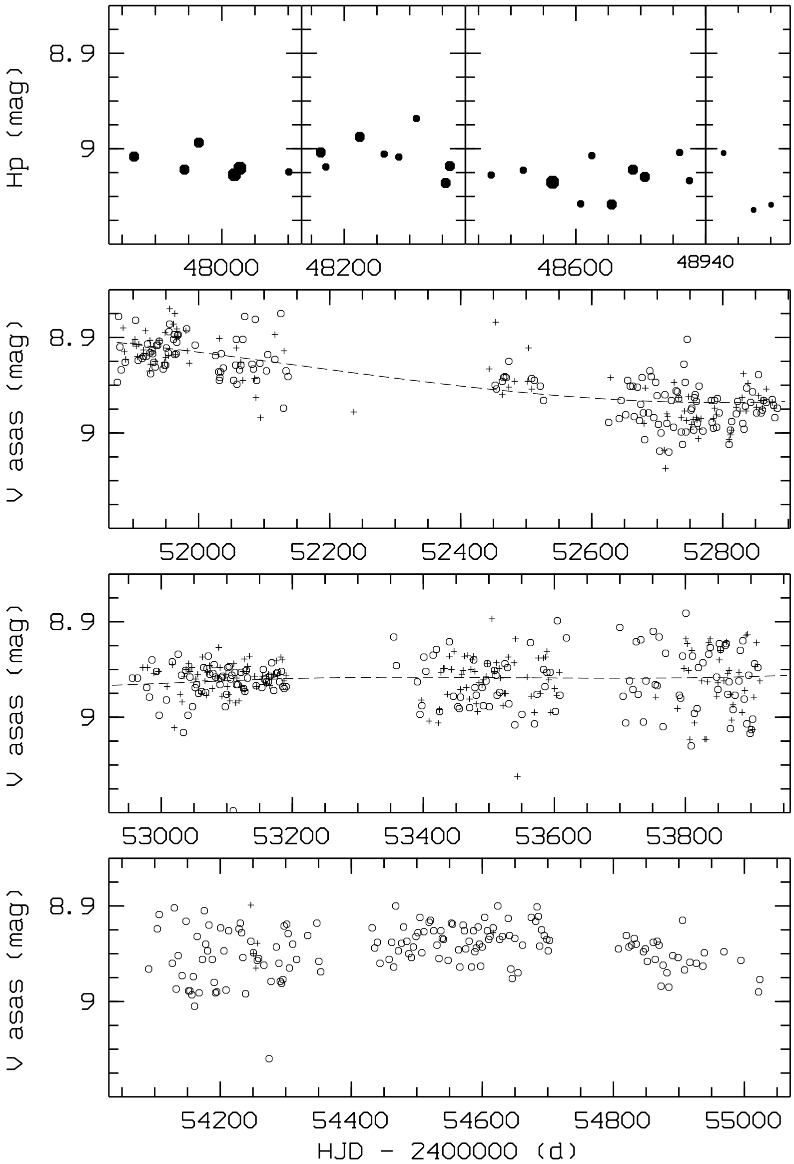

Figure 35: Long-term trends in the aperture–3 ASAS and the HIPPARCOS photometry of HD 108568. Three sizes of symbols refer to the average of respectively 1–3, 4–6 and 8–9 HIPPARCOS measurements obtained in less than two days. Only the 101 individual data with uncertainties up to 0.020 mag were included. ASAS data sets (Table 1) are represented by different symbols in the mid- and lower panels. The dashed line traces a tentative smoothed (s = 19.5) cubic spline long-term detrending.

obtained in the interval 2005–2007 is well represented by a sine fit with a peak-to-peak variation 0.059 mag and a period of $1^{\mathrm{d}}.76982$ (minimum light at HJD 2 453 794.445). In 2008 and 2003 the variation is still easily discernible, but with a lower range of 0.036 and 0.026 mag, respectively, and a slightly different cycle length (Fig. 36). In the earlier and (sparse) most recent data, the cycle is not detectable and this cannot be attributed to the uncertainties in the long-term detrending.

The HIPPARCOS data give an inconclusive signal in the range of the frequencies detected by ASAS. A detailed study suggests that the data taken before HJD 2 448 030 and those taken after HJD 2 448 560 support $P \approx 1^{\mathrm{d}}.7669$ with a peak-to-peak variation of 0.039 mag (Fig. 36), although it is not an independent detection. A slow brightening of the star during part of the intermediate time interval (Fig. 35), which is not easily removed in an objective way, significantly influences the power diagrams for the complete data set (see zoom window in upper part of Fig. 36). If this is a spotted variable, we can estimate $R \sin i$ = 2.0 solar radii.

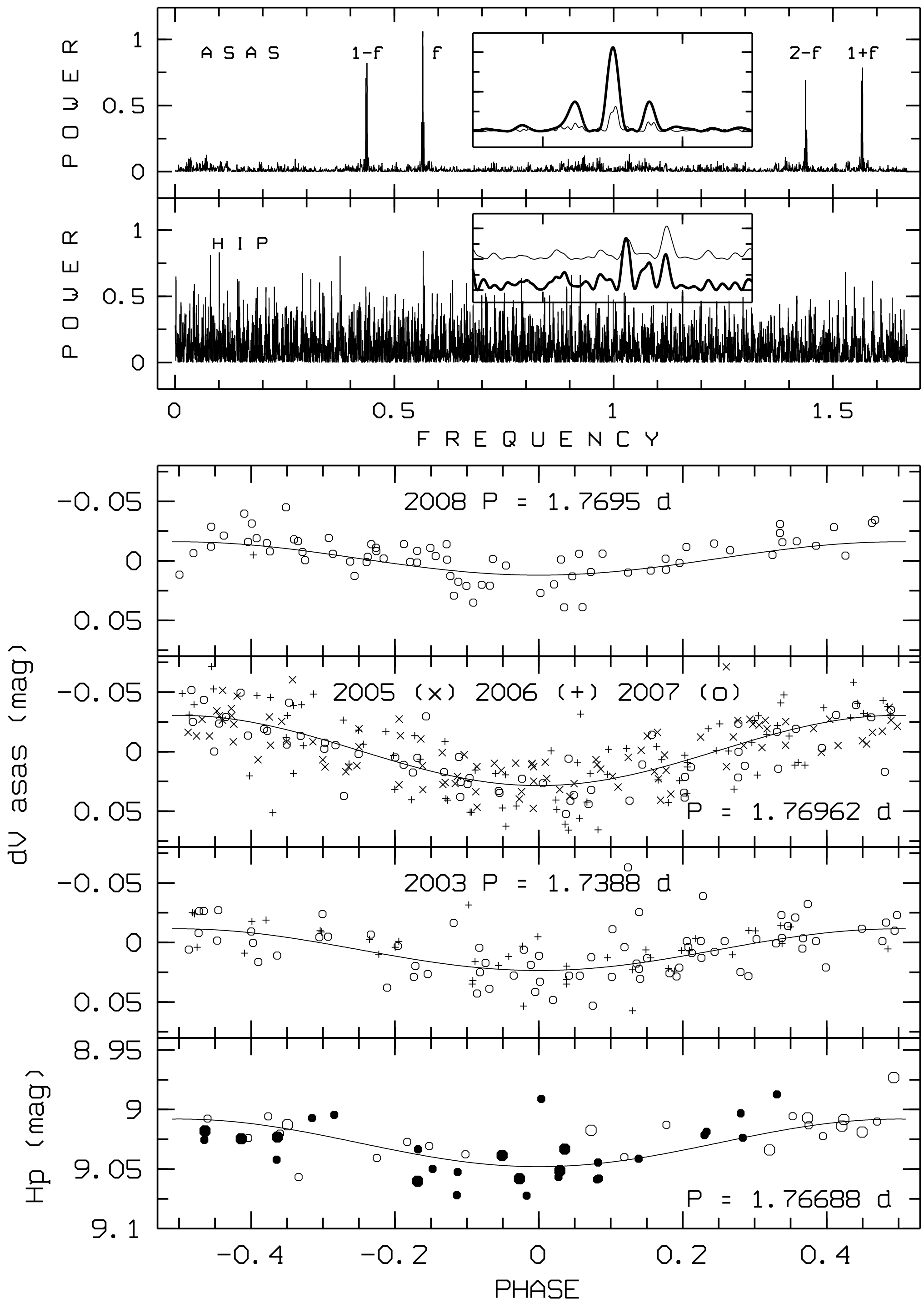

Figure 36: Evidence for a short-term cycle in HD 108568. The upper part of the figure shows the Scargle power for the 2005–2007 ASAS data and for the selected HIPPARCOS data (see text). The zoom window shows the power for these sets around f with a thick line, and for the complete ASAS set and for all 101 HIPPARCOS data with uncertainties up to 0.02 mag with a thin line (shifted by 0.5 in the HIPPARCOS panel). Tickmarks on the horizontal axes in the zoom window correspond to $f = 0.56$ and $f = 0.57$ cycles per day. The lower four panels show the phase diagrams at different times (cycle length indicated in the figure) with the sine fits discussed in the text. In the HIPPARCOS panel, open circles refer to the data obtained before HJD 2 448 030 and filled symbols to those obtained after HJD 2 448 560, with larger sizes for paired observations. In the ASAS panels, 'o' and '+' symbols refer to the two data sets, as in Fig. 35, except for the 2005–2007 panel that discerns between data obtained in different years. In the latter panel, two anomalously faint measurements are not shown, and another one falls outside the range of the panel with the 2003 data. Size and time coverage of the subsets are as follows: 2003: 115 data in HJD 2 452 625–883; 2005: 98 data in HJD 2 453 354–618; 2006: 86 data in HJD 2 453 699–913; 2007: 60 data in HJD 2 454 090–353 and 2008: 71 data in HJD 2 454 431–702.

5.2.3 HD 105070 = HIP 58996

Wichmann et al. (2003) identify HD 105070 as member of a tight kinematical group of ten very young and highly active G-type stars with extremely high lithium equivalent widths, yet at the same time showing a large dispersion in space. In another paper, Wichmann & Schmitt (2003) argue that these stars are dispersed in the field from either LCC, UCL or Per OB3. HD 105070 was identified as a light variable in the HIPPARCOS catalogue. The ASAS photometry reveals that the major part of the light variability is irregular on a long-term scale (Fig. 37). The tentative smoothed (s = 16) cubic spline detrending shown in that figure allows us to detect underlying periodic or cyclic variability (Fig. 38). While the HIPPARCOS data are too sparse for such detrending, and cannot uniquely reveal periodicity, the subset obtained before the fading between HJD 2 448 520–600 (limited further to the 82 data with uncertainties of 0.020 mag and less) shows power at the primary frequency detected in the ASAS data, even without any long-term detrending. One of the highest Scargle power peaks is situated at $f_{\rm hip}$ = 0.3881 cycles per day, overlapping with $f_{\rm ASAS}$ = 0.387118 cycles per day. The longer HIPPARCOS series of data obtained within a substantial fraction of a day at HJD 2 448 030.55–31.26, HJD 2 448 165.67–66.65 and HJD 2 448 168.07–69.05 do not lend any support for the power peaks detected in the ASAS data at higher frequencies aliased to $f_{\rm ASAS}$, above one cycle per day.

After prewhitening the ASAS data for $f_{\rm ASAS}$, there remains significant power in the frequency interval 0.37–0.38 cycles per day. Hence, we analysed yearly subsets to investigate how persistent are the multiple peaks (Fig. 38) in this range. The strongest frequency in the subsets corresponds to the strongest one in the total set only for the years 2004 (HJD 2 452 962–3 190), 2007 (HJD 2 454 106–340) and 2008 (HJD 2 454 430–703), but remains distinguishable in other years. In the remaining four years, the subsets show a stronger peak at the position of the next two frequencies in the total set, which remain unresolved in the yearly sets: f_1 = 0.37782 cycles per day and

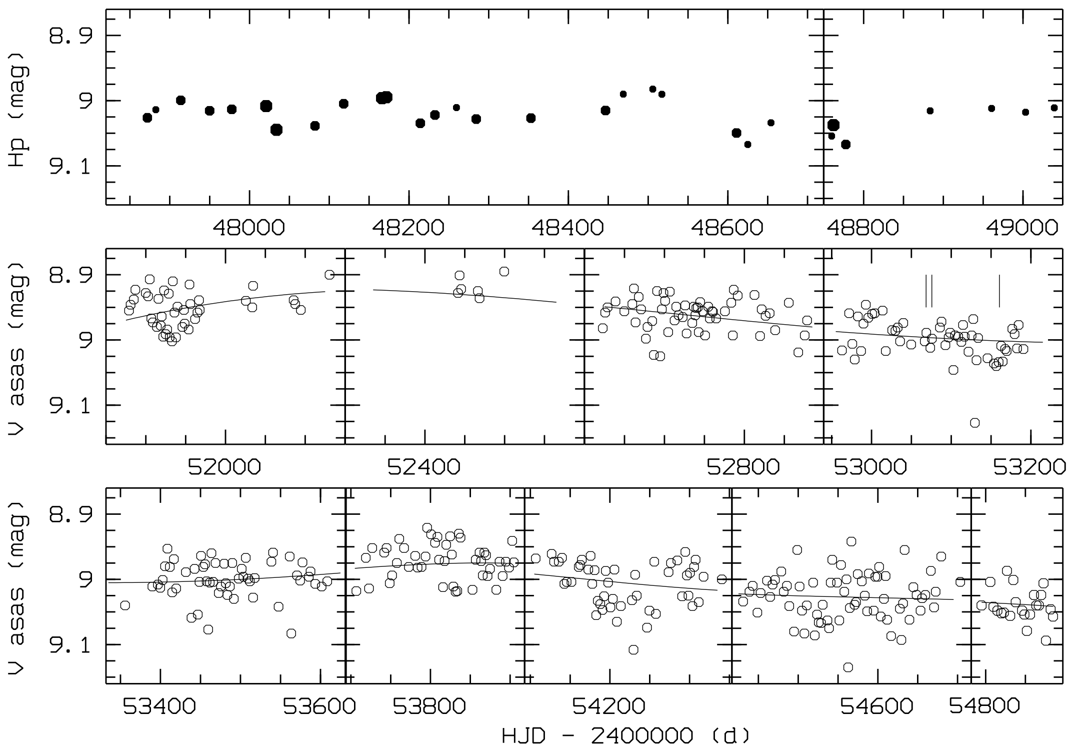

Figure 37: Light variability of HD 105070. HIPPARCOS photometry is averaged over series within a day, increasing symbol size representing 1–2, 3–6 and 9–15 measurements. Only individual measurements with uncertainties of 0.020 mag or less were included. The ASAS aperture–3 photometry is shown with the smoothed (s = 16) cubic spline used for long-term detrending. Three vertical lines in the right-hand side panel in the middle row indicate the times at which spectra were taken.

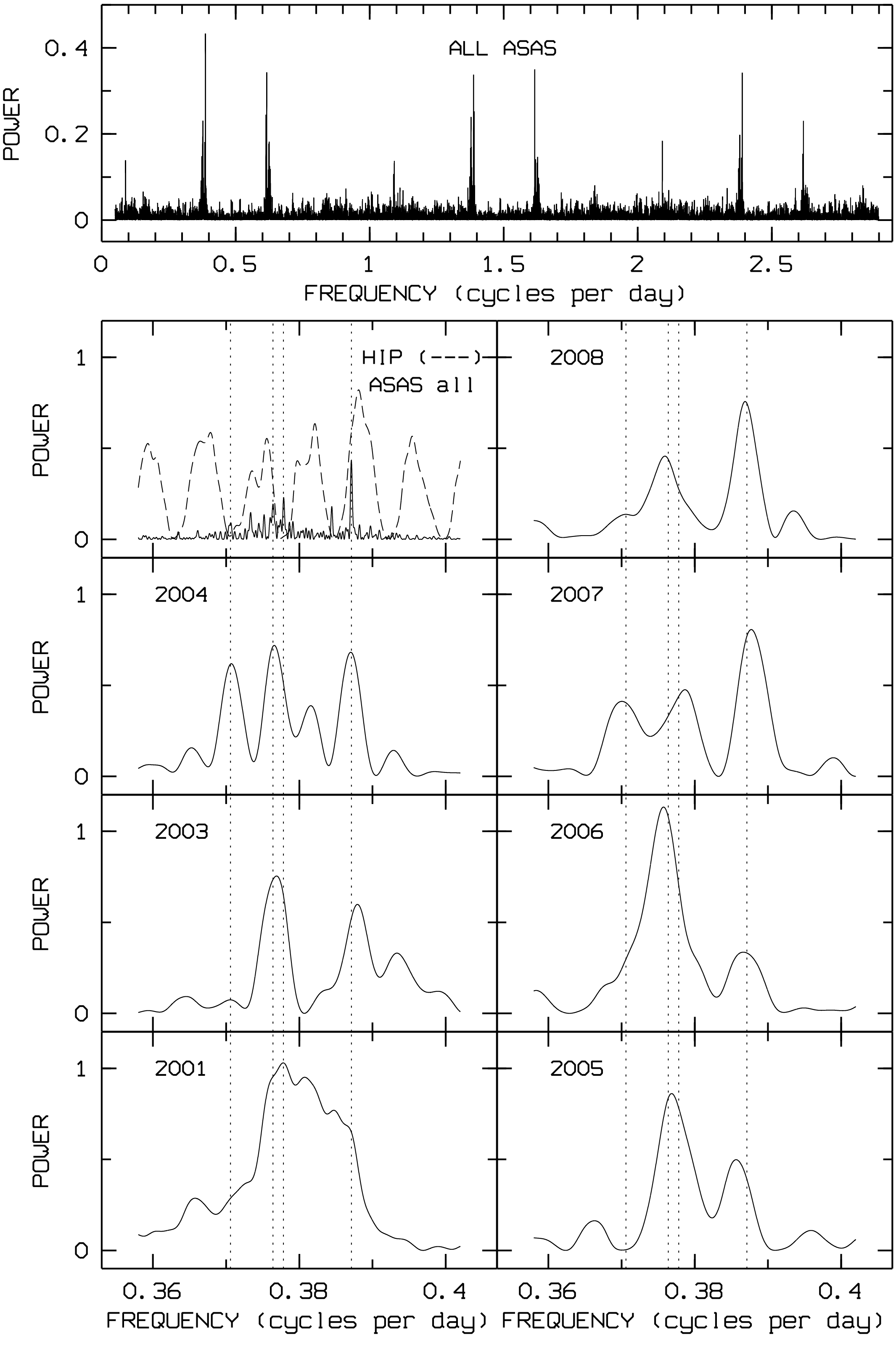

Figure 38: Frequency analysis of HD 105070 for all selected ASAS data (upper panel) and yearly subsets. Smaller panels zoom in on the 0.36–0.4 cycles per day frequency interval for the indicated year and for the HIPPARCOS subset defined in the text. The latter panel also shows the result for the complete ASAS set. Vertical dashed lines refer to the frequencies discussed in the text. The number of data in yearly subsets is 41 (2001; HJD 2 451 878–2 130), 56 (2003; HJD 2 452 622–878), 52 (2004; HJD 2 452 962–3 190), 54 (2005; HJD 2 453 355–608), 47 (2006; HJD 2 453 718–904), 49 (2007; HJD 2 454 106–340), and 68 (2008; HJD 2 454 430–703).

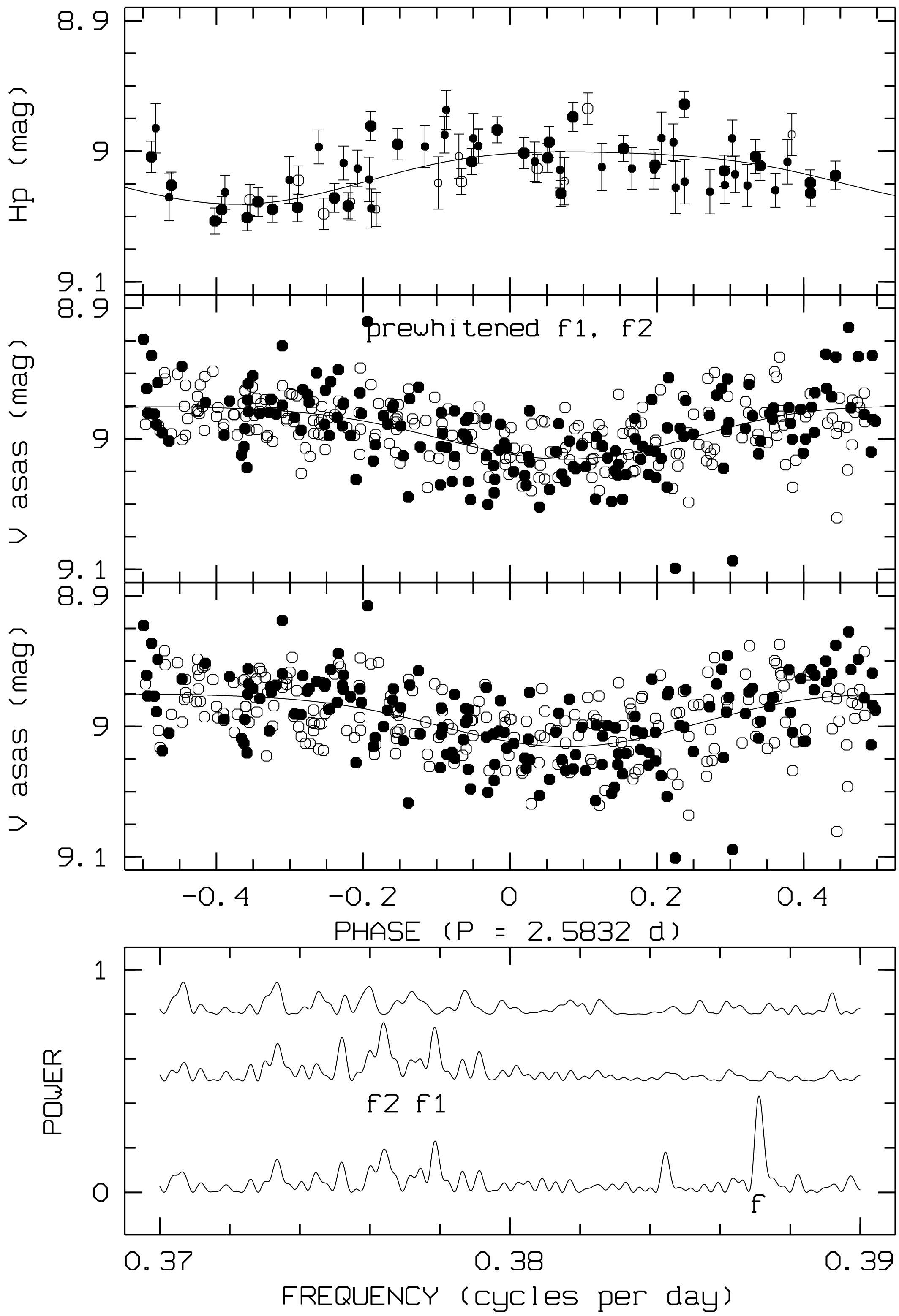

Figure 39: Short-term light variability of HD 105070. Lower panel: Scargle power functions for the long-term detrended ASAS aperture–3 data (bottom), and, shifted upwards, after prewhitening for f (middle) and additionally for both f_1 and f_2 (top). The other panels present phase diagrams for the main frequency f. From bottom to top: long-term detrended ASAS data; same data prewhitened for f_1 and f_2; and the HIPPARCOS data. No long-term detrending was applied to the latter, but data in the time interval HJD 2 448 600–800 (open circles) were shifted upwards by 0.03 mag. Larger symbols represent paired observations. One ASAS data point (out of 396) falls outside the figure. The curve is the model for the ASAS data ($8.992 + 0.0199 \cos 2\pi(\phi - 0.0689) + 0.00372 \cos 4\pi(\phi - 0.0877)$), shifted 0.025 mag down and −0.45 in phase in the HIPPARCOS panel. Phase zero is at HJD 2 453 541.7116. In the ASAS panels, filled symbols refer to the years 2004, 2007 and 2008 (see text).

f_2 = 0.37639 cycles per day. This peak is particularly prominent (relative to f_{ASAS}) in 2005 (HJD 2 453 355–608) and 2006 (HJD 2 453 718–904). A fourth frequency reaches comparable amplitude in 2004 (HJD 2 452 962–3 190) and 2007 (HJD 2 454 106–340), f_3 = 0.3706 cycles per day.

The phase diagram corresponding to f_{ASAS} does not reveal any systematic difference between the shape defined by the data of the years 2004, 2007 and 2008, and those where the power peak is not the dominant one (Fig. 39). Nor are there obvious phase shifts. This remains true after prewhitening the data for the next strongest two frequencies. This suggests that a strict periodicity for this mode cannot be excluded based on the ASAS data alone. The data are better represented if we include a second order Fourier term allowing for a faster rise to maximum light. Applying strictly the main ASAS frequency to the HIPPARCOS data results in a large phase shift. A 3σ change in frequency to $f = 0.38703$ cycles per day reconciles the phases at the expense of a slightly worse fit for the ASAS data.

The power peaks at f_1 and f_2 each have similar heights, twice smaller than the one at f_{ASAS}. Hence sine fits were made simultaneously. Whether these frequencies correspond to strict periodicity or cyclic character is not clear, in view of the beat period of 700 days. Further prewhitening suggests additional frequencies below f_2. The lowest one is the frequency f_3 that appears resolved in some yearly subsets. However, at this level it becomes inappropriate to interpret the ASAS data any further. We tentatively conclude that a strictly periodic component at frequency f_{ASAS} might be hidden in a more complex variability pattern. The length of any of the period(s) is not incompatible with a rotation period ($v \sin i$ = 32–35 km/s (Wichmann et al. 2003; Torres et al. 2006; Chen et al. 2011, respectively) implying $R \sin i$ = 1.7 solar radii).

Three spectra were obtained within three months in 2004, at phases 0.85, 0.60 and 0.43 with respect to the $2\overset{\mathrm{d}}{.}583272$ period (phase 0.0 as defined in Fig. 39); the last one is very similar to the second one (with a slight Dopper shift) and is not shown in Fig. 40 to avoid confusion. The spectra exhibit substantial chromospheric emission in the Ca II H and K lines (reported earlier by Chen et al. 2011). In addition, the line profiles (and principally those from weaker lines) at phase 0.85 are different from those in the other two spectra, obtained near to maximum brightness in the short cycle, where they are very similar. Hence, spectrum variability (also in a quite subtle way in the strength of the Ca II emission and the H α line profile) might be linked to this short cycle.

Finally, we measure in the three spectra a radial velocity of 16.6 ± 0.6 km/s (rms uncertainty), in contrast to published measurements of 11.9 km/s (Wichmann et al. 2003) and 13 km/s (Torres et al. 2006). While the latter agree within their quoted uncertainties, ours hint at the possibility that the star is a long-period spectroscopic binary. If confirmed, it would place the star nearer to the main-sequence than concluded presently (Wichmann et al. 2003). This also raises the question whether the complex light variability has contributions from two objects.

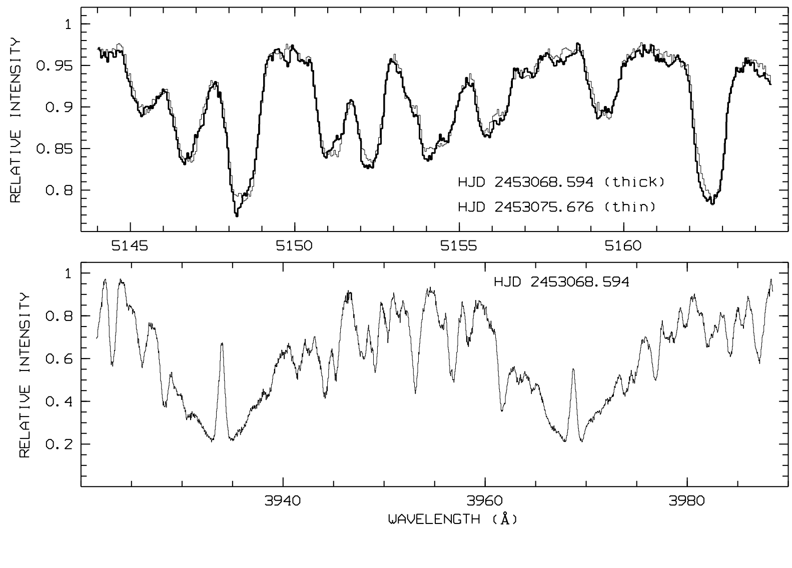

Figure 40: HD 105070: chromospheric emission in the Ca II lines (bottom panel) and subtle line variability shown in a wavelength region slightly blueward of the prominent Mg I lines.

5.2.4 HD 116402 = HIP 65423

HD 116402 is a single, fast-rotating solar type star (35 km/s, Cutispoto et al. (2002); 27 ± 2 km/s, Chen et al. (2011)). The ASAS photometry shows long-term irregular variations with a peak-to-peak amplitude of 0.14 mag as indicated by a smoothed ($s = 14$) cubic spline representation (Fig. 41). Detrending lowers the rms of the aperture–3 photometry from 40 to 26 millimag.

A period search after detrending shows power at several frequencies (Fig. 42). Aliasing due to the once-per-night observing strategy distributes power over frequencies f and, approximately, $1 - f$, $1 + f$ and $2 - f$ in a way that does not allow us to definitely favour frequencies around 0.5 cycles per day over those around 1.5 cycles per day. Multiple power peaks are present near 0.46, 0.54, 1.46 and 1.54 cycles per day, and their power varies significantly from one yearly subset to the next.

A straightforward multiple-period analysis on the whole set suggests $f_1 \approx 0.53793$ cycles per day as the main frequency (with the three next strongest peaks being aliases, and the fourth strongest enhanced by an alias, as prewhitening shows) followed by $f' \approx 1.44976$ cycles per day, originally the fifth strongest peak. But because of aliasing, it is possible that the true frequencies are much nearer one to the other, for example f_1 and $f_2 = 2 - f'$ would differ only by 0.015 cycles per day. Not all power disappears accounting for f_1 and f', or for aliases of them. Prewhitening even slightly strengthens a less prominent power peak at a much lower frequency of ≈0.0987 cycles per day (and at some aliases of it).

If we assume that we are dealing with a differentially rotating spotted variable exhibiting spot-latitude dependent effects varying with time, and that f_1 and f_2 are the main rotational frequencies, then $R \sin i$ estimates permit us to favour the frequencies around 0.5 cycles per day. The f_1 frequency would imply $R \sin i = 1.3$ solar radii.

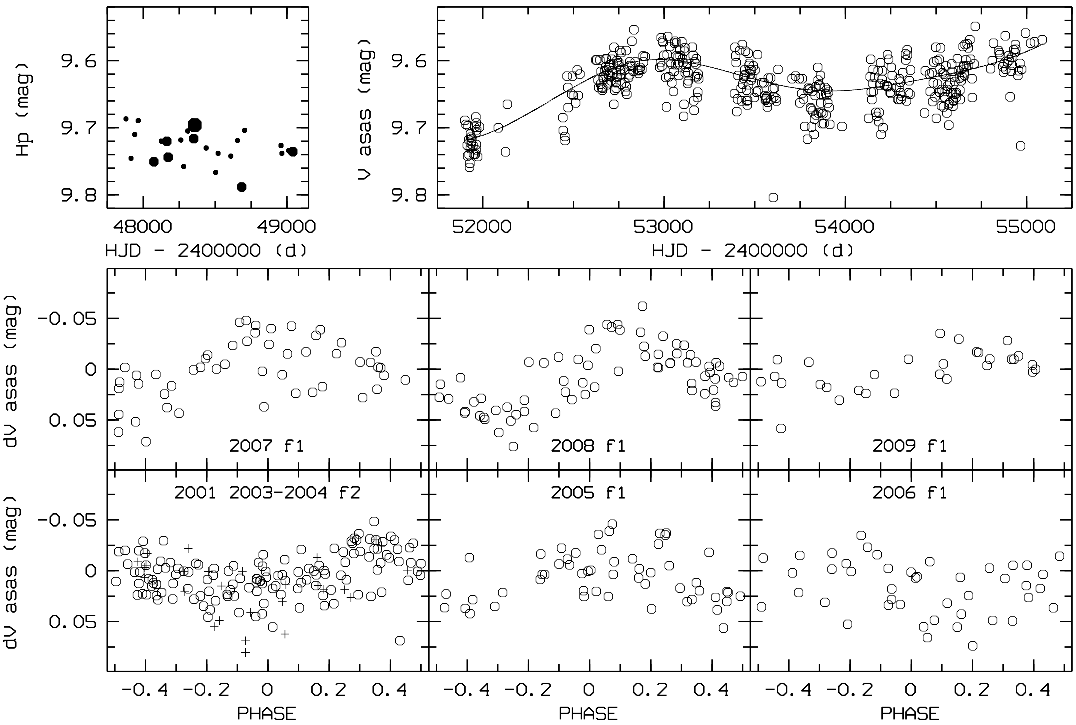

Figure 41: Photometry of HD 116402. Upper panels show the HIPPARCOS data, averaged over ≈ 1 day, and the ASAS aperture–3 data with the applied long-term trend (smoothed cubic spline, $s = 14$). Three anomalously faint ASAS measurements (out of a total of 425 data) are not shown. Increasing symbol sizes in the upper left panel indicate averaging over 1–3, 4–7, and 15 HIPPARCOS observations. The lower panels show phase diagrams for subsets of data with $f_1 = 0.53793$ cycles per day (see Fig. 42 for size and time range), except for the earliest data (173 data, left bottom panel) that are shown with a slightly different frequency $f_2 = 0.5529$ cycles per day. In this panel, '+' symbols indicate the data after HJD 2 453 140 (mid-May 2004). The data were detrended as shown in the upper right panel.

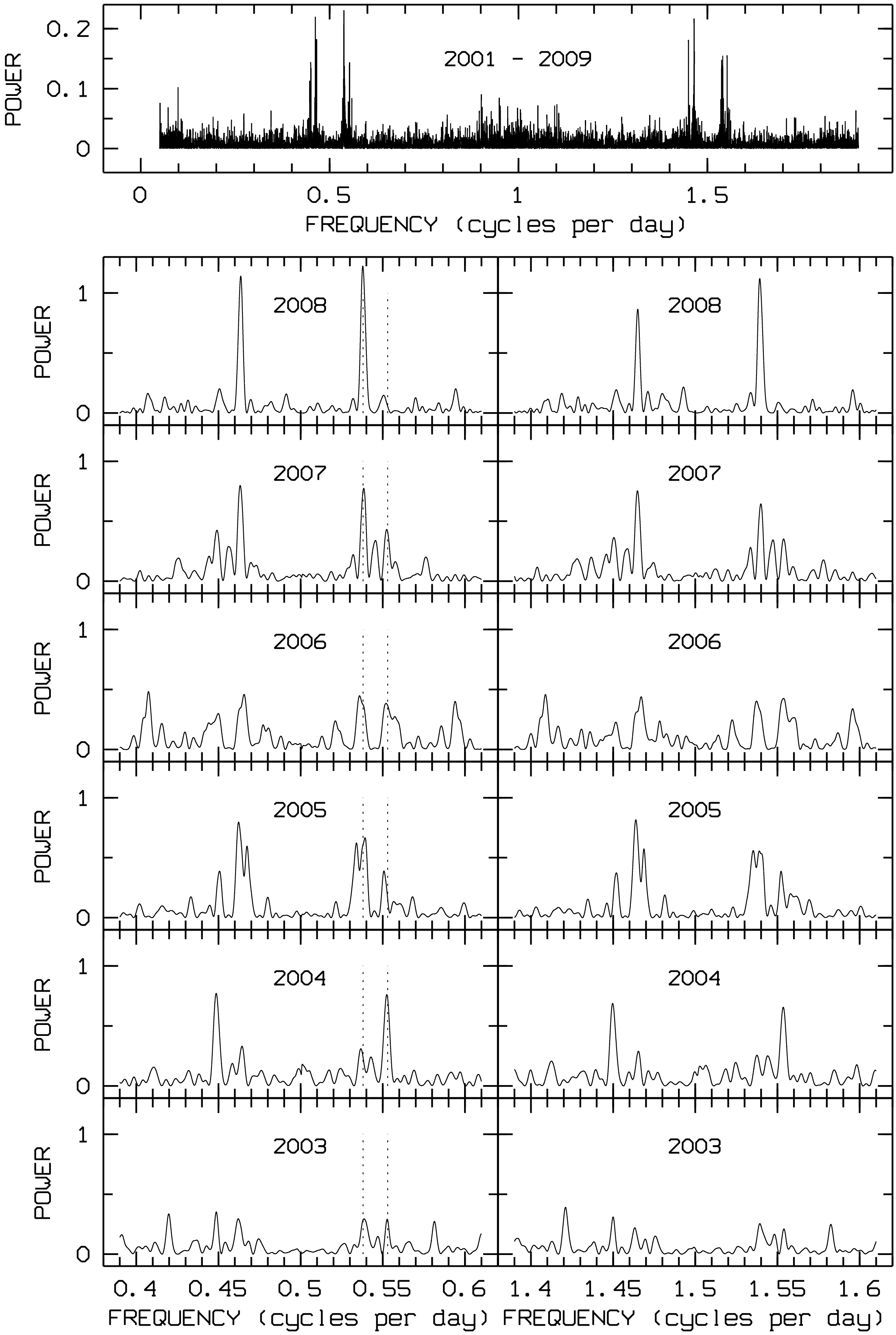

Figure 42: Frequency spectrum of the long-term detrended data of HD 116402 for all data (upper panel), and around the main frequency peaks for yearly subsets (2003: 72 data in HJD 2 452 623–895; 2004: 56 data in HJD 2 452 975–3 190); 2005: 54 data in HJD 2 453 387–628); 2006: 44 data in HJD 2 453 705–981; 2007: 50 data in HJD 2 454 127–359; 2008: 70 data in HJD 2 454 436–716). The dashed vertical lines indicate f_1 = 0.53793 and f_2 = 0.5529 cycles per day.

The HIPPARCOS data do not reveal any of these frequencies, even if only the 82 data with uncertaincies of 0.025 mag and less are selected. This is understandable in view of the smaller size of the sample, the complex variability pattern revealed by the ASAS data, and the dominating long-term irregular variations that are hard to estimate from the sparser data over the shorter HIPPARCOS baseline. This star deserves a detailed light analysis with better sampling at shorter time scales, eliminating the severe alias problems in the present data set. Table 4 mentions only the dominant frequency as indicator of quasi-periodicity.

5.2.5 HD 106725 = HIP 59854

HD 106725 is a G1IV pre-main sequence (Mamajek et al. 2002) binary with a separation of 0.2 arcseconds (CCDMJ12165-5009AB). It shows smooth, low-amplitude light variations (Fig. 43), and short-term cyclic variability characteristic of BY Dra-type variables. The ASAS data show significant power at frequencies near 0.43 and 0.57 cycles per day, and higher-frequency aliases. The HIPPARCOS data, although insufficient to provide a unique response, show power nearby the forementioned frequencies (the highest power peak being near 0.57 cycles per day) and allow us to exclude the aliases at higher frequencies (Fig. 44), as well as to exclude strict periodicity. A deeper analysis of ASAS subsets for different time intervals clarifies that the power peaks are almost entirely due to data obtained after November 2005 (HJD > 2 453 706). A sine fit for this subset at $f = 0.42922$ cycles per day removes all other significant power peaks. The peak-to-peak amplitude is 0.036 mag.

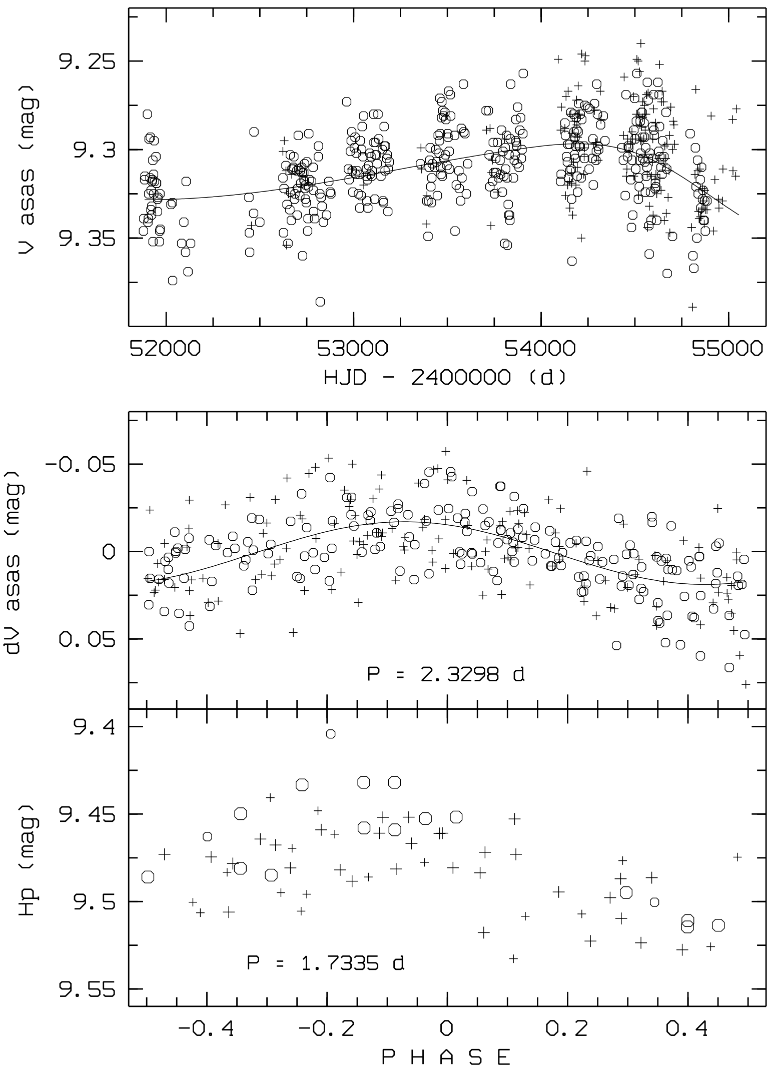

Figure 43: Upper panel: ASAS aperture–4 photometry of HD 106725 and assumed long-term variability represented by a smoothed ($s = 17.5$) cubic spline. Two faint measurements out of 550 fall outside the magnitude range shown in the figure. Mid panel: ASAS residuals after subtracting the long-term drift and folded on the detected cycle length. In both panels, 'o' and '+' correspond to the two data sets mentioned in Table 1. The smaller '+' set was shifted to 0.006 mag fainter magnitudes. The overplotted curve is a sine with peak-to-peak amplitude of 0.036 mag and maximum light at HJD 2 452 647.165. Lower panel: HIPPARCOS data folded on the alternative cycle length (see Sect. 5.2.5). 'o' symbols correspond to the subset obtained in 10 days in May 1990 (HJD 2 448 021–030). Larger symbols represent paired observations. Phase 0.0 corresponds to HJD 2 454 385.0 (mid panel) and HJD 2 448 307.0 (bottom panel), respectively.

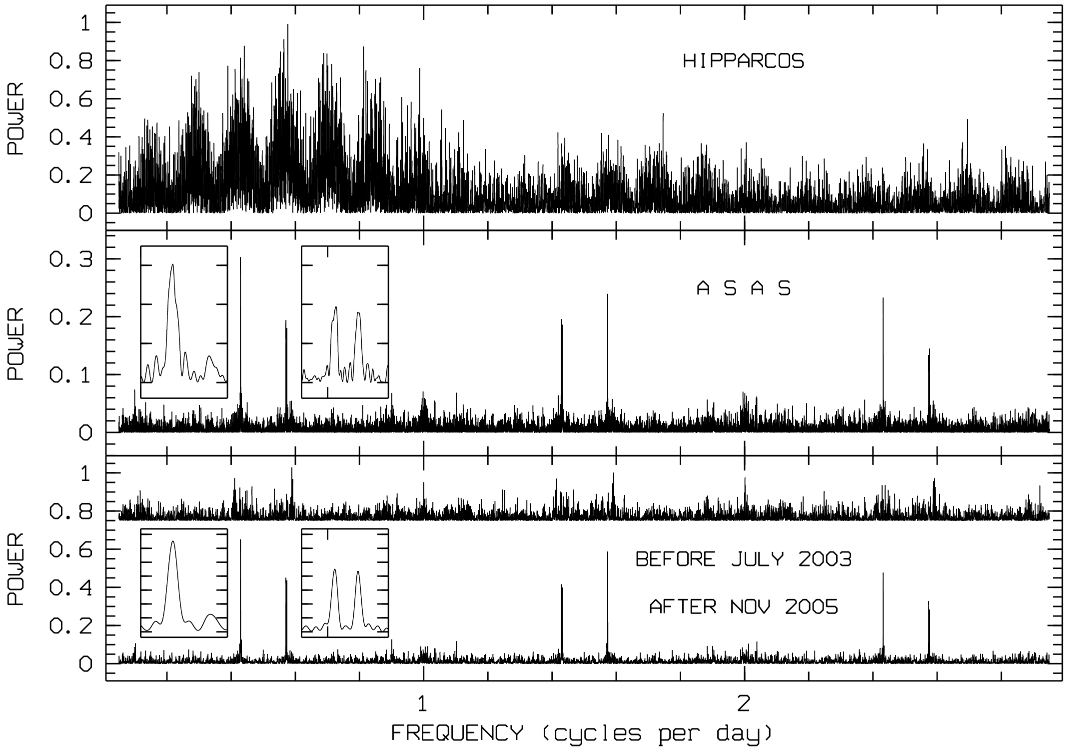

Figure 44: Scargle analysis of HD 106725; Upper panel: HIPPARCOS data. A subset of 113 data points with uncertainties up to 0.026 mag was used. Data taken with time differences of 20 minutes were averaged. Mid panel: all selected ASAS data. Details are shown for intervals $f = 0.43 \pm 0.003$ and $f = 0.572 \pm 0.005$. Lower panel: same for the 322 data points obtained after November 2005 (HJD > 2 453 706) and, shifted upwards by 0.75, for the 170 data points obtained before July 2003 (HJD < 2 453 200). The analysis of the ASAS data was made after detrending using the smoothed $s = 17.5$ cubic spline shown in Fig. 43.

5.2.6 HD 113466 = HIP 63847

HD 113466 is a post-T Tauri mid-G star showing low-level long-term light variability over 0.05 mag, and in addition a cyclic variability in $\approx 2\overset{d}{.}9159$ with a peak-to-peak amplitude of 0.023 mag (Fig. 45). The figure shows the data prewhitened for the long-term or the cyclic variability in the upper and lower panel respectively. The long-term trend was modelled by a smoothed ($s = 15.5$) cubic spline, the cyclic variability by the sine model mentioned above, with phase 0.0 corresponding to HJD 2 453 670.906. After prewhitening for the cyclic variability, the rms in the yearly subsamples is reduced in all but one of them, indicating that the cycle was rather persistent over the covered decade.

These conclusions cannot be confirmed independently using the HIPPARCOS data, nor can it be firmly denied that a similar short cyle would be hidden in the HIPPARCOS data. Firstly, the uncertainty on the long-term trend is large. Secondly, the power spectrum is sensitive to the choice of a cut-off in uncertainty on the data to be used in the analysis. Actually this choice can be made so that there is a peak for a cycle one percent shorter than the one revealed by ASAS (65 data with uncertainties up to 0.023 mag, and without application of any long-term detrending); however, within this selection the data before HJD 2 448 030 and those after HJD 2 448 610 respectively, concentrate on different phases of the cycle. Therefore there is a risk of artificially ‘improving’ the phase diagram by the application of a subjective long-term detrending. If we assume that the short-term variations have a rotational origin, using $v \sin i = 33$ km/s (Chen et al. 2011) implies $R \sin i = 1.9$ solar radii.

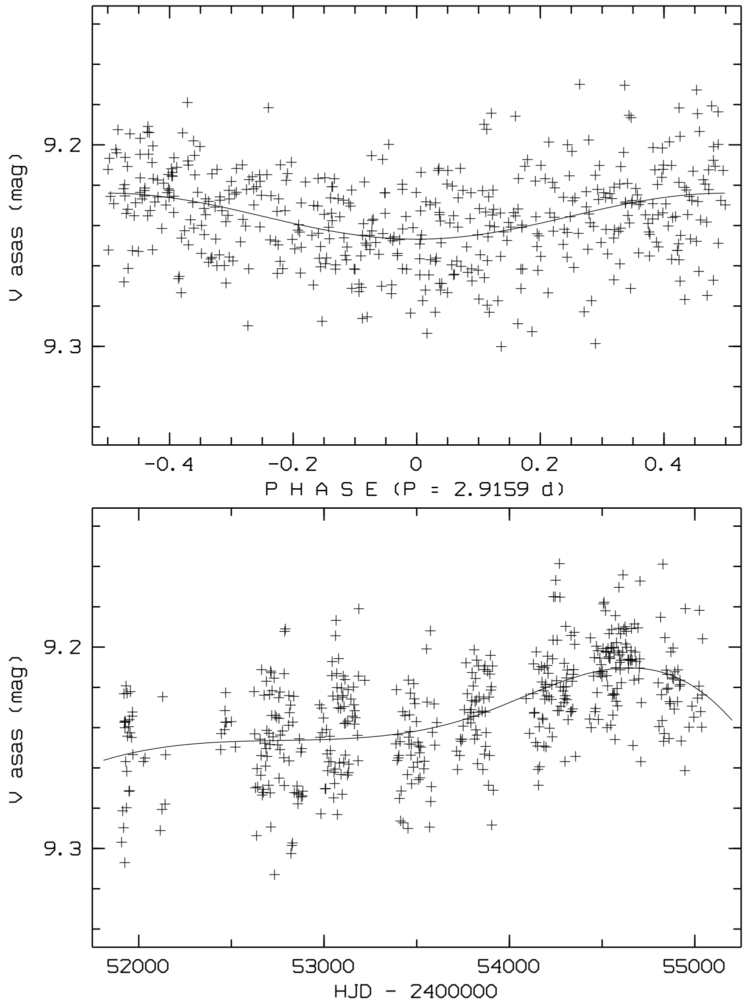

Figure 45: Aperture–4 ASAS data of HD 113466. Upper panel: phase diagram after long-term detrending with the smoothed (s = 15.5) cubic spline shown in the lower panel. Lower panel: ASAS data after prewhitening with the sine curve plotted in the upper panel (peak-to-peak amplitude 0.023 mag, phase 0 corresponding to HJD 2 453 670.906). Two data points fainter than V = 9.35 (out of a total of 464) are not shown.

5.3 Irregular variables

5.3.1 HD 100453 = HIP 56354

HD 100453 is an isolated, ≈10 Myr old Herbig A9Ve star with a 0.2–0.3 solar mass M4V weak-lined T Tauri companion at ≈120 a.u. (Chen et al. 2006; Collins et al. 2009). It shows evidence for circumstellar dust through an infrared excess, without silicate emission bands shortward of 30 μm (Meeus et al. 2002). Guimarães et al. (2006) estimate $T_{\rm eff}$ = 7400 K, $\log g$ = 4.2 and $v \sin i$ = 48 km/s. Malfait et al. (1998) estimate E($B - V$) = 0.08 with a minor part (0.02) due to interstellar extinction. Collins et al. (2009) present a very detailed multi-wavelength analysis of the stars and their environment, suggesting that the disk is in an unusual evolutionary state between a gas-rich protoplanetary disk and a gas-poor debris disk.

The star is an unsolved light variable of HIPPARCOS. Analyzing the 32 series of up to 12 measurements obtained within up to 20 h, no strong evidence of fast variability is found; therefore we formed average values that are displayed in the upper panels of Fig. 46, with error bars computed from the individual uncertainties listed in the catalogue. Three consecutive series within a time interval of 70 days between HJD 2 448 700 and HJD 2 448 800 are 0.06–0.08 mag fainter than the bulk of the observations and cause the variability classification. Fluctuations among the other series do not exceed 0.02 mag, taking into account the noise contributions.

The two ASAS sets each contain roughly 400 selected observations (Table 1). The middle and lower panels of Fig. 46 illustrate a constant or very slightly fluctuating brightness level with very rare obscuration events within the 0.1 mag range. The occurrence of two such events with a separation of roughly 50 days around HJD 2 453 000 suggest that the HIPPARCOS event may be

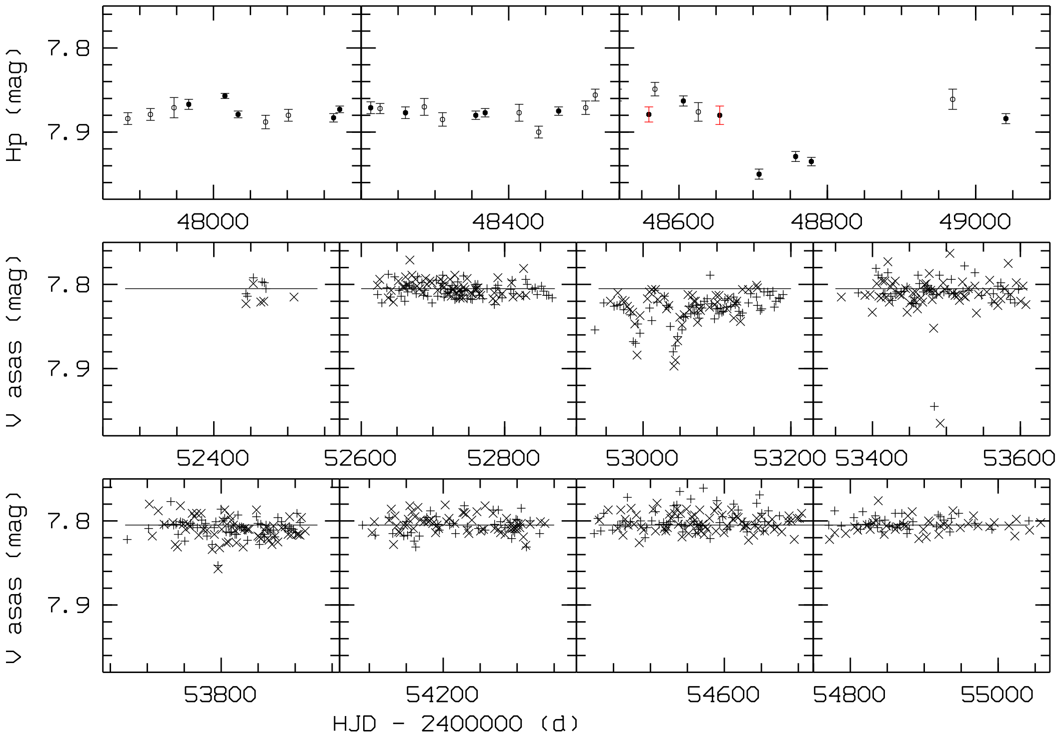

Figure 46: The light variations of HD 100453. Plusses (392) and crosses (407) indicate aperture–3 data from two ASAS sets (Table 1). No magnitude shifts were applied. A horizontal line is shown at magnitude 7.805 in order to guide the eye judging low-level fluctuations (see text). Three data points ($V < 8.1$) fall outside the range of the figure (see text). HIPPARCOS data averaged within one day (filled discs indicating at least 4 contributing measurements) are given in the upper panels. Red error bars indicate uncertainties on the mean computed from the scatter of contributing data, rather than from the HIPPARCOS uncertainties, in cases where this scatter exceeds the expected uncertainty by a factor of 1.5 or more.

similarly 'double' rather than uninterrupted over 70 days. A larger obscuration near HJD 2 453 500 is less well covered and one or both of the faint data could be bad photometry that survived the selection procedure. Another three single data points with magnitudes as faint as 8.1–8.2 at HJD 2 453 392.8, HJD 2 454 438.8 and HJD 2 454 866.8, respectively, are presumably due to bad photometry. HD 100453 is now a confirmed irregularly variable star.

5.3.2 HD 106444 = HIP 59716

HD 106444 is a visual binary consisting of a mid-F star and a G9Ve: pre-main sequence secondary at 23″, 2MASS J12145229-5547037, which contributes roughly one third of the light (SIMBAD database). The companion has a clear impact on the photometry. All HIPPARCOS data were flagged (code 16+), and the ASAS magnitudes brighten roughly 0.06 mag, between each of the apertures 0 and 1, 1 and 2, and 2 and 4. The larger apertures 3 and 4 encompass most light of the system while the HIPPARCOS data measure principally the brighter component, resulting in a noticeable magnitude offset.

Notwithstanding this complexity, the photometry is not useless. The ASAS data indicate a long-term trend, perhaps in a 2800-day cycle, with a peak-to-peak amplitude of 0.07 mag (Fig. 47). No trend is detected over the three-year HIPPARCOS mission. This is best illustrated gaining accuracy by averaging the data over consecutive satellite orbit cycles. The filled symbols in the lower panel of Fig. 47 indicate the observations for which the internal scatter is reasonably consistent with the expectation value computed from the uncertainties on individual measurements listed in the HIPPARCOS photometry annex, while the internal scatter is at least a factor 1.5 above the expectation value for data represented by open circles. The latter averages, tending to brighter magnitudes,

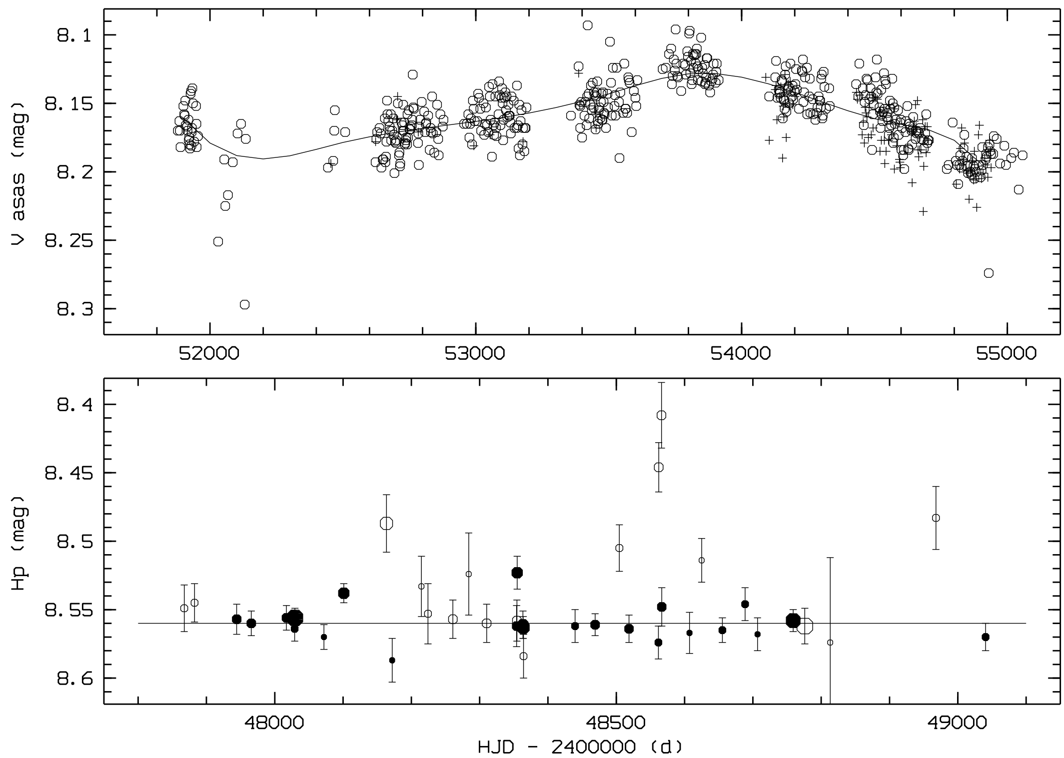

Figure 47: Photometry of HD 106444. Upper panel: the two ASAS data sets (Table 1, circles refer to the larger one). Plusses were shifted to 0.005 mag brighter aperture–4 magnitudes. The full line is a smoothed (s = 0.019) cubic spline representation of the long-term trend. Lower panel: short-term averaged HIPPARCOS data (see Sect. 5.3.2) with the size of the symbols proportional to the number of contributing measurements (3 to 9). Open symbols identify the data presumably most strongly affected by the 2nd component (see Sect. 5.3.2).

presumably include measurements strongly biased by the secondary component. The trend seen in the ASAS but not in the HIPPARCOS data, and the fact that the trend in the ASAS data is somewhat more pronounced in the larger apertures suggests that the observed variability is caused rather by 2MASS J12145229-5547037 than by HD 106444.

5.3.3 HD 113901 = HIP 64044

HD 113901 is a mid–F star showing irregular light variability (Fig. 48). We searched for an underlying cyclic component, first selecting the relatively 'quiet' time interval 2 454 100–900 and then detrending with the smoothed (s = 20.6) cubic spline shown in Fig. 48. Some power was found near 0.32, 1.32 and 2.32 cycles per day, but not strong enough to raise it above the level of suspected cyclic variability. An extensive series of 63 HIPPARCOS measurements in 3.75 d gave additional support for f = 1.32 while rejecting the aliases mentioned above. However, further scrutiny of the other HIPPARCOS data does not support such cycle and this cannot be easily ascribed to a smooth long-term variability. Hence, cyclic variability is not proven and, if present, its detection would require a much denser time coverage. We notice that such cycle length would be compatible with the rotation period of the star. Using $v \sin i$ = 93 km/s (Chen et al. 2011) implies $R \sin i$ = 1.4 solar radii. Three FEROS spectra obtained in 2004 (dates shown in Fig. 48) indicate a radial velocity of 16 ± 1 km/s.

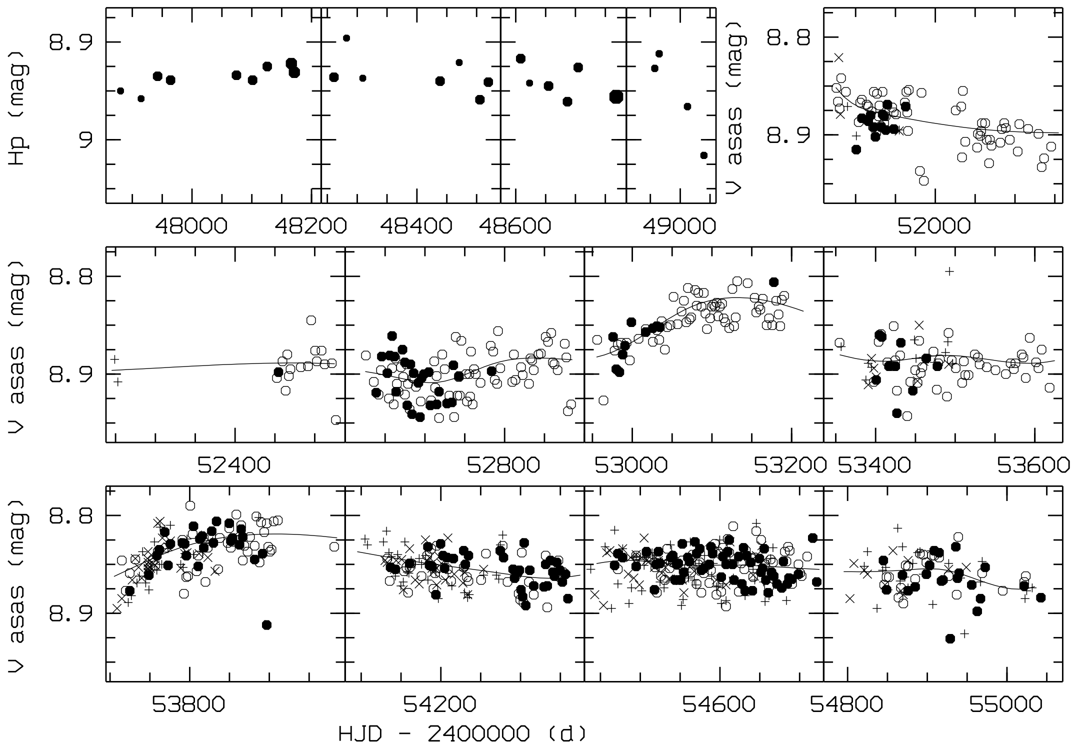

Figure 48: Light variability of HD 113901. HIPPARCOS photometry is averaged over series within a day (increasing symbol size representing 1–2, 3–5 and 8 measurements) and over 3.75 days (largest symbol). Only the 150 measurements with uncertainties of 0.025 mag or less were included. The ASAS aperture–3 photometry is composed of four data sets (Table 1). The sets represented by filled dots, '+' and 'x' were shifted in magnitude by −0.003, +0.004 and −0.007 mag with respect to the largest data set ('o'). Two faint data points fall out of the magnitude range shown. The curve in the ASAS panels is the smoothed (s = 20.6) cubic spline used for the tentative long-term detrending. Three vertical lines in the third panel of the middle row, indicate the times at which spectra were taken.

5.3.4 HD 108016 = HIP 60567

HD 108016 has four large sets of photometry in the ASAS project (Table 1), resulting in 800 useful measurements. The HIPPARCOS data contain, in addition to the widely spaced data, two denser series within one week, at HJD 2 448 022 and 027. The ASAS data show quite different scatter from year to year. The fact that the ASAS aperture includes one star which is two magnitudes fainter (TYC 8243-1367-1, V = 11.65), and two stars three magnitudes fainter, all at distances of 32 to 41″, causes $V_{\rm ASAS}$ to be bright with respect to Hp in comparison with other mid- to late-F stars. Nevertheless, the influence on the rms between data in different apertures is small.

No clear cyclic signal fitting a significant part of the ASAS and HIPPARCOS data could be found, although the complete ASAS set shows some weak but discernible power peaks in the intervals $(n + 0.04, n + 0.07)$ for $n = 0, 1, 2$ which are not supported by the whole HIPPARCOS set nor by its denser series. In the early ASAS data of 2001 (HJD 2 451 895–975, leftmost panel in the mid-row of Fig. 49), a clear pattern of several dimming events during one or a few weeks is visible over 80 days but such event does not recur on this timescale later-on. Clearly, irregular patterns dominate the variability of this object.

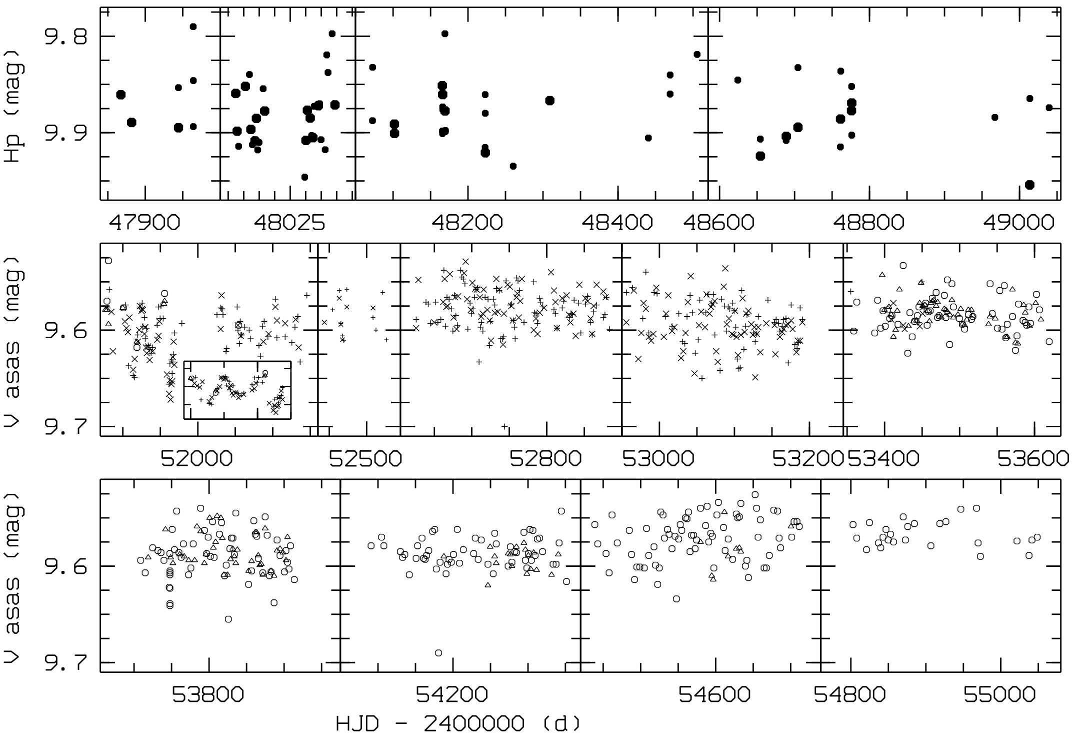

Figure 49: The ASAS (aperture–3) and HIPPARCOS photometry (restricted to the 113 individual data with uncertainties ≤ 0.032 mag) of HD 108016. Larger symbols in the upper panels correspond to the average of two HIPPARCOS measurements within 20 minutes. The second panel from the left shows the denser series, the small tickmarks indicating a one-day spacing. Different ASAS data sets (Table 1) are represented by 'o', triangles (shifted to 0.008 mag fainter magnitudes), '+' (+0.006 mag) and 'x' (+0.012 mag). The small panel inside the leftmost mid-row panel shows in more detail the pattern seen in the time interval HJD 2 451 895–975, with tickmarks each 25 days and 0.05 mag.

5.3.5 HD 117524 = HIP 66001

HD 117524 is a mid-G, pre-main sequence, proper motion binary (Makarov & Kaplan 2005). Photometrically, it shows long-term irregular variability, sometimes with slow trends during a whole observing season (e.g. in 2008, see mid-panel of bottom row of Fig. 50) and at certain epochs also variations on very short time-scales (e.g. around HJD 2 452 700, Fig. 50). In some years, variability was much less prominent. There is no indication of a cyclic component in the variability.

A similar variety of characteristics is seen in the HIPPARCOS data. There is no indication of long-term variability above the 0.02 mag level before HJD 2 448 200; the rms scatter in series of observations within a fraction of a day never exceeds its expected value of ≈0.025 mag before HJD 2 448 600. However, thereafter the observed rms scatter within a fraction of a day is often larger and data taken within a week or few weeks show a significantly different light level (Fig. 50).

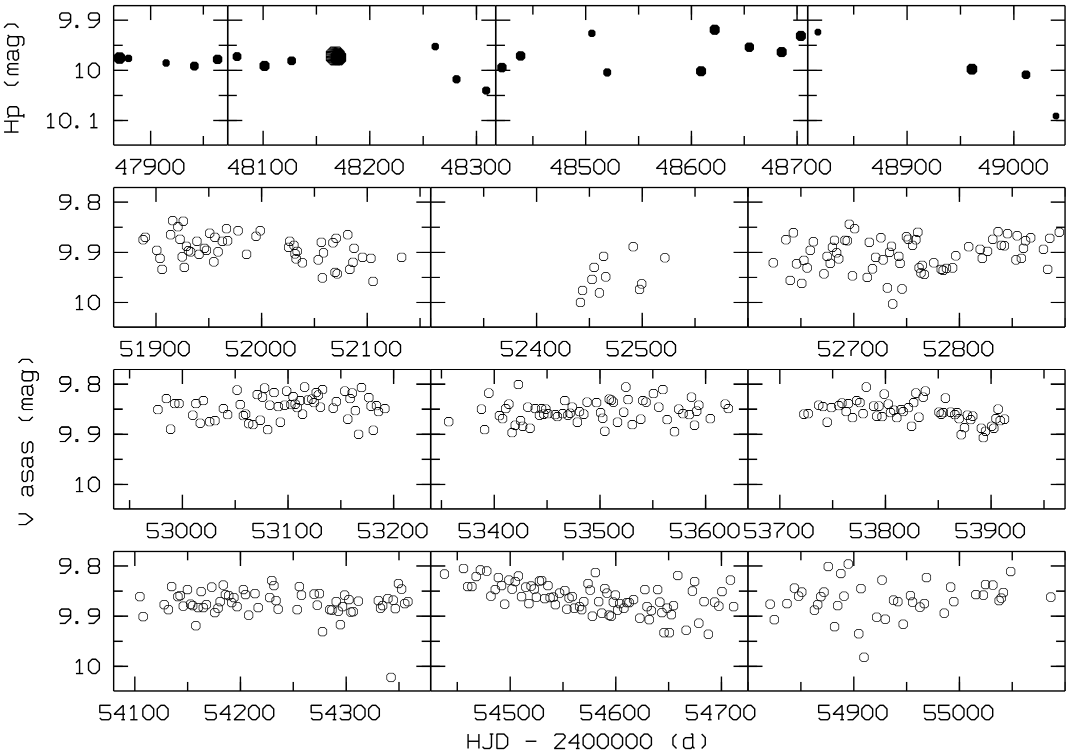

Figure 50: The irregular variability of HD 117524. The upper row summarizes the HIPPARCOS data, averaged over time intervals within one day, with symbol size growing linearly with the number (1–19) of contributing data. The ASAS data are from aperture 2.

5.3.6 HD 111170 = HIP 62445

HD 111170 is the variable star V940 Cen identified during the HIPPARCOS mission and classified as a BY Dra-type variable (Kazarovets et al. 1999). Mamajek et al. (2002) list it as a post-T Tauri star. Addition of the ASAS data sets shows that the light variation is larger than the one covered by the HIPPARCOS mission (Fig. 51). While the star was then significantly fainter, and still dimming during the HIPPARCOS epoch at a rate of 0.115 mag per 1 000 days, it passed through a brightness maximum in recent years (2007, HJD 2 454 230) with $V_{\rm ASAS} \approx 9.30$ as compared to $Hp \approx 9.7$. The difference in passband accounts roughly for $Hp - V_{\rm ASAS} \approx 0.12$ mag.

We notice that the HIPPARCOS data set is quite unusual in the sense that for about three quarters of the cases only one of the two measurements within 20 minutes survived as a catalogue entry. Apparently some particular problem occurred quite often for this object.

After removal of the long-term trend (linear in the HIPPARCOS epoch and by a smoothed ($s = 18$) cubic spline in the ASAS epoch), a search for short periods was made since the subset residual scatter of ≈ 0.02 mag rms is a bit higher than usual. A unique period for the 20-year time interval covered by the observations was not found, although some interesting points may be noticed. The best-quality HIPPARCOS data (74 entries with uncertainty up to 0.021 mag, extending over HJD 2 447 880–9 012, 19 of them representing paired observations) support a frequency $f = 2.39205$ cycles per day and a peak-to-peak variation of about 0.04 mag, but such periodicity is not found in the ASAS data and is not supported by the lower-quality HIPPARCOS data. At best, such cycle is relevant only when the star is fainter. In both data sets there is noteworthy power near 2 and 3 cycles per day, but never at compatible frequencies in both sets. The ASAS window function has significant peaks near such frequencies, so interpretation is not straightforward. Summarizing, we suspect short-term microvariability with, possibly, cycles of length between one half and one third of a day, but a more adequate sampling and precision is needed to substantiate this. The slow long-term variation over several tenths of a magnitude is well-established.

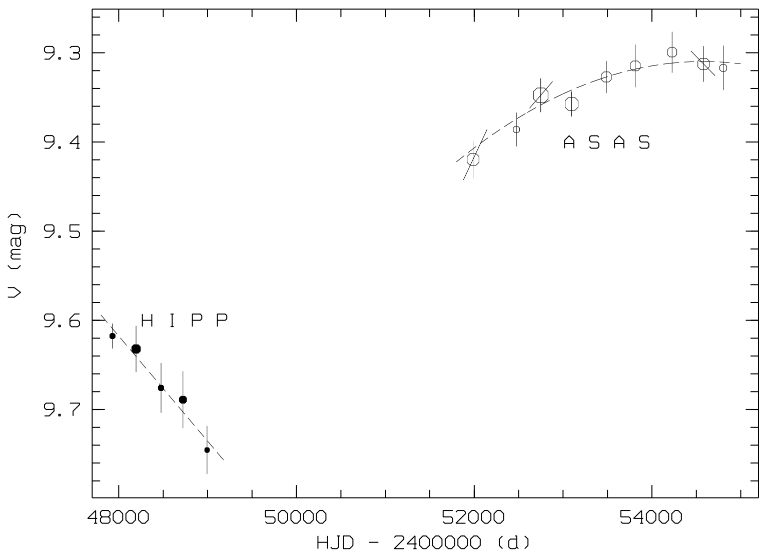

Figure 51: Long-term variability of HD 111170 (V940 Cen). The magnitudes averaged over subsets of HIPPARCOS data (comprising 9 data during HJD 2 447 881–964; 45 during HJD 2 448 074–309; 11 during HJD 2 448 418–519; 29 during HJD 2 448 607–754; 3 during HJD 2 448 956–9 013) and 'yearly' (actually starting in December of the previous year) averages of ASAS data (80 in 2001, HJD 2 451 879–2 145; 19 in 2002, HJD 2 452 242–526; 111 in 2003, HJD 2 452 623–883; 93 in 2004, HJD 2 452 976–3 191; 61 in 2005, HJD 2 453 359–606; 59 in 2006, HJD 2 453 709–914; 53 in 2007, HJD 2 454 091–347; 76 in 2008, HJD 2 454 439–711 and 27 in 2009, HJD 2 454 803–5 049) are shown, with bars indicating the rms of individual measurements around the mean of the subset. Gradients within the subsets are shown when exceeding their 3σ uncertainty. Symbol size grows linearly with the number of contributing data.

5.3.7 HD 116650 = HIP 65517

In the Michigan Spectral Survey (Houk 1982) HD 116650 appears as K0/2V + (G) but the classification is noted as less reliable. Mamajek et al. (2002) list it as a pre-main sequence star of type G1.5IV and notice that the $b - y$ and $B - V$ colours support the spectral type. Chen et al. (2011) determine $v \sin i = 37 \pm 3$ km/s. The HIPPARCOS catalogue suggests it is a β Lyrae type eclipsing binary with a period of almost $1\overset{d}{.}09$. In the Variable Star Name List dealing with the detection of variable stars by HIPPARCOS, it is suggested to be possibly an RS CVn-type binary (Kazarovets et al. 1999).

The ASAS data set excludes the suggested short periodicity. Fig. 52 shows the dominantly slow variability pattern visible in the ASAS data as well as, less detailed, in the HIPPARCOS data. The main trend in the latter set is a slow dimming of the star. The relatively small size of the HIPPARCOS set (Fig. 1) has given the opportunity to fold the data successfully in the spurious $1\overset{d}{.}09$ period.

A search for an underlying cyclic component was done on the raw data and after detrending with the smoothed ($s = 16.9$) cubic spline shown in Fig. 52. There is some power at frequencies of 1.64785 and 0.66757 cycles per day but only at a level that would lead us, in the absence of irregular variations, to *suspect* a cyclic variation (peak-to-peak variation below 0.02 mag). There is no power at the period proposed in the HIPPARCOS catalogue. The binary character of the star is questionable. Nevertheless, two HIPPARCOS epochs with 4 and 8 measurements, HJD 2 448 519 and HJD 2 448 702, respectively, indicate that larger variations at least occasionally occur on timescales shorter than one day. These may contribute to some extent to the scatter noticed in the ASAS panels of Fig. 52.

Acknowledgements. Part of this work was supported by the European ESA/PRODEX project number 14732/00NL/SFe(IC). The authors acknowledge extensive use of ESO-MIDAS, the Simbad and Vizier databases at CDS, Strasbourg, France and the SAO/NASA ADS services at Harvard-Smithsonian CfA, US.

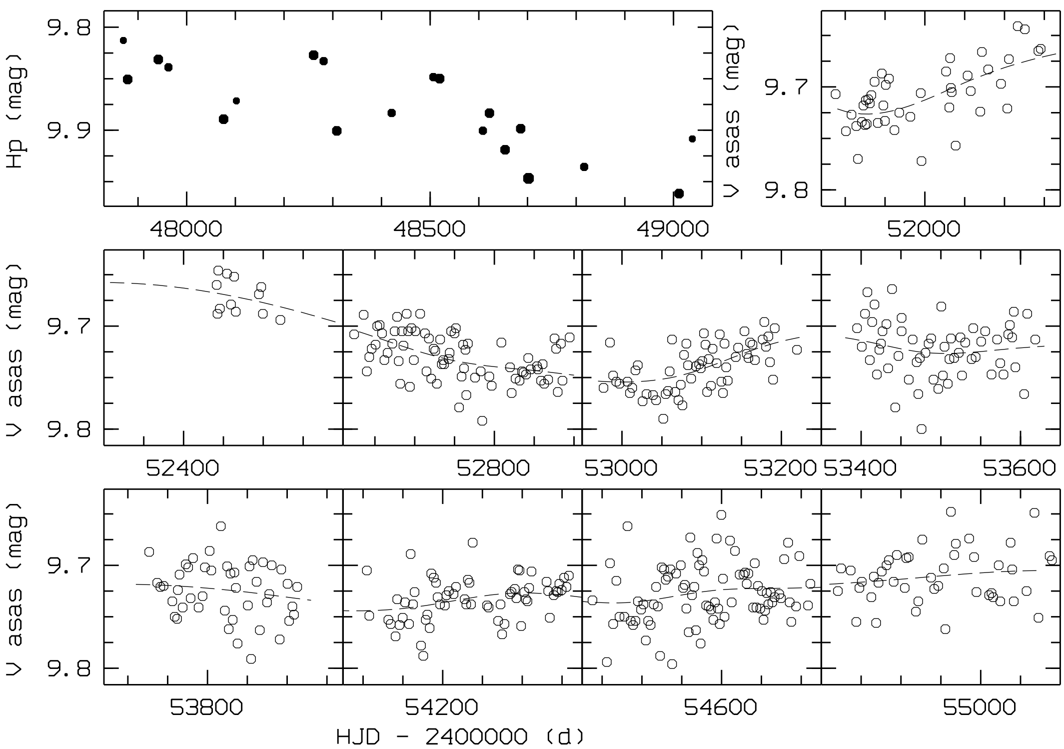

Figure 52: Light variability of HD 116650, from HIPPARCOS and ASAS aperture–4 photometry. Five of 489 measurements fall outside the magnitude range shown in the figure. The dashed line in the ASAS panels is the smoothed (s = 16.9) cubic spline used for tentative long-term detrending. HIPPARCOS data are represented by dots of different sizes depending on the number of observations (1, 2–3, 4–6, 8) obtained within one day.

References

Adelman, S. J., Dukes, Jr., R. J., & Pyper, D. M. 1992, AJ 104, 314

Alencar, S. H. P., Melo, C. H. F., Dullemond, C. P., et al. 2003, A&A 409, 1037

Alencar, S. H. P., Teixeira, P. S., Guimarães, M. M., et al. 2010, A&A 519, A88

Andersen, J., Lindgren, H., Hazen, M. L., & Mayor, M. 1989, A&A 219, 142

Borra, E. F., Beaulieu, A., Brousseau, D., & Shelton, I. 1985, A&A 149, 266

Brown, A. G. A. & Verschueren, W. 1997, A&A 319, 811

Carmona, A., van den Ancker, M. E., & Henning, T. 2007, A&A 464, 687

Catalano, F. A. & Leone, F. 1993, A&AS 100, 319

Chen, C. H., Mamajek, E. E., Bitner, M. A., et al. 2011, ApJ 738, 122

Chen, X. P., Henning, T., van Boekel, R., & Grady, C. A. 2006, A&A 445, 331

Christiansen, J. L., Derekas, A., Kiss, L. L., et al. 2008, MNRAS 385, 1749

Collins, K. A., Grady, C. A., Hamaguchi, K., et al. 2009, ApJ 697, 557

Cutispoto, G., Pastori, L., Pasquini, L., et al. 2002, A&A 384, 491

David, M., Hensberge, H., & Nitschelm, C. 2013, A&A 557, A47

de Zeeuw, P. T., Hoogerwerf, R., de Bruijne, J. H. J., Brown, A. G. A., & Blaauw, A. 1999, AJ 117, 354

Dierckx, P. 1982, Computer Graphics and Image Processing, 20, 171

Fukagawa, M., Tamura, M., Itoh, Y., Hayashi, S. S., & Oasa, Y. 2003, ApJL 590, L49

Garrison, R. F. 1967, ApJ 147, 1003

Guimarães, M. M., Alencar, S. H. P., Corradi, W. J. B., & Vieira, S. L. A. 2006, A&A 457, 581

Harmon, R. O., Robinson, R., & Roy, A. 2011, in Bulletin of the American Astronomical Society, Vol. 43, American Astronomical Society Meeting Abstracts #217, 342.08–

Henry, G. W., Fekel, F. C., & Henry, S. M. 2007, AJ 133, 1421

Henry, G. W., Fekel, F. C., & Henry, S. M. 2011, AJ 142, 39

Hoffmeister, C. 1930, Astronomische Nachrichten 240, 193

Houk, N. 1982, Michigan Catalogue of Two-dimensional Spectral Types for the HD stars. Volume 3. Declinations -40° to -26°., ed. Houk, N.

Houk, N. & Cowley, A. P. 1975, University of Michigan Catalogue of two-dimensional spectral types for the HD stars. Volume I. Declinations -90° to -53°., ed. Houk, N. & Cowley, A. P.

Houk, N. & Smith-Moore, M. 1988, Michigan Catalogue of Two-dimensional Spectral Types for the HD Stars. Volume 4, Declinations -26° to -12°., ed. N. Houk & M. Smith-Moore

Kazarovets, A. V., Samus, N. N., Durlevich, O. V., et al. 1999, Information Bulletin on Variable Stars 4659, 1

Koen, C. & Eyer, L. 2002, MNRAS 331, 45

Köhler, R., Kunkel, M., Leinert, C., & Zinnecker, H. 2000, A&A 356, 541

Kraus, A. L. & Hillenbrand, L. A. 2007, ApJ 662, 413

Krautter, J., Wichmann, R., Schmitt, J. H. M. M., et al. 1997, A&AS 123, 329

Lanz, T. & Mathys, G. 1991, A&AS 90, 365

Makarov, V. V. & Kaplan, G. H. 2005, AJ 129, 2420

Malfait, K., Bogaert, E., & Waelkens, C. 1998, A&A 331, 211

Mamajek, E. E., Meyer, M. R., & Liebert, J. 2002, AJ 124, 1670

Mathys, G. 1991, A&AS 89, 121

Mathys, G. 1994, A&AS 108, 547

Mathys, G. & Lanz, T. 1992, A&A 256, 169

Meeus, G., Bouwman, J., Dominik, C., Waters, L. B. F. M., & de Koter, A. 2002, A&A 392, 1039

Mora, A., Merín, B., Solano, E., et al. 2001, A&A 378, 116

Neuhäuser, R. & Brandner, W. 1998, A&A 330, L29

North, P. 1984, A&AS 55, 259

Perryman, M. A. C. 1997, The Hipparcos and Tycho Catalogues (ESA SP-1200), Vol. 1 (ESTEC, Noordwijk, The Netherlands: ESA Publication Division)

Pojmański, G. & Maciejewski, G. 2004, Acta Astronomica 54, 153

Royer, F., Gerbaldi, M., Faraggiana, R., & Gómez, A. E. 2002, A&A 381, 105

Scargle, J. D. 1982, ApJ 263, 835

Schwarzenberg-Czerny, A. 1991, MNRAS 253, 198

Shaya, E. J. & Olling, R. P. 2011, VizieR Online Data Catalog, 2192, 20002

Shevchenko, V. S., Grankin, K. N., Ibragimov, M. A., Mel'Nikov, S. Y., & Yakubov, S. D. 1993, Ap&SS 202, 121

Thompson, I. B., Brown, D. N., & Landstreet, J. D. 1987, ApJS 64, 219

Torres, C. A. O., Quast, G. R., da Silva, L., et al. 2006, A&A 460, 695

Vander Linden, D. & Sterken, C. 1986, A&A 168, 155

Waite, I. A., Carter, B. D., Marsden, S. C., & Mengel, M. W. 2005, PASA 22, 29

Waite, I. A., Marsden, S. C., Carter, B. D., et al. 2011, PASA 28, 323

Wichmann, R. & Schmitt, J. H. M. M. 2003, MNRAS 342, 1021

Wichmann, R., Schmitt, J. H. M. M., & Hubrig, S. 2003, A&A 399, 983

Wichmann, R., Sterzik, M., Krautter, J., Metanomski, A., & Voges, W. 1997, A&A 326, 211

Zinnecker, H., Christou, J., Ridgway, S., & Probst, R. 1990, in Astronomische Gesellschaft Abstract Series, Vol. 5, Astronomische Gesellschaft Abstract Series, 67–